Final Report

DEVELOPMENT OF A WORLDWIDE MODEL FOR F-LAYER-PRODUCED SCINTILLATION

By: E. J. FREMOUW C. L. RINO

Prepared for:

NATIONAL AERONAUTICS AND SPACE ADMINISTRATION
GODDARD SPACE FLIGHT CENTER
GREENBELT, MARYLAND 20071

CONTRACT NAS5-21551

STANFORD RESEARCH INSTITUTE
Menlo Park, California 94025 · U.S.A.

STANFORD RESEARCH INSTITUTE
Menlo Park, California 94025 · U.S.A.

Final Report *November 1971*

DEVELOPMENT OF A WORLDWIDE MODEL FOR F-LAYER-PRODUCED SCINTILLATION

By: E. J. FREMOUW C. L. RINO

Prepared for:

NATIONAL AERONAUTICS AND
SPACE ADMINISTRATION
GODDARD SPACE FLIGHT CENTER
GREENBELT, MARYLAND 20071

SRI Project 1079

CONTRACT NAS5-21551
Contract Period: 3 February through
3 December 1971
Principal Investigator: E. J. Fremouw
(415) 326-6200
Ext. 2596
Technical Officer: T. S. Golden
(301) 982-4297

Approved by:

DAVID A. JOHNSON, *Director*
Radio Physics Laboratory

RAY L. LEADABRAND, *Executive Director*
Electronics and Radio Sciences Division

Copy No. 111

ABSTRACT

An empirical approach to modeling the electron-density irregularities in the F layer of the earth's ionosphere that are primarily responsible for scintillation of transatmospheric VHF-UHF signals has been devised and tested. The work was directed toward two major goals: first, development of a worldwide model for describing the rms fluctuation in signal strength to be expected on an arbitrary satellite-to-earth communication link under average ionospheric conditions; and, second, investigation of the feasibility of similar modeling for description of the complete first-order distribution of signal strength.

In the work on rms fluctuation, a model for scintillation-producing irregularities was postulated as a function of geomagnetic latitude, local time of day, season, and sunspot number. The primary parameters of the irregularities that were postulated were the strength (rms fluctuation in electron density) and the scale-size transverse to the geomagnetic field. The irregularities were assumed to be aligned along the field, and their axial ratio was taken as constant, as were their height and the thickness of the irregular layer.

The model was tested by computing the fractional rms fluctuation in received power (square of real amplitude) to be expected in a given experimental circumstance and comparing against values of this or related quantities reported in the literature. The model then was improved by iteration. The iterative model development made use of twelve data sets from eight contributions to the scintillation literature; final testing employed these twelve data sets plus an independent one from an additional publication.

The feasibility investigation into modeling amplitude distribution involved a theoretical development of scattering in the complex domain, based solely on requirements of the Central Limit Theorem. From the theoretical results, a technique for evaluating the expected amplitude distribution in a given observational circumstance was devised.

The technique was tested against a single data set obtained from observations near the geomagnetic equator, and the test showed a high degree of agreement between the calculated and observed results. This success was demonstrated to be non-fortuitous by means of a second test, employing a change in a single assumed ionospheric parameter, which considerably reduced the agreement.

As a result of the above, it is concluded that distribution modeling is feasible for conditions of moderate scintillation. It is recommended that the limitations of the technique devised be tested empirically and that a theoretical effort be undertaken to extend the technique's range of validity.

The rms model developed is offered as a tool for systems planning on a worldwide basis, except poleward from about 70 degrees geomagnetic latitude, where testing was not possible. Other limitations are described in the report. The model is expected to yield better than order-of-magnitude estimates of scintillation to be encountered in most circumstances.

CONTENTS

CONTENTS (Concluded)

ILLUSTRATIONS

TABLES

ACKNOWLEDGMENT

This work depended heavily on man/computer interaction. We hereby acknowledge with thanks the important contributions of Mrs. Odile de la Beaujardiere and Mrs. Dolores McNeil in performing the sometimes frustrating task of writing, testing, and perfecting the evolving computer programs used.

I INTRODUCTION

As a result of earlier work on ionospheric effects on transatmospheric radio signals, personnel of Stanford Research Institute (SRI) presented a paper at the U.S. Spring 1970 meeting of the International Radio Science Union (URSI), entitled "A Proposed Empirical Model for Worldwide VHF-UHF Scintillation." In view of system-design needs for evaluating signal scintillation in this frequency range, NASA requested a proposal for work on improving, quantifying, and testing the suggested model. SRI responded with a proposal for refining the model and testing it against published scintillation data; this document is the final report on the ensuing research project.

A. Objectives

There were two major objectives of the research carried out. The first was to describe worldwide scintillation behavior in such a manner that quantitative predictions can be made of the root-mean-square (rms) fluctuation in signal strength to be expected under average ionospheric conditions on an arbitrary satellite-to-earth communication path. The description is to account for diurnal, seasonal, and solar-cycle trends of scintillation and for geometric effects. The second objective was to determine the feasibility of similarly modeling not only the rms fluctuation, but rather the entire first-order statistical distribution of signal strength on such a path, over the full range of ionospheric conditions.

The rms model developed--including its limitations--is described herein, along with an evaluation of the feasibility of distribution

modeling. The rms modeling work is reported in Section II and the distribution feasibility investigation in Section III; general conclusions and recommendations are made in Section IV. The research contract called for a "catalogue" of calculated scintillation magnitude, based on the rms model. Such a catalogue is presented, in graphical form, in Appendix A. The computer program (card deck and complete listing) used for calculating the catalogue entries is being delivered to NASA under separate cover.

Appendix B is a partial guide to the scintillation literature, and Appendix C discusses the Nakagami distribution as related to the work described in Section III.

B. Background

The signal-strength fluctuations, called scintillation, that are experienced by exterrestrial VHF-UHF signals passing through the earth's atmosphere are caused almost entirely by scattering in the ionosphere, especially in the F layer. These amplitude scintillations--as well as (to a lesser extent) phase, angle, and polarization scintillation--have been studied by numerous workers observing radio stars and satellites. The measurement of scintillation usually involves determining an index of scintillation activity. Until recently, the most common method was to assign activity indices by qualitatively examining the records, thus making quantitative comparison of data difficult.

More recently, indices have been developed that involve calculating (or that are related to) the ratio of the change in amplitude (or power) to the average amplitude (or power) of the signal, such as computing the fractional rms fluctuation or the fractional mean deviation. Briggs and Parkin (1963) used diffraction theory to relate the rms fluctuation of power analytically to the strength and size of the scattering ionospheric

irregularities, as a function of scattering-layer height and thickness, magnetic-field geometry, zenith angle, and observing frequency.

Briggs and Parkin also related the rms fluctuation of power to other quantitative indices, based on an assumption about the underlying signal statistics. Some other observers have related their subjective indices empirically to the quantitative indices of Briggs and Parkin--notably Little, Reid, Stiltner, and Merrit (1962) and Preddey, Mawdsley, and Ireland (1969). The index suggested by Whitney, Aarons, and Malik (1969) also has been so evaluated by Bischoff and Chytil (1969), again subject to certain assumptions of statistics (see Section III-D and Appendix C for discussion of this point).

In the work of Briggs and Parkin, the fractional rms fluctuation of power was found to be directly proportional to the rms fluctuation of electron density in the ionosphere, other observational and irregularity parameters being equal. There are essentially no direct measurements of the electron-density fluctuation.* However, several workers have performed remote measurements of the other two parameters that are most important for purposes of scintillation modeling--irregularity scale-size and scattering-layer height (Hewish, 1952; Yeh and Swenson, 1964; Aarons and Guidice, 1966; Kent and Koster, 1966; Lansinger and Fremouw, 1967).

The measurements of scale-size and height were judged sufficiently consistent for various geographic and geophysical conditions that it was proposed to treat these quantities as constants in rms modeling. During the course of the work, it was found that such an assumption was not adequate for scale-size, especially where frequency dependence of scintillation is of concern. The assumption was somewhat relaxed, as described in Section II-C-5.

---

* The first such measurements have recently been reported by Dyson (1969, 1971), using an in situ technique.

Aside from the treatment of scale-size, the approach to modeling was to assume that observed variations in scintillation index result solely from changes in the rms fluctuation of electron density in the F layer. The general behavior of scintillation as a function of geographic and geophysical conditions has been reviewed by Aarons, Whitney, and Allen (1971), and by Fremouw and Bates (1971).

The modeling procedure was to postulate dependences of the rms fluctuation of electron density on latitude, sunspot number, season, and time of day, and then to calculate the resulting scintillation dependences to be expected, using the diffraction theory of Briggs and Parkin. The calculated result was then compared with observations reported in the literature and the postulated model was improved by iteration; the starting model was based on the morphological review by Fremouw and Bates. The method will be more fully described in Sections II-A, B, and C.

II RMS MODELING

A. The Basis for Modeling

1. Theory and Assumptions

The theoretical basis for the work described in Section II was laid by Briggs and Parkin (1963). In their diffraction theory, the irregular ionospheric layer is assumed to produce only phase perturbations (i.e., absorption is ignored), which is appropriate at all frequencies of interest here. There are two steps in employing their theory: first, to calculate the rms fluctuation of phase at the output plane of the irregular layer, and then to calculate the fractional rms fluctuation of power in the diffraction-perturbed wavefront arriving at the receiver.

There are several assumptions inherent in the work of Briggs and Parkin. The most important are the following:

(1) Angular deviations of radio rays within the scattering medium are small, so that integration may be carried out along straight lines in the medium.

(2) The scattering medium is several times thicker than the size of an individual irregularity.

(3) The thickness of the layer is small compared with its distance from the receiver.

(4) The spatial autocorrelation function of the irregularities may be expressed as a gaussian with symmetry about the geomagnetic-field direction.

(5) The rms fluctuation in phase at the output plane of the scattering medium is less than one radian (weak-single-scatter assumption).

The above assumptions for the most part are acceptable for a working model of the normal F-layer scattering region for frequencies of concern here, although Assumption 4 is probably an idealization. Assumption 2 may not hold in special circumstances such as in scattering directly associated with isolated auroral forms, but this is probably of limited importance for our endeavor of calculating average scintillation magnitude. The origin and nature of the above assumptions should become clear upon reading Section III, where the same conditions are invoked for developing the theory of amplitude distribution.

Assumption 5, above, represented the most serious limitation of Briggs and Parkin's theory for employment in rms modeling. Except in the mid-latitude region, it becomes invalid rather often at the common scintillation observing frequencies of 40 and 50 MHz. In the lower end of the operational band of interest (say, 100 to 200 MHz), the assumption becomes invalid for a few hours on most nights in the auroral and equatorial regions, and apparently even at sub-auroral latitudes (boundary region) during periods of high sunspot number. Above 200 MHz, the weak-scatter assumption is rarely invalid, mainly in the midnight hours near the geomagnetic equator and under conditions of auroral disturbance.

In general, in the low-sunspot-number period of 1972-75, strong scatter should be sufficiently unusual in the 100-to-2300 MHz spectral regime to be unimportant in calculating most averages. The computer program developed for rms modeling, including the version released to NASA for systems planning, contains a feature for flagging situations where strong scatter is encountered. This permits avoiding undue error from breakdown of the weak-scatter assumption, and makes particularly troublesome communication conditions immediately obvious.

Again, this condition is most likely to be encountered near the lower end of the operational band of interest (such as at 136 MHz), near the geomagnetic equator at night and in aurorally active regions.

Based on the above-listed assumptions, Briggs and Parkin gave the following expression [their Eq. (20)] for the fractional rms fluctuation in signal intensity (square of real amplitude) observed at the ground as a function of ionospheric and geometrical (illustrated in Figure 1) parameters:

$$S = \sqrt{2}\,\phi_o \left[1 - (\cos u_1 \cos u_2)^{1/2} \cos \frac{1}{2}(u_1 + u_2)\right]^{1/2} . \qquad \text{(II-1)}$$

The quantities u_1 and u_2 are geometrical ones dealing with the ratio of Fresnel-zone size to the scale-size of the scattering irregularities. They are defined as follows:

$$u_1 = \tan^{-1} \frac{2\lambda z}{\pi \xi_o^2} \quad , \quad u_2 = \tan^{-1} \frac{2\lambda z}{\pi \beta^2 \xi_o^2} \qquad \text{(II-2)}$$

where

$$\beta = (a^2 \sin^2 \psi + \cos^2 \psi)^{1/2} \qquad \text{(II-3)}$$

which describes the orientation of the irregularities, and where

$$z = \frac{z_1 z_2}{z_1 + z_2} \quad . \qquad \text{(II-4)}$$

The square of the Fresnel-zone size appears in Eq. (II-2) as the product λz. The variables used in Eqs. (II-2), (II-3), and (II-4) are the following:

λ = Wavelength of the radio wave

z_1 = Distance from the receiver to the center of the scattering region

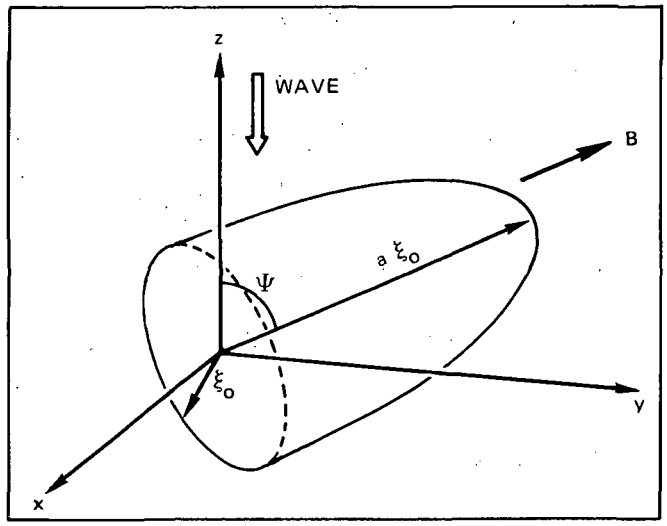

(a)

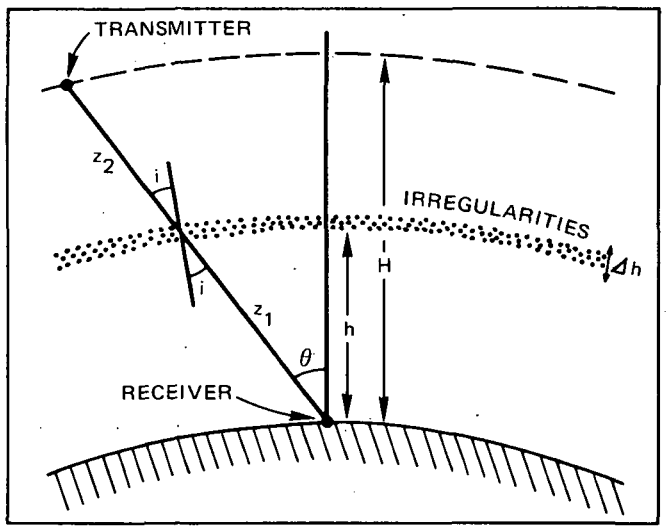

(b)

LA-1079-6

FIGURE 1 THE SCATTERING GEOMETRY OF BRIGGS AND PARKIN (1963). (a) A typical scattering irregularity, elongated along the geomagnetic field B, which lies in the (y,z) plane at an angle Ψ to the radio line of sight. (b) The overall geometry.

z_2 = Distance from the center of the scattering region to the transmitter

ξ_o = Transverse scale-size of the ionospheric irregularities (distance over which the spatial autocorrelation function drops to e^{-1} transverse to the geomagnetic-field direction)

a = Axial ratio of the ionospheric irregularities (ratio of longitudinal scale-size to ξ_o)

ψ = Angle between the negative of the radio-propagation vector and the geomagnetic field direction, along which the longitudinal axis of the irregularities is aligned.

All ionospheric parameters and the remaining geometrical ones appear in the factor ϕ_o, derived by Briggs and Parkin [their Eq. (13)] on the basis of the assumptions listed earlier, with the following result:

$$\phi_o = \pi^{1/4} r_e \lambda \frac{\left(a\xi_o \sec i\right)^{1/2}}{\beta^{1/2}} (\Delta h)^{1/2} (\Delta N) \quad . \qquad \text{(II-5)}$$

The quantity ϕ_o is the rms fluctuation in radio-frequency phase across a plane at the output boundary of the scattering layer. In addition to the variables defined above, ϕ_o depends on the following:

r_e = Classical radius of an electron

i = Angle of incidence of the radio-propagation vector on the scattering layer, measured from the local vertical

Δh = Thickness of the scattering layer

ΔN = rms fluctuation in electron density in the scattering region (i.e., $\Delta N \triangleq \langle (N - \langle N \rangle)^2 \rangle^{1/2}$, where $\langle\ \rangle$ indicates mean).

The geometry is further specified as follows:

$$i = \sin^{-1} \frac{R_o \sin \theta}{R_o + h} \tag{II-6}$$

$$z_1 = (R_o^2 \cos^2 \theta + 2R_o h + h^2)^{1/2} - R_o \cos \theta \tag{II-7}$$

$$z_2 = (R_o^2 \cos^2 \theta + 2R_o H + H^2)^{1/2} - (R_o \cos^2 \theta + 2R_o h + h^2)^{1/2}$$

where

θ = Zenith angle of the transmitter as viewed at the receiver

R_o = Distance from center of the earth to the receiver

h = Center height of the scattering layer above the receiver

H = Height of the transmitter above the receiver.

Equations (II-1) through (II-7) were coded along with a number of auxiliary expressions, to permit calculation of the Briggs and Parkin scintillation index, S, as a function of the F-layer model being developed and various satellite and radio-star observing conditions. Conceptually, the two major steps in the principal calculation are described by Eqs. (II-5) and (II-1). The main modeling endeavor was to provide proper parameter values for use in calculating the rms phase fluctuation, ϕ_o.

By far the greatest effort was put into selecting the appropriate worldwide behavior of rms electron-density fluctuation, ΔN. Before describing the ΔN modeling, we shall discuss selection of the other geophysical quantities involved in the calculations.

The simplest to handle was the scattering-layer thickness, Δh. Since it (more precisely, its square root) appears only in Eq. (II-5) as a multiplicative factor along with ΔN, it was possible to treat it entirely as a constant. If the desired end result were an accurate

model of ΔN for geophysical purposes, then much more attention would have to be given to Δh. For developing a model that will predict scintillation index, it is really only the product $\Delta N(\Delta h)^{1/2}$ that is important, and separating the effects of the two variables would be quite impossible from published scintillation data. Nonetheless, in order to model ΔN as accurately as was consistent with the available data and the needs of the project, the value chosen for Δh was taken from measurements reported in the literature--namely, 100 km (Liszka, 1964b; Yeh and Swenson, 1964; Kent and Koster, 1966).

The center height, h, of the scattering layer enters the calculations through the incidence angle, i, in Eq. (II-5), and more importantly through the Fresnel-distance parameters, u_1 and u_2, in Eq. (II-1). The works of Liszka (1964b), Yeh and Swenson (1964), and Kent and Koster (1966) cited above for layer thickness, are also the best sources of information regarding layer height. It is possible that, from time to time, the center height varies through most of the F layer, but there is no evidence of trends associated with the independent variables of interest in this study--time of day,* season, sunspot number, and latitude. The published observations all suggest that the scattering layer is located, on the average, at about 350 km altitude, regardless of the above independent variables, and this value was used in the modeling.

The axial ratio, a, of the scattering irregularities enters directly in the numerator of Eq. (II-5) and through the quantity β in both Eq. (II-5) and Eq. (II-1). Where it enters directly, it is quite

---

*Our effort is directed at modeling F-layer-produced scintillations only, and there is no attempt to account for the daytime scintillations produced in the E layer that have been reported at various latitudes by a number of observers. The latter are generally quite weak compared with those produced in the F layer, with which we are concerned.

acceptable to treat it as a constant, for the same reasons invoked for Δh. The situation is more subtle where the axial ratio enters through β, which describes the projection of the field-aligned irregularities viewed by the receiver. Here the magnetic-field geometry also is involved. In practice, the effect of axial ratio on the way scintillation varies with magnetic-field geometry is important only when the radio line of sight approaches being parallel to the field (in which case the irregularities would be viewed end-on).

Some variations in axial ratio apparently occur, but there is no reported evidence of systematic trends with most of the independent variables of concern here. Observations under a variety of observing conditions (Jones, 1960; Liszka, 1963; Koster, 1963) suggest using a value of 10 for axial ratio in calculating average scintillation index, and this value was chosen.

More recent observations of Kent and Koster (1966) and especially of Koster, Katsriku, and Tete (1966) show that the irregularities can be very much more elongated in the equatorial region. Fortunately, in this region the field-aligned irregularities are nearly horizontal, so they can be viewed nearly end-on only for low elevation angles toward the north and south. Indeed, near the equator they can never be viewed exactly end-on because of the ionosphere's curvature and the greater curvature of the geomagnetic field lines.

While treating axial ratio as a constant with a value of 10 is thought adequate for most applications, and while this approach has been used in the current work, further pursuit of this question would be appropriate in more refined modeling. While it would be unimportant for applications such as equatorial communication via synchronous satellite, it may be of some concern for, say, tracking of high-inclination satellites from stations several degrees away from the geomagnetic equator.

Another problem related to field alignment is selection of a model for the geomagnetic field itself. Excellent mathematical models exist (e.g., Cain and Cain, 1968), and they could be employed in scintillation modeling. This would be straightforward in principle but costly in computer time. Calculating the field direction for use in evaluating β would be reasonably economical. However, an important variable in the model of electron-density fluctuation, which will be discussed in Sections II-B, C, and D, is the geomagnetic latitude of the ionospheric location in question. This could be calculated for an accurate field model through the invariant-latitude parameter L (McIlwain, 1961), but it would involve essentially tracing field lines--an expensive procedure.

Consequently, a simple earth-centered but axially tipped dipole magnetic-field model was used in the current work, permitting a simple analytical calculation of geomagnetic latitude. In more refined modeling--where the added computer expense might be justified--a higher-order field model would quite likely give better data fits than have been achieved in the present effort. It does not seem that the expense would be justified, however, prior to refinement of other parameters, especially irregularity scale-size, which will now be discussed.

With the height of the ionospheric scattering layer being reasonably well described as constant at 350 km, the most important variable other than ΔN (more precisely, $\Delta N(\Delta h)^{1/2}$) in establishing the magnitude of scintillation is the scale-size, ξ_o, of the irregularities transverse to the geomagnetic field. This is because the amplitude scintillations develop gradually by diffractive interference during post-scattering propagation. The propagation distance required for development of scintillation to a given magnitude depends on the scale-size of the irregularities, through the Fresnel-zone relation contained in the bracketed factor of Eq. (II-1), subject to the definitions (II-2).

At the outset of the work it was decided to treat ξ_o as a constant, using the value 1 km. This was based on observations by Hewish (1952) and Aarons and Guidice (1966) near the scintillation boundary; by Lansinger and Fremouw (1967) in the auroral zone, and by Kent and Koster (1966) in the equatorial region. It was recognized that this represented something of a compromise, ignoring some small variation of scale-size with latitude. As stated in the project proposal, "A better empirical formula would allow at least for some variation in scale-size (Fremouw and Lansinger, 1967; Singleton, 1969) and in axial ratio (Kent and Koster, 1966)."

The matter of axial ratio has been discussed above. Regarding scale-size, it was thought that treating it as a constant would not have an important effect on calculating average scintillation index. During the course of the modeling, however, it was found to be more important than anticipated. It is particularly so for predicting frequency dependence of scintillation. Therefore, near the end of the work, a small step was taken toward more sophisticated modeling than that proposed--namely, treating scale-size as well as the fluctuation of electron density as a latitudinal variable. The model selected for irregularity scale-size, ξ_o, which is considered rudimentary in comparison with that for irregularity strength, ΔN, is described in Section II-C-5.

2. Selection of Data

The essence of the modeling procedure was to postulate a model for ΔN (and for ξ_o, as discussed above), to insert the model values in Eq. (II-5) along with the other parameters needed, and then to employ Eqs. (II-5) and (II-1) to calculate the value of S expected for a given set of published scintillation observations. In this manner, the model was tested and improved. Thus, a time-consuming but very necessary step in the procedure was to select published data that would be useful for model testing.

Given the time and funds available, it was known to be feasible to test the model against about ten sets of observational data, and it was important that the sets be selected judiciously. The first step in this process was to inspect and categorize approximately seventy-five papers and reports on scintillation observations,* about fifty of which had been accumulated prior to commencing the work. The remainder were more recent papers, gleaned from scanning appropriate journals and symposium proceedings.

About fifty papers were found, dating from 1958 to 1971, that treated some aspect of scintillation morphology. These were inspected more carefully and about twenty were chosen for closer review and more detailed categorization. The most common reason for discarding the others was that the author(s) used a subjective scintillation index and provided no basis for relating it to the quantitative indices defined by Briggs and Parkin (1963). Table 1 shows the papers retained, categorized according to the latitudinal regime(s) of the observations and the scintillation dependence(s) that might be tested with each paper.

Its appearance in Table 1 does not necessarily mean that a paper is very useful for direct quantitative model testing. Some have been retained in the table even if an uncalibrated, subjective index was used by the author, if the paper falls in a sparsely populated category. This is true expecially at equatorial and polar latitudes. Some such papers might become useful for modeling if the index used can be calibrated against a quantitative one; this would be useful, for instance, for modeling sunspot dependence in the equatorial region, where long-term observations have been carried out, but only in terms of a subjective index.

---

*These papers are listed in five major categories in Appendix B, as a partial readers' guide to the scintillation literature.

Table 1

PAPERS FROM WHICH SELECTIONS WERE MADE FOR MODELING

DEPENDENCE	EQUATORIAL LATITUDES	MIDDLE LATITUDES	BOUNDARY LATITUDES	AURORAL LATITUDES	POLAR LATITUDES
LATITUDE		Yeh & Swenson (1964) Whitney, Allen, Aarons (1967) * JSSG (1968) Aarons, Mullen, Whitney (1969) * Preddey (1969)	Aarons, Mullen, Basu (1963) * Aarons, Mullen, Basu (1964) Basu, Allen, Aarons (1964) Yeh & Swenson (1964) Whitney, Allen, Aarons (1967) * JSSG (1968) Aarons, Mullen, Whitney (1969) * Preddey (1969) Aarons & Allen (1971)	Little, Reid, Stiltner, Merritt (1962) Liszka (1964a)	Frihagen (1969) Whitney, Allen, Aarons (1967)
TIME	Koster (1958) Koster & Wright (1963) * Koster (1968) Bandyopadhyay & Aarons (1970) Aarons, Whitney, Allen (1971)	Yeh & Swenson (1964) Whitney, Allen, Aarons (1967) * Preddey (1969) * Preddey, Mawdsley, Ireland (1969)	* Lawrence, Jespersen, & Lamb (1961) Aarons, Mullen, Basu (1964) Yeh & Swenson (1964) Whitney, Allen, Aarons (1967) Aarons, Mullen, Whitney (1969) Preddey, Mawdsley, Ireland (1969) * Preddey (1969) Aarons & Allen (1971)	* Little, Reid, Stiltner, Merritt (1962) * Fremouw (1966)	Frihagen (1969) Whitney, Allen, Aarons (1967)
SEASON	Koster (1963) Koster & Wright (1963) * Koster (1968)	Yeh & Swenson (1964) Preddey (1969) Preddey, Mawdsley, Ireland (1969)	Aarons, Mullen, Basu (1964) Yeh & Swenson (1964) Preddey, Mawdsley, Ireland (1969)	Fremouw (1966)	
SUNSPOT NUMBER	Koster (1958) Koster & Wright (1963)	Yeh & Swenson (1964)	Briggs (1964) Yeh & Swenson (1964)	Little, Reid, Stiltner, Merritt (1962) Fremouw (1966)	
FREQUENCY			Lawrence, Jespersen, Lamb (1961) Basu, Allen, Aarons (1964) Aarons, Allen, Elkins (1967)	Little, Reid, Stiltner, Merritt (1962) Fremouw (1966) * Lansinger & Fremouw (1967)	
AZIMUTH AND/OR ELEVATION		JSSG (1968)	Lawrence, Jespersen, & Lamb (1961) Basu, Allen, Aarons (1964) Jesperson & Kamas (1964) Yeh & Swenson (1964)	Little, Reid, Stiltner, Merritt (1962)	

* Employed in refinement and/or quantitative testing of the model.

The entries in Table 1 that actually were used for quantitative refinement and/or testing of the model are identified by asterisks. Initial selections were made with an eye to evaluating as many scintillation dependences over as great a range of geomagnetic latitude as possible. Some selections were changed during the course of the work, as model needs and the value of data sets clarified.

Again, the number of data sets used was limited by time and funds available. Some improvement in the model developed in this work probably could be achieved by use of additional data sets appearing in Table 1. A discussion of alternatives for more refined (and therefore more accurate and more broadly useful) modeling appears in Section IV.

B. The Approach to Modeling

If all scintillation observations were made under identical and simple experimental conditions, there would be little need to perform the extensive model-building calculations carried out on this project. In particular, the situation would be most simple if all observations were performed with the transmitter at the receiver's zenith on a frequency that encountered only weak, single scatter and if such observations were available for all latitudes, times, etc., of interest. In this situation, subject to the assumptions described in Section II-A-1, it would be possible to calculate ΔN directly from measurements of scintillation index, S, via Eqs. (II-1) and (II-5). The result could then be used for the reverse calculation to estimate the magnitude of scintillation in an arbitrary observing situation.

In practice, the world's large collection of scintillation data has been obtained under conditions far from the above ideal. First, a large majority are given only in terms of subjective indices that are difficult if not impossible to relate to theory. Second, a great many observations

have been performed at 40 and 54 MHz, at which frequencies the condition of weak, single scatter often is violated. Third, the observations are necessarily made under a variety of elevation angles, magnetic aspect angles, and other geometrical factors. Finally, various workers have performed different types of averaging and have sorted and displayed their data in a variety of ways.

Under the above circumstances, the most practical approach to modeling is to postulate the parameters of the scattering irregularities to be modeled--in our case, primarily their strength, ΔN--and then to calculate the scintillation index to be expected as a check on the postulated model. This was the approach taken, and the calculations were performed with an eye to reproducing or simulating the manner in which the actual data were obtained and treated.

The transmitter and receiver locations (and motions, if any) were chosen to be representative of the actual ones, the magnetic field geometry was accounted for on the basis of a dipole model, and other experimental circumstances were considered. After the scintillation index was calculated, averages were performed in a manner identical or similar to those performed by the observer on the actual data. The final result then was compared with the reduced data presented in the observer's paper or report.

The scintillation index first calculated in the program is the S developed by Briggs and Parkin (1963), which they later called S_4. The program used in modeling also converted S to any of the other three indices defined by Briggs and Parkin, on demand. Briggs and Parkin's four indices are defined as follows, where A is the real signal amplitude and $< >$ indicates averaging:

$$S_1 \triangleq \frac{\langle |A - \langle A \rangle| \rangle}{\langle A \rangle} = 0.42\ S$$

$$S_2 \triangleq \frac{\langle (A - \langle A \rangle)^2 \rangle^{1/2}}{\langle A \rangle} = 0.52\ S$$

$$S_3 \triangleq \frac{\langle |A^2 - \langle A^2 \rangle| \rangle}{\langle A^2 \rangle} = 0.73\ S \qquad \text{(II-8)}$$

$$S_4 \triangleq \frac{\langle (A^2 - \langle A^2 \rangle)^2 \rangle^{1/2}}{\langle A^2 \rangle} = S \quad .$$

The version of the program released to NASA calculates S_2 (the fractional rms fluctuation in amplitude) and S_4 (the fractional rms fluctuation in power).

The papers and reports used for quantitative modeling gave scintillation magnitude either as one of the above four indices or as some other index calibrated in terms of one of the above. In the latter case, the quoted index was converted to one of the above for comparison with the calculations. The data were tabulated in a form convenient for computer visual comparison against calculation, by scaling off values from a data-presentation figure in the report or paper (a two-dimensional graph, or, in some cases, a contour plot). The tabulation was committed to the computer on punched cards and then reproduced by the computer in graphical form. The computer plotted model-calculation results in the same form and on the same scale for comparison with the plotted data and for iterative improvement of the model. Several examples of such pairs of plots (observed and calculated scintillation indices) appear in Section II-D.

The initial model used for the first tests against observed scintillation index was that suggested in the project proposal. In terms of the notation used in Eqs. (II-2), (II-3), (II-5), and (II-6),

it contained the following parameters describing the scintillation-producing, F-layer irregularities of electron density: $\xi_o = 1$ km, $a = 10$, $h = 350$ km, $\Delta h = 100$ km, and $\Delta N = \Delta N_e + \Delta N_m + \Delta N_h$.

The three terms specifying ΔN are equatorial, mid-latitude, and high-latitude contributions to the rms fluctuation of electron density, respectively. As given in the proposal, they were of the following form:

$$\Delta N_e = K_e(1 + K_{er}R)\left[1 - K_{es}\cos\frac{\pi}{91}(D + 10)\right] \left[e^{-t^2/T_e^2} + e^{-(t-24)^2/T_e^2}\right]_e e^{-\lambda^2/\lambda_e^2} \qquad \text{(II-9)}$$

$$\Delta N_m = K_m(1 + K_{mt}\cos\frac{\pi t}{12}) \exp\left[-\frac{(\lambda - \lambda_o)^2}{\lambda_m^2}\right] , \qquad \text{(II-10)}$$

and

$$\Delta N_h = K_h\left[1 + \text{erf}\left(\frac{\lambda - \lambda_b}{\lambda_h}\right)\right] \qquad \text{(II-11)}$$

where

$$\lambda_b = \lambda_1 - \lambda_r R - \lambda_t \cos \pi t/12 \qquad \text{(II-12)}$$

and

$$\lambda_h = K_h\lambda_b \ . \qquad \text{(II-13)}$$

The independent variables in the above model for ΔN are the following:

R = Mean sunspot number

D = Day of the year

t = Time of day, in hours

λ = Geomagnetic latitude.

The characteristic time T_e and the subscripted K's and λ's not otherwise defined above are constants to be evaluated by comparison of model-based

calculations of scintillation index against observed values. The initial values chosen for testing were as follows:

$K_e = 1.3 \times 10^9 \text{el/m}^3$, $K_{er} = 0.02$, $K_{es} = 0.5$, $T_e = 4$ hrs , $\lambda_e = 12^o$;

$K_m = 1.5 \times 10^9 \text{el/m}^3$, $K_{mt} = 0.5$, $\lambda_o = 35^o$, $\lambda_m = 10^o$;

$K_h = 3.2 \times 10^9 \text{el/m}^3$, $\lambda_1 = 70^o$, $\lambda_r = 0.01^o$, $\lambda_t = 10^o$, $K_{h\lambda} = 0.1$.

The above model, including most of the initial constants, was postulated on the basis of the qualitative review of the scintillation literature by Fremouw and Bates (1971). It is essentially empirical, but there is some geophysical basis for its general form. In particular, describing ΔN by means of three rather independent terms based on geomagnetic latitude is quite reasonable in the light of ionospheric knowledge.

There is a widely known ionospheric region lying within about $\pm$ 15 degrees of the geomagnetic equator that has unique properties. It is essentially coincident with that region in which the geomagnetic field lines that reach the ionosphere return downward without penetrating above it. In contrast, at middle latitudes, the field lines penetrate the ionosphere and return to the opposite hemisphere, again penetrating the (conjugate) ionosphere.

At high latitudes, the field lines penetrate the ionosphere and continue to great altitude, where they are distorted by the solar wind and may even merge with interplanetary field lines. Solar and magnetospheric-tail processes, such as precipitation of auroral-producing and other particles, are dominant forces on ionospheric dynamics in this region. The characteristics of these three latitudinal regimes, as they impact on the production and behavior of ionospheric irregularities, have been reviewed by Elkins (1969).

The transition between the middle-latitude and the high-latitude ionosphere occurs in a rather complicated region (in the vicinity of 60^{o} geomagnetic latitude, but with the latitude varying considerably with time of day and solar and geomagnetic activity) that is bounded by the main ionization trough (Muldrew, 1965) and the auroral oval (Feldstein and Starkov, 1967). For scintillation morphology, the transition is characterized by sometimes sharp increases in index poleward of the boundary, as compared with equatorward of the boundary (Kent, 1959; Yeh and Swenson, 1964; Kaiser and Preddey, 1968).

For modeling of average scintillation, it is necessary to know the average effect of such abrupt transitions in scintillation magnitude at a latitude that may vary. To this end, let us suppose that a single realization of the F layer contains a latitudinal transition in rms electron-density fluctuation that can be described as a step function whose argument is a random variable with a gaussian distribution. That is, let

$$\Delta N_h = \langle \delta N \rangle$$

and let

$$\delta N = H(\lambda - \lambda_t) = \begin{cases} 0 \text{ for } \lambda < \lambda_t \\ 1 \text{ for } \lambda \geq \lambda_t \end{cases}$$

where λ_t is normally distributed with mean λ_b and variance λ_σ^2. Then

$$\Delta N_h = \frac{1}{\sqrt{2\pi}\,\lambda_\sigma} \int_{-\infty}^{\infty} H(\lambda - \lambda_t) \exp\left[- \frac{(\lambda_t - \lambda_b)^2}{2\lambda_\sigma^2} \right] d\lambda_t$$

$$= \frac{1}{\sqrt{2\pi}\,\lambda_\sigma} \int_{-\infty}^{\lambda} \exp\left[- \frac{(\lambda_t - \lambda_b)^2}{2\lambda_\sigma^2} \right] d\lambda_t \quad . \tag{II-14}$$

Noting that the right side of Eq. (II-14) approaches unity for $\lambda \to \infty$, and changing the variable of integration to $x = \frac{\lambda_t - \lambda_b}{\sqrt{2}\,\lambda_\sigma}$, we have

$$\Delta N_h = 1 - \frac{1}{\sqrt{\pi}} \int_y^\infty \exp\,[-x^2]\,dx$$

where $$y = \frac{\lambda - \lambda_b}{\sqrt{2}\,\lambda_\sigma} ,$$

so that $$\Delta N_h = 1 - \frac{1}{2}\,\mathrm{erfc}\; y = \frac{1}{2}\left[1 + \mathrm{erf}\left(\frac{\lambda - \lambda_b}{\sqrt{2}\,\lambda_\sigma}\right)\right] . \qquad \text{(II-15)}$$

Eq. (II-15) is the basis for the error-function form of Eq. (II-11). The trends in the location of the boundary latitude are given by Eq. (II-12). The error-function form in fact turns out to describe rather well the average increase in scintillation with increasing latitude in the boundary region.

The entire empirical basis for the initial model was described in the project proposal and can be found in the Fremouw and Bates review. Most of its features are consistent with Elkins' 1969 summary of scintillation morphology, in his Table 8. Briefly, quoting from the proposal:

> "Average scintillation level can be divided into components that depend primarily on latitude and time. In a narrow band of latitudes centered on the geomagnetic equator, F-layer scintillations are primarily a nighttime phenomenon, varying with season and with epoch of the solar cycle. At midlatitudes, there is a variation with time of day and with latitude but apparently no variation with season or solar activity. High-latitude scintillation shows a sharp equatorward boundary that depends on time of day and solar activity. Poleward of the boundary, scintillation is always strong, showing little diurnal or seasonal variation, some variation with latitude, and possible variation with solar epoch."

For the most part, the changes in the initial model that came about through iterative testing against published observations were in the nature of evaluating the various constants that appear in Eqs. (II-9) through (II-13). Some changes in form were made, however--most notably, the addition of a fourth term in the ΔN model to account for what is believed to be aurorally associated scintillation. The resulting model is presented in Section II-D. Comparisons are also made there of predicted scintillation index and the observations used for model testing.

C. Calculational Procedure

1. Mid-Latitude ΔN Term

The first term of the ΔN model to be tested was the mid-latitude term, because of its simple form. Referring to Eq. (II-10), it is seen to consist of a simple diurnal variation and a guassian latitudinal behavior. It contains no seasonal or sunspot-number dependence because there is no clear evidence for such trends at middle latitudes.

The data of Singleton (1969) show slight summer and winter increases in mid-latitude scintillation as compared with that at the equinoxes (his Figure 2) for the year 1965. Preddey, Mawdsley, and Ireland (1969), however, present a somewhat more extensive collection of mid-latitude data (their Figures 3 through 7), and this behavior does not appear consistent. We conclude that such a seasonal dependence is not a strong, persistent feature of mid-latitude scintillation, and it is not included in our model.

Elkins (1969) lists a positive sunspot variation for mid-latitude scintillation in his summarizing table, but the supporting papers quoted (in his Table 4b) are reports of observations near and through the scintillation boundary region and not through the mid-latitude ionosphere, in the sense used in this report. In fact, there

seem to be no continuous, long-term observations of true mid-latitude scintillation reported in the literature. The question is regarded as open but of relatively little significance for systems applications because of the generally low level of scintillation at middle latitudes.

The latitudinal dependence of scintillation in the mid-latitude regime is most evident in the data of Preddey (1969), and they were used for testing this feature of the model. The data were obtained by observing the 40-MHz beacon on satellite BE-B with a shipboard receiver during voyages from New Zealand to McMurdo Sound, Antarctica, and from New Zealand to islands in the South Pacific. Thus, they were useful for testing both the mid-latitude and the high-latitude terms of the ΔN model. The data were given in terms of S_4 as defined in Eq. (II-8) and so were particularly convenient for model testing.

Preddey presented his data in two ways. First, he plotted individual points that represented an average scintillation index for an entire satellite pass when the ship was at a given geomagnetic latitude, using data only for satellite elevation angles greater than 15°. Second, he plotted curves representing the scintillation index averaged over 5° intervals of the point at which the line of sight penetrated the ionosphere. The latter presentation was more appropriate for our model testing. Preddey presented separate curves for daytime and for nighttime observations (his Figures 1 and 2).

To simulate Preddey's observing and data-reduction procedure, we had to perform a time average and two kinds of spatial averaging. First, the value of ΔN was obtained by averaging the model over 8.5 hours and over 5° of geomagnetic latitude. Next we had to account for the fact that observations for any given location of the ionospheric penetration point--and hence the 5° average values--contained contributions from a range of azimuths and elevations corresponding to a number of

satellite passes when the ship was located at different places. To do this, we averaged the scintillation index given by Eq. (II-1) over all azimuths and over elevation from 15^{o} to 90^{o}, holding ΔN constant at the 5^{o} average value.

The latter averaging accounted for the range of magnetic aspect angles encountered, by means of the quantities β and ψ that appear in Eq. (II-3) and the geomagnetic field model included in the computer program. It also accounted for the range of Fresnel distance, z, defined in Eq. (II-4) and calculated from Eqs. (II-7), and for the range of incidence angle, i, computed from Eq. (II-6). The azimuth-elevation averaging was done in such a manner as to simulate several north-south passes, at different longitudes relative to that of the receiver, of a satellite in a circular orbit at an altitude of 1000 km. This adequately approximates the behavior of BE-B, which has a perigee of 888 km and an apogee of 1075 km in a 79.6^{o}-inclination orbit, according to a recent NASA Satellite Situation Report.

Following the above procedure, the average nighttime scintillation index was calculated for each 5^{o} of geomagnetic latitude between 17.5^{o} and 42.5^{o}. To simplify the first calculations, only the mid-latitude term of the model was used in calculating ΔN. The values listed in Section II-B were used for the initial model parameters. All but K_m had been estimated from the qualitative scintillation review by Fremouw and Bates (1971). The initial value for K_m was chosen, essentially arbitrarily, to be on the order of 1% of the presumed background electron density. The value of 1.5×10^{9} el/m^3 was immediately found to be too large by a factor of about three.

Aside from K_m, only small changes in mid-latitude model parameters were necessary. In two successive calculations, an acceptable fit to the Preddey data was obtained with values for λ_o and λ_m of

32.5^{o} and 7^{o}, respectively. Using only Preddey's nighttime data, it was not actually possible to independently evaluate K_m and the mid-latitude, diurnal-variation parameter, K_{mt}. What was obtained was the following quantity:

$$K_m (1 + 0.8 K_{mt}) = 7.5 \times 10^8 \text{ el/m}^3 \qquad \text{(II-16)}$$

where the 0.8 came from averaging $\cos \frac{\pi t}{12}$ over the hours 19.5 to 04.0, in accordance with Preddey's time averaging of his data.

To carry out the desired separation of parameters, the next set of calculations performed was designed for testing the model's diurnal behavior against that of data presented by Preddey, Mawdsley, and Ireland (1969). These data also were obtained from observations of the 40-MHz beacon aboard BE-B, in this case from a series of fixed, ground-based receivers. Most appropriate for our purpose were data obtained from the northern (equatorward) half of the sky at Brisbane, Australia (magnetic invariant latitude = 35.5^{o}).

The calculations were similar to, but somewhat simpler than, those described above for the Preddey data, because of the fixed receiver. In essence, the scintillation index was calculated according to Eq. (II-1) and averaged over azimuth from 0 to $\pm 90^{o}$ and over elevation from 15^{o} to 90^{o}. The averaging again was done in such a manner as to simulate that obtained from a number of passes over and to the east and to the west of the station by satellite BE-B. The satellite position was incremented in earth-centered angle along a great circle, which reproduces the averages obtained from using equal time increments in data reduction, as actually performed by Preddey, Mawdsley, and Ireland (1969).

The above-described average scintillation index was calculated for every two hours from 02 to 24 hours and compared with points scaled

from Figure 7 of the paper by Preddey et al. for a day in June, 1965, the same month as (but a year earlier than) that in which the Preddey data described earlier were collected. The data of Preddey et al. were given in the paper in terms of a subjective index, but they were converted to S_4 by means of a calibration formula provided by the authors. On the basis of Eq. (II-16) and the earlier assumption that $K_{mt} = 0.5$, a value of 5.4×10^8 el/m^3 was used for K_m in the calculation. These values gave quite an acceptable fit to the Brisbane data.

The above calculations completed the first iteration of testing and quantifying the mid-latitude term of the ΔN model. It remained unchanged throughout the subsequent calculations, except for small adjustments of the constants to provide better agreement with high-latitude and equatorial data, which will be discussed later. The final model parameters and graphical comparisons of the calculations with published data are given in Section II-D.

2. Scintillation-Boundary ΔN Term

As compared with the mid-latitude term, a good deal more difficulty was encountered and many more calculations were required for modeling ΔN near and poleward of the scintillation boundary. The first paper used--to evaluate the basic latitudinal dependence of scintillation in the boundary region--was that of Aarons, Mullen and Basu (1964). In this paper, the authors presented results of observing the 54-MHz beacon on Transit 4A from a single receiver location--Sagamore Hill, near Boston, Massachussetts (geomagnetic latitude = 54°).

The calculational procedure for testing the model against the data of Aarons et al. was similar to that used for modeling mid-latitude scintillation; the main difference was in the manner of averaging. The observations used were presented as measurements of S_3, as defined in

Eq. (II-8), averaged over many satellite passes within a 16^{o} longitude swath centered on the receiver longitude. The presentation was of average scintillation index vs. latitude of the ionospheric penetration point (Figure 1 of the paper). The data we used were averaged over all hours of the day and over the one-year observing period, for quiet and moderate magnetic activity periods (Fredericksburg K = 0,1,2).*

To simulate the observing and data-reduction procedures of Aarons and his coworkers, we calculated S_3 over the appropriate range of subionospheric latitudes and averaged the values over $\pm 8^{o}$ of longitude relative to the receiving station. The transmitter was assumed to be at an altitude of 940 km; this approximates the geometry provided by Transit 4A, which is listed as having a perigee of 878 km and an apogee of 997 km in a recent NASA Satellite Situation Report.

In the first boundary-region calculations, the equatorial and mid-latitude terms were set to zero for simplification. The initial values for the model parameters appearing in Eqs. (II-11), (II-12), and (II-13), as quoted in Section II-B, were found generally to place the average location of the scintillation boundary too far poleward. After several trial calculations, an excellent fit to the data was obtained in the boundary region, with the following parameter values:

$$K_h = 2 \times 10^{9}\ \text{el/m}^3 \quad , \quad K_{h\lambda} = 0.2 \quad , \quad \text{and} \quad \lambda_1 - 44\lambda_r = 61.6^{o} \qquad \text{(II-17)}$$

where the value 44 is the sunspot number assumed for the calculations.

---

*More sophisticated modeling would take into account variations in scintillation index with such geophysical variables as magnetic activity. In doing so, care would be needed not to account doubly for behavior such as diurnal and seasonal variations. In the present work, we were aiming only at describing average scintillation as a function of the latter type of variable, independently of geophysical variables that might be invoked to identify departures from this average behavior.

As in all calculations, the sunspot number was taken from reports of Solar-Geophysical Data, published in Boulder, Colorado by the Department of Commerce, selected as representative of the observing period involved (in this case, for the year beginning July 1, 1961).

With the above values inserted in the model, the calculations were redone with the addition of the mid-latitude term as evaluated from the data of Preddey and of Preddey et al. As expected, addition of the mid-latitude term did not appreciably affect the data fit in the boundary region. It improved the fit to the south of the receiving station, but the model gave generally smaller values of scintillation index there than those reported from the observations.

The above implies that there is in fact an increase in ionospheric irregularity toward the south from about geomagnetic latitude 50^{o} in the eastern North American sector, which had not been recognized previously. Indeed, the effect apparently was at least as strong in the data of Aarons et al. as in the data on which the mid-latitude term of the model was based (i.e., the data of Preddey and Preddey et al.).

As is seen in Eq. (II-17), the modeling performed on the basis of the Aarons, Mullen, and Basu data did not permit evaluation of solar-cycle migration of the scintillation boundary, nor did it permit evaluation of its diurnal variation. As a first attempt at evaluating the latter two dependences, testing was performed against the data of Lawrence, Jespersen, and Lamb (1961), who had conducted observations of the radio star, Cygnus A, for all hours of the day in an epoch of much larger sunspot number.

Lawrence et al. observed Cygnus A following its rise at Boulder, Colorado (geomagnetic latitude = 48.9^{o}) for "three or four hours each day" from February, 1958 through February, 1959. In this way, they observed in the same part of the sky for all hours of the

day, (albeit on different days). They observed on both 53 and 108 MHz, which, it was hoped, would provide a model test of frequency dependence. However, the calculations showed that the assumption of weak, single scatter was questionable near midnight even for 108 MHz, under the high-sunspot-number (184) conditions involved. This means that the calculations would be invalid for most hours at 53 MHz, so model testing and evaluating was limited to 108 MHz. The data were given as the square of S_2, as defined in Eq. (II-8), so the index S_2 was calculated from the model.

To approximate the observing conditions, the transmitter was taken to be at very great distance at the latitude and longitude corresponding to the celestial coordinates of Cygnus A at the sidereal time equivalent to two hours after its rise at Boulder. This corresponded to a northeasterly azimuth at an elevation angle just under twenty degrees. Holding the geometry fixed, time was simply advanced in one-hour increments through twenty-four hours in the subroutine containing the ΔN model. Since the mid-latitude and boundary-region model terms contain no seasonal dependence, it was not necessary to account for the fact that the observation for each hour was made on a different day of the year. (The effect of the equatorial term, which does contain a seasonal dependence, is totally negligible at the latitude of Boulder.)

Using the Boulder data, it was not very difficult to evaluate λ_t and to separate λ_l and λ_r, consistent with Eq. (II-17). However, this procedure alone did not represent a strong test of the model because it did not involve any redundant calculations for consistency checking. To provide such a consistency check, the data of Preddey (1969) again were invoked--for the boundary region at night and during the day at two different epochs of a solar cycle (sunspot number = 30 and 103). The calculational procedure was exactly as described for the Preddey data in Section II-C-1.

These calculations revealed that the starting model--particularly Eq. (II-12)--did not completely describe the sidereal and solar-cycle dependences of the scintillation-boundary latitude. In particular, Preddey's data (his Figures 1 and 2) showed a greater diurnal variation in boundary latitude when the sunspot number was 103 (January, 1968) than when it was 30 (June, 1966). To describe this behavior, the last term in Eq. (II-12) was modified to make the diurnal excursion of the boundary latitude a function of sunspot number. The form of the modification is given in Eq. (II-19).

3. Auroral-Oval ΔN Term

At this point in the procedure, the model for ΔN still contained only three terms, one each for equatorial, middle, and high latitudes. To test this form at a latitude well up on the scintillation boundary--in the auroral zone, in fact--the data of Fremouw (1966) were invoked. The plan was to use his observations of the diurnal variation of 68-MHz and 223-MHz scintillation index at College, Alaska, in 1965 (his Figure 11). These observations were taken near solar minimum (sunspot number = 15), and they were to be compared against the 223-MHz, solar-maximum data of Little, Reid, Stiltner, and Merritt (1962), obtained at the same location in 1957-58 (sunspot number = 200).

Little and his coworkers had devised a subjective scintillation index for use with their 223-MHz observations and then calibrated it against S_3 as defined in Eq. (II-8). The calibration curve is quite nonlinear and contains considerable uncertainty for very small values of scintillation index. Fremouw resumed 223-MHz observations at College (geomagnetic latitude = 64.7°) several years after Little et al. had ceased theirs, and he found the level of scintillation greatly diminished. He then augmented the 223-MHz effort with observations at 68 MHz, continuing to use the index of Little et al.

As a result of the uncertainty in the index for small values and the very strong dependence of auroral-zone scintillation on sunspot number, the 223-MHz observations of Fremouw were found of little value for quantitative modeling. An exception, to which we shall return in Section II-C-5, consists of carefully edited samples of the data reduced without resort to a subjective index (Lansinger and Fremouw, 1967). Presently, we are concerned only with Fremouw's 68-MHz data.

Both Little et al. and Fremouw used interferometers to observe radio stars at College, Alaska. Thus, the basic procedure in calculation was similar to that used for the Boulder data, as described in Section II-C-2. However, at College the radio star used (Cassiopeia A) is circumpolar. The Alaskan workers observed around the clock and then obtained the diurnal variation of scintillation index, independently of the local hour angle of the source, by averaging data for a given time of day through all days of the year.

The above data-reduction procedure was accounted for in the model calculations by coding an advance of sidereal time (and hence of the source's local hour angle) relative to solar time of day, at the rate of just under four minutes per day. The resulting values of S_3 for a given solar hour were then averaged through the year.

When the above procedure was applied to Fremouw's 68-MHz data, using the previously established parameters for the mid- and high-latitude terms of the three-term model for ΔN, reasonably good agreement was found. The average level of scintillation calculated was quite close to that observed, although the calculated diurnal variation was somewhat stronger than the observed. The latter discrepancy was simply suggestive of a need for minor parameter revision--a small decrease in the scintillation boundary latitude, coupled with a small decrease in the strength of the high-latitude term. It was decided to proceed immediately to the 223-MHz, solar-maximum data of Little et al.

The calculation procedure for the data of Little et al. was exactly as described above; the frequency and sunspot number were simply changed. The result, however, was quite different and somewhat surprising; the calculated values of S_3 were considerably too low, for all hours of the day. This result quantified a fact that had been realized only qualitatively at the outset of Fremouw's radio-star observations at College: that auroral-zone scintillation is very strongly dependent on sunspot number. It seemed unlikely that the proposed three-term model for ΔN could adequately describe scintillation behavior both at subauroral locations such as Boston and Boulder, and at auroral-zone locations such as College.

In the light of ionospheric knowledge, the least arbitrary way out of the above-described dilemma is a fourth term in the ΔN model, describing scintillation irregularities essentially coincident in latitude with the auroral oval. Such a term, therefore, was added after review of auroral morphology under both solar-maximum (Davis, 1961) and solar-minimum conditions (Stringer and Belon, 1967).

There followed a round of calculations seeking to optimize the parameters of the four-term model as it applied to auroral and subauroral scintillations. This involved iterative calculations and parameter adjustments based on the data of Preddey (1969); Aarons, Mullen, and Basu (1964); Fremouw (1966) and Little, Reid, Stiltner, and Merritt (1962). The model and the degree to which it can account for the observations is described in Section II-D.

4. Equatorial ΔN Term

The final term of the ΔN model to be tested and evaluated was the equatorial term, because it was desired to use data of Koster (1968), which were not available in the open literature and which were obtained

from the University of Ghana only after an unanticipated delay. There are many observations from the equatorial region in the open literature, but they are in terms of a subjective index that has not been calibrated against one of those defined in Eq. (II-8).

In view of the great range of scintillation activity encountered near the magnetic equator and of the nonlinear calibration curve that had been found for the subjective index of Little, Reid, Stiltner, and Merrit (1962), it did not seem satisfactory to employ the subjective equatorial index for quantitative modeling. It was therefore necessary to await arrival of the data of Koster (1968), which are in the form of S_3 as obtained by the Air Force Cambridge Research Laboratory technique (Whitney, Aarons, and Malik, 1969; Bischoff and Chytil, 1969).

The data used were presented in terms of contours of S_3 on a grid of date and time of day, from May 1967 through May 1968 (Koster's Figure 14). Values were scaled as a function of time of day on January 31 and as a function of day of the year at 0200 GMT (which is coincident with local standard time). The observations were of the 136-MHz beacon on the synchronous satellite Canary Bird and were made from Legon, Accra, Ghana (geomagnetic latitude = 9.4^{o}). The transmitter was essentially stationary, which was a most convenient situation for the modeling calculations, to the southwest of the receiver at an elevation angle of 75^{o}.

In the computations, the receiver and transmitter were held at fixed locations, the latter at synchronous altitude; the scintillation index, S_3, was calculated first as a function of time of day, with day of year held constant, and then as a function of day of year, with the time of day held constant. The sunspot number was assumed to be 107 for the calculation of diurnal variation (appropriate for January, 1968), and 97 for the calculation of seasonal variation (more representative of the one-year period from May 1967 through May 1968).

Referring to Eq. (II-9), it is seen that the originally proposed equatorial term for the ΔN model had a guassian diurnal variation that was symmetrical about midnight. Subsequently, however, it was noted that essentially all reports of equatorial scintillation show a rather rapid growth of activity in the post-sunset hours and a slower decay in the pre-sunrise hours (cf. Figure 20 of Aarons, Whitney, and Allen, 1971). Therefore, prior to beginning the equatorial calculations, the form of the equatorial model term was altered slightly to permit description of this diurnal asymmetry.

With the above modification introduced, the first calculation showed a promising fit to the diurnal data of Koster (1968), although the general strength of equatorial scintillation was considerably underestimated with the first choice of parameters. A revised choice for K_e resulted in a much better fit, and the observed seasonal dependence also was rather readily matched by the model. Unfortunately, no data have been obtained to permit direct testing of the latitudinal dependence of the equatorial term. However, the width of the equatorial disturbed region in the model has been set to provide a smooth transition to the mid-latitude data of Preddey (1969).

More important, no equatorial scintillation data in the form of a quantitative index such as those defined in Eq. (II-8) seem to be available over a sufficiently long period to evaluate sunspot-number dependence. We shall return to this deficiency of the present model in Section II-D.

5. Scale-Size Behavior

As discussed in Section II-A-1, it was supposed at the outset of this work that the size of the F-layer irregularities responsible for scintillation could be taken as a constant throughout the calculations.

This assumption was kept for the calculations described in Sections II-C-1 and II-C-2, using the value of 1 km for the distance over which the ionospheric spatial autocorrelation function drops to e^{-1} in a direction transverse to the geomagnetic field. As a check on this assumption, and as a means of evaluating the frequency dependence predicted by the model, calculations were prepared for comparison with two-frequency radio-star observations of Lansinger and Fremouw (1967) at College, Alaska.

Lansinger and Fremouw used some of the same data as those reported on by Fremouw (1966), but performed very much improved data reduction. The observations were of Cassiopiea A at 68 and 223 MHz, and Fremouw used them for a resumption of the studies begun by Little, Reid, Stiltner, and Merritt (1962) by scaling strip-chart records in terms of a subjective index devised by the earlier workers. In addition to strip-chart recording, however, some of the data were digitized and tape-recorded, making them much more amenable to quantitative analysis.

For a three-month period beginning in October of 1965, the tape-recorded data were carefully edited to avoid periods of interference, which was important for accurate use of the 223-MHz data because of the very low level of scintillation activity at so high a frequency near solar minimum. For the remaining data, the scintillation index S_4 was calculated for 223 MHz and 68 MHz directly from the definition given in Eq. (II-8). Whenever S_4 exceeded a threshold (0.04 at 223 MHz) set by system noise, the ratio of S_4 at 68 MHz to that at 223 MHz was calculated. Lansinger and Fremouw used the observed ratios to deduce an irregularity scale-size of about 600 meters for their auroral-zone location and noted a trend toward larger irregularities with increasing latitude.

For comparison with the data of Lansinger and Fremouw, the calculational routine described in Section II-C-3 for testing against the data of Fremouw and of Little et al. was modified. The most important modification consisted simply of performing the S_4 calculations once for each frequency and then taking the ratio. In addition, it was necessary to perform averaging over only three months rather than over a full year, as in the previous cases, when accounting for the change in source look angles from day to day for a given time of day (i.e., the asynchronism between solar and sidereal time). The result was plotted as a function of source hour angle rather than solar time of day, in order to simulate the authors' presentation (a modification of their Figure 2).

The result of the above calculation with the then-existing model, which assumed a fixed irregularity scale-size of 1 km, was about 30% larger than the scintillation-index ratio of 68 to 223 MHz observed by Lansinger and Fremouw. This discrepancy was judged unacceptable, and the calculations were redone using 600 meters for the transverse scale-size, with a much improved result.

Based on the foregoing experience with the auroral-zone scale-size, it was decided to abandon the simplification of taking the same value at all latitudes, substituting instead values measured at different latitudes. For the equatorial region the value of 300 meters was chosen, based on observations of Koster, Katsriku, and Tete (1966), and of Golden (1970). This choice has been further strengthened by comparison of calculated amplitude distributions with observed ones from a set of equatorial data supplied by NASA, as demonstrated in Section III-E.

At middle and scintillation-boundary latitudes (below the auroral zone) and at polar latitudes (above the auroral zone), values

of 1500 meters and 1000 meters, respectively, were used. In the former regime, the value was based on observations of Aarons, Allen, and Elkins (1967), together with a heuristic suggestion by Singleton (1969). In the latter regime, it was based on the observation by Lansinger and Fremouw (1967) that scale-size increases again poleward of the auroral zone.

The above scale-sizes were inserted in the computer program by means of a model for scale-size as a function of latitude that consists essentially of steps at particular geomagnetic latitudes. In order to avoid discontinuities, the steps are described by error functions whose widths are about six degrees. This model obviously is rudimentary as compared with that developed for the rms electron-density fluctuation in the F-layer. It is a considerable improvement over assuming a constant value for scale-size, however, especially as regards the frequency dependence of scintillation. The data fits shown in Section II-D were obtained using the described latitudinal model for scale-size, and its mathematical form will be given there, along with the final model for electron-density fluctuation.

D. The Resulting Model and Its Limitations

As a result of the procedure described in the foregoing sections, the following empirical model for scintillation-producing irregularities in the F-layer of the earth's ionosphere is put forth:

- Center height of the irregular layer = 350 km
- Thickness of the irregular layer = 100 km
- Ratio of scale-size along geomagnetic field to that transverse = 10
- Transverse scale-size (to e^{-1} spatial autocorrelation) = ξ_o
- Rms fluctuation of electron density (irregularity strength) = ΔN.

Mathematical expressions are given for ξ_o and ΔN in Eqs. (II-18) and (II-19), respectively, in terms of the following independent variables:

λ = Geomagnetic latitude in degrees

t = Local time of day in hours

D = Day of year out of 365

R = Sunspot number.

$$\xi_o = 300 + 600\left[1 + erf\left(\frac{\lambda - 12}{3}\right)\right] - 450\left[1 + erf\left(\frac{\lambda - 62}{3}\right)\right] + 200\left[1 + erf\left(\frac{\lambda - 69}{3}\right)\right] \text{ meters} \qquad \text{(II-18)}$$

$$\Delta N = \left(5.5 \times 10^9\right)\left(1 + 0.05R\right)\left[1 - 0.4\cos\left(\frac{D + 10}{91.25}\right)\right]\left\{\exp\left[-\left(\frac{t}{4}\right)^2\right] + \exp\left[-\left(\frac{t - 23.5}{3.5}\right)^2\right]\right\}\left\{\exp\left[-\left(\frac{\lambda}{12}\right)^2\right]\right\}$$

$$+ \left(6.0 \times 10^8\right)\left(1 + 0.4\cos\frac{\pi t}{12}\right)\left\{\exp\left[-\left(\frac{\lambda - 32.5}{10}\right)^2\right]\right\}$$

$$+ \left(2.7 \times 10^9\right)\left\{1 + erf\left[\frac{\lambda - 79 + 0.13R + (5 + 0.04R)\cos(\pi t/12)}{17.8 - 0.026R - (1 + 0.008R)\cos(\pi t/12)}\right]\right\}$$

$$+ \left(5.0 \times 10^7\right) R\left\{\exp\left[-\left(\frac{\lambda - 70 + 2\cos(\pi t/12)}{0.03R}\right)^2\right]\right\} \quad el/m^3 \qquad \text{(II-19)}$$

Comparisons of scintillation index calculated from the above model with the observations used in iterative evaluation of the model are shown in Figures 2 through 9, starting with equatorial observations and progressing generally poleward. This is followed, in Figure 10, by comparison of calculated values with a set of observed values not employed in development of the model. In all cases, observed values are shown as discrete points and calculated values are shown as smooth curves. The calculated curves are solid where the assumption of weak, single scatter

is satisfied ($\phi_o < 0.7$), and dashed where the assumption is questionable ($0.7 \leq \phi_o \leq 1.0$). Where the assumption is invalid ($\phi_o > 1.0$), no calculated value is given.

Comparison of calculated results with the observations of Koster (1968) appear in Figure 2, with the diurnal variation shown on top and the seasonal variation shown on the bottom. The fit is seen to be reasonably close for both types of behavior, where the assumption of weak, single scatter holds. The more abrupt rise of the observed values in the evening hours than those calculated could be accounted for by a change in form of the equatorial term of the ΔN model, and parameter adjustments could reduce other discrepancies. This hardly seems justified, however, in the light of two more serious limitations of the model at equatorial latitudes, which will now be discussed.

The first limitation stems from lack of an opportunity to test the model's predicted sunspot-number dependence of scintillation. There appear to be no long-term equatorial data available in terms of quantitative indices, although there remains the possibility of calibrating some earlier observation results in such terms (Koster, private communication). Thus, the equatorial term of the scintillation model may be considered relatively reliable under average ionospheric conditions for sunspot numbers on the order of 100 (typical of solar-maximum), but for other sunspot numbers it is only an untested estimate.

The second limitation referred to above probably is inherent in the average nature of the model, but is of some practical concern. In the past few years, instances of significant scintillation on surprisingly high frequencies (as high as 6 GHz) have been reported by equatorial observers (Kuegler, 1969; Craft, 1971; Christiansen, 1971; Skinner, Kelleher, Hacking, and Benson, 1971). The model developed in this work would not have predicted this turn of events, which apparently is

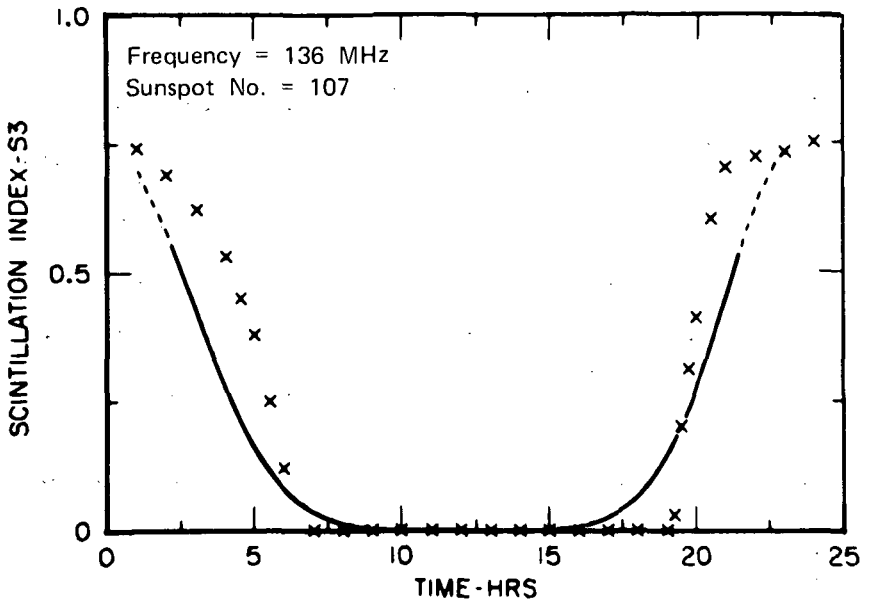

KOSTER (1968), DIURNAL

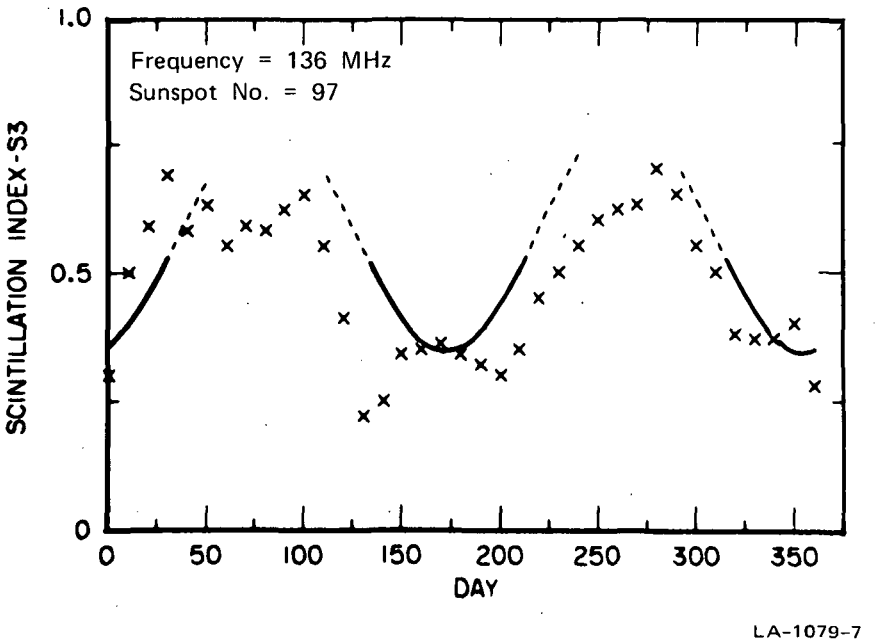

KOSTER (1968), SEASONAL

FIGURE 2 COMPARISON OF MODEL CALCULATIONS WITH GEOSTATIONARY-SATELLITE OBSERVATIONS FROM GHANA. As in all figures in Section II, the observations are shown as discrete points and the calculations as a curve. The curve is solid where an important assumption on which the calculations are based is valid, and dashed where the assumption is questionable. Where the assumption is invalid, no calculated results are given (see text).

not a manifestation of "average ionospheric conditions," but which still is of decided practical concern for communication systems.

At middle latitudes the model produced quite acceptable fits to the data of Preddey, Mawdsley, and Ireland (1969), and of Preddey (1969). Figure 3 shows the comparison of calculated diurnal variation of scintillation at middle latitudes, with the former data.

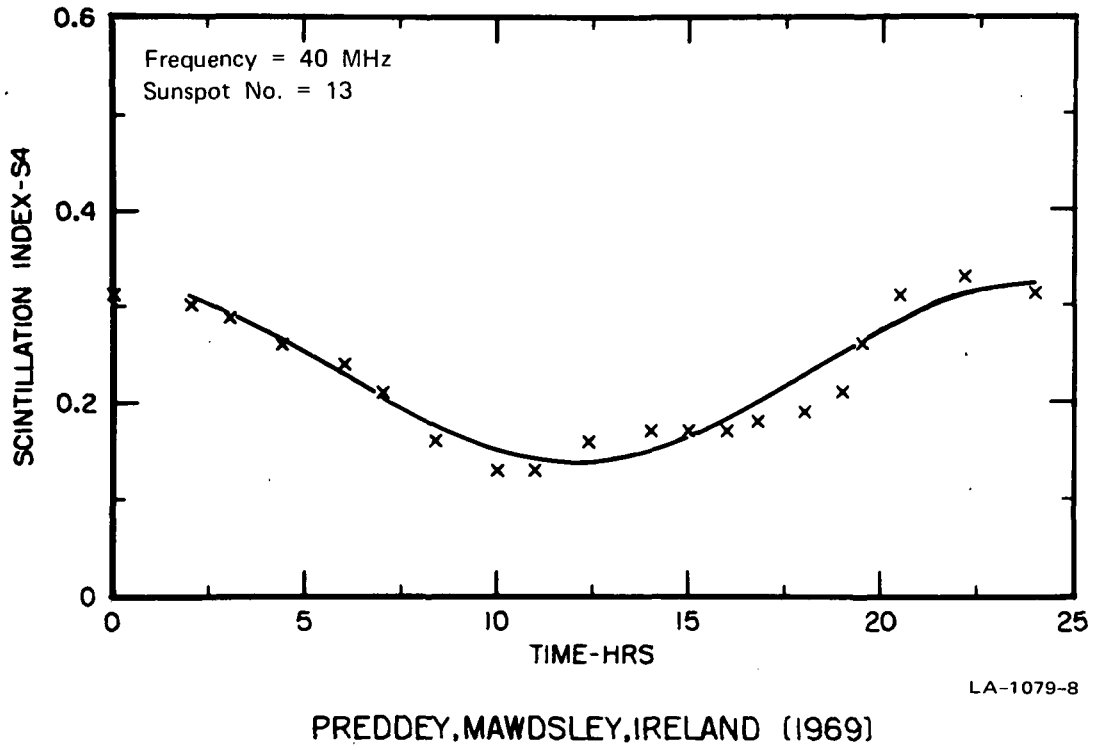

FIGURE 3 COMPARISON OF MODEL CALCULATIONS WITH HIGH-INCLINATION-SATELLITE OBSERVATIONS OF THE DIURNAL VARIATION OF SCINTILLATION FROM BRISBANE, AUSTRALIA

Figure 4 compares calculated and observed latitudinal dependence for daytime and for nighttime, using the data of Preddey (1969). The bars shown on the Preddey data points represent some of the few indications given in the literature, of variations from the average results reported. They indicate the range of day-to-day variations observed in scintillation index. (They are not measurement uncertainties.)

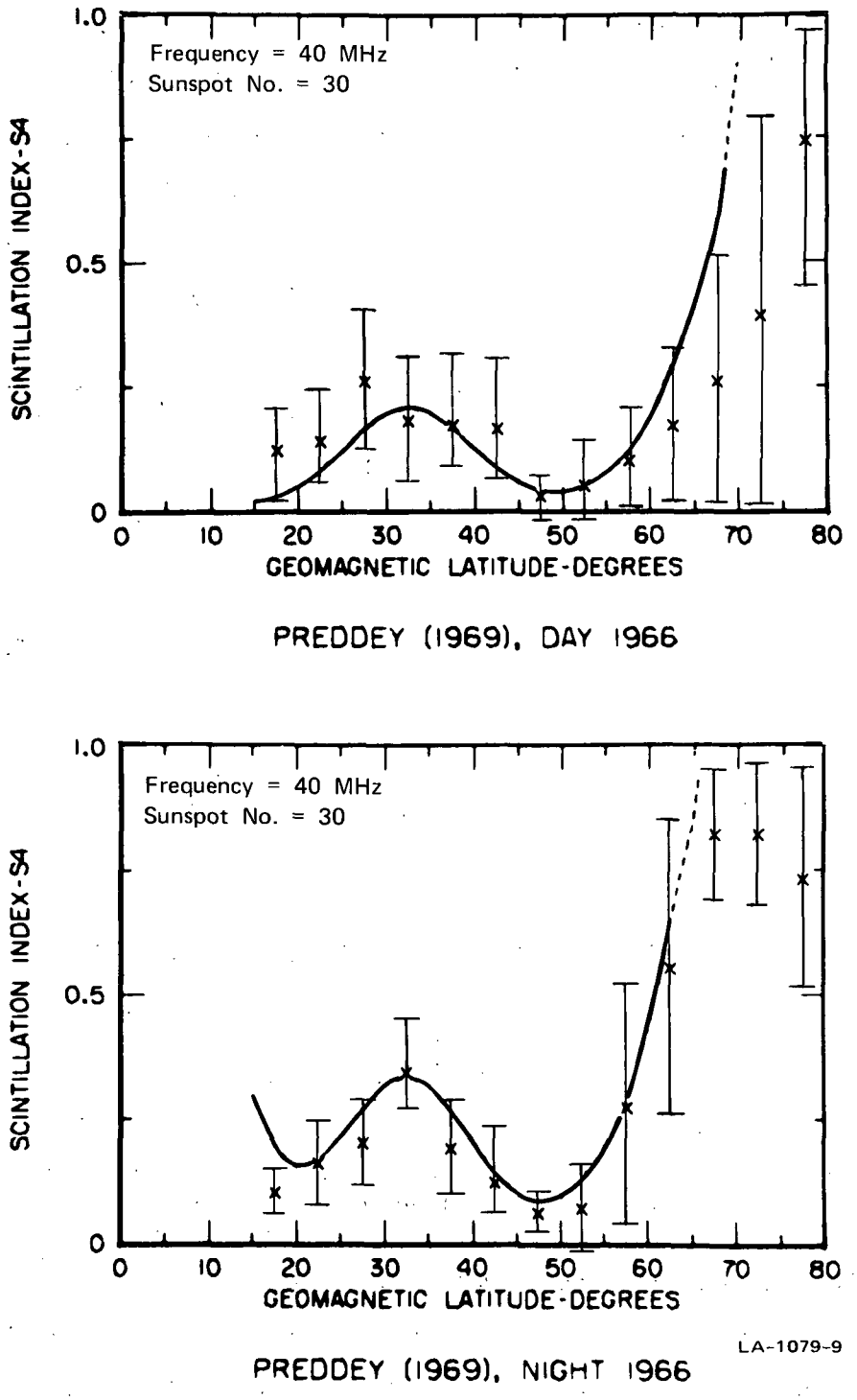

FIGURE 4 COMPARISON OF MODEL CALCULATIONS WITH HIGH-INCLINATION-SATELLITE OBSERVATIONS IN THE MIDDLE-LATITUDE AND SCINTILLATION-BOUNDARY REGIONS OF THE SOUTH PACIFIC, NEAR SOLAR MINIMUM.

Figure 4 also compares the calculated latitudinal dependence in the scintillation-boundary region with that observed by Preddey, under essentially solar-minimum conditions (sunspot number = 30). The fit is seen to be quite good at night--the time of most practical concern. The match is less satisfactory in the daytime, reflecting the dictates of data sets from other stations, notably the observations of Aarons, Mullen, and Basu (1964) and of Fremouw (1966).

Similar observations performed by Preddey near solar maximum (sunspot number = 103) are compared with boundary-region calculations in Figure 5. In general, the fit is not as close as for solar-minimum conditions, with the nighttime results again being better than those for the daytime. The mismatch is due largely to the dictates of the extreme solar-maximum (sunspot number = 184) data obtained by Lawrence, Jespersen, and Lamb (1961) at Boulder, Colorado, during the IGY.

Comparison of the calculated diurnal variation of 108-MHz scintillation with the Boulder data is given in Figure 6. In general, the fit is seen to be quite good, although there is some discrepancy both near noon and near midnight. The midday discrepancy is due to at least two causes. First, most midday scintillations at Boulder were ascribed by Lawrence, Jespersen, and Lamb to E-layer irregularities, on the basis of ionosonde data, whereas our model is for F-layer irregularities only. Secondly, the influence of the Preddey data shown in Figure 5 was to depress the calculated daytime scintillation index in the latitude region of the Boulder observations. Regarding the midnight discrepancy, little can be said because the calculations indicate breakdown of the weak, single scatter assumption even at 108 MHz in the Boulder IGY data. It will be recalled that the IGY coincided with the strongest solar maximum on record.

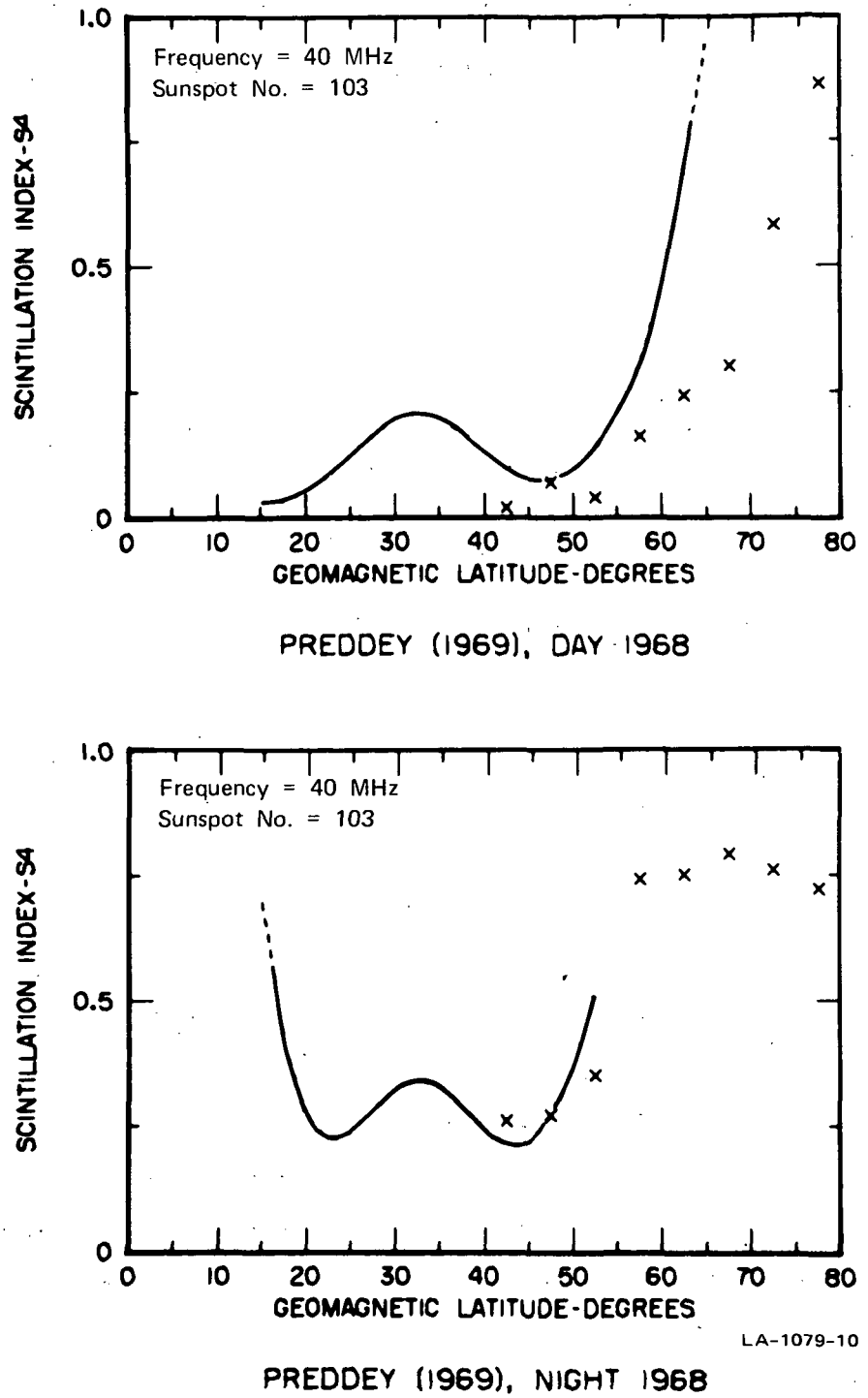

FIGURE 5 COMPARISON OF MODEL CALCULATIONS WITH HIGH-INCLINATION-SATELLITE OBSERVATIONS IN THE SCINTILLATION-BOUNDARY REGION OF THE SOUTH PACIFIC, NEAR SOLAR MAXIMUM

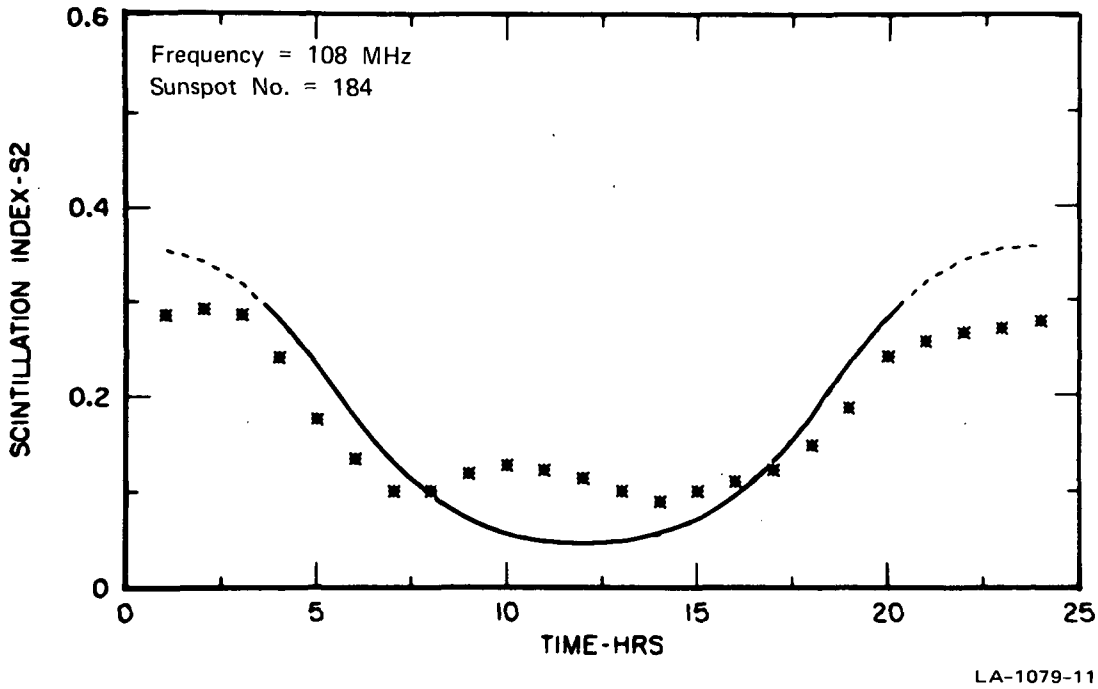

FIGURE 6 COMPARISON OF MODEL CALCULATIONS WITH RADIO-STAR OBSERVATIONS OF THE DIURNAL VARIATION OF SCINTILLATION FROM BOULDER, COLORADO

The scintillation model was tested against 13 data sets scaled from nine different papers and reports. Of these, one of the most disappointing comparisons of calculated results with observation was for the data of Aarons, Mullen, and Basu (1964), as shown in Figure 7. While a good fit was obtained in the scintillation-boundary region at an early stage of the modeling, incorporation of additional data--especially those of Preddey--caused a deterioration. It simply was not possible to maintain consistently good fits between the model and the various data sets.

Faced with the above condition, the modeling involved some compromise between different data sets, since there was little basis for evaluating relative data quality. It appears that a somewhat revised set of model parameters--especially in the scintillation-

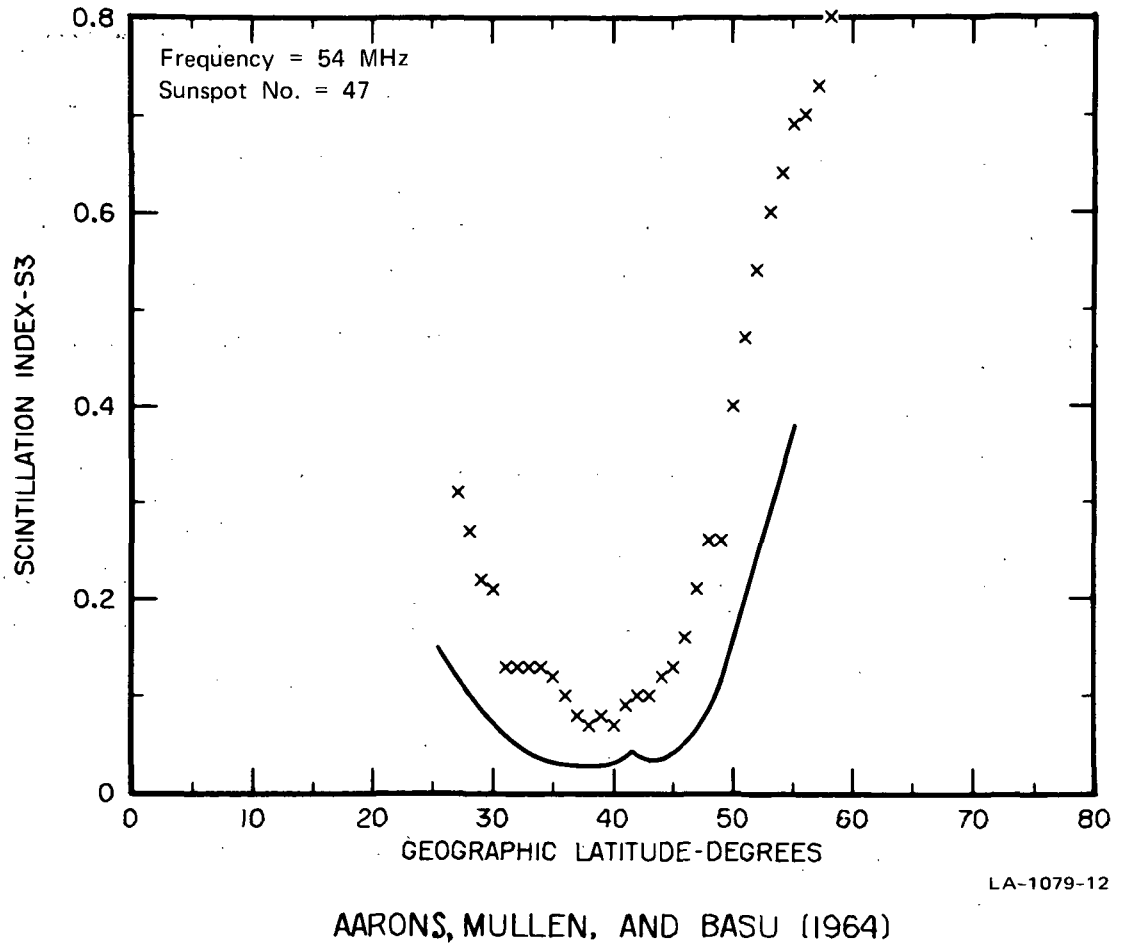

FIGURE 7 COMPARISON OF MODEL CALCULATIONS WITH HIGH-INCLINATION-SATELLITE OBSERVATIONS IN THE MIDDLE-LATITUDE AND SCINTILLATION-BOUNDARY REGIONS OF EASTERN NORTH AMERICA

boundary term of the expression for ΔN--would produce a better fit to the data of Aarons et al. and of Lawrence et al., at the expense of the Preddey data.

Since the former two data sets are from the northern hemisphere and the latter from the southern, one might suppose a hemispheric asymmetry to be involved (due in part, perhaps, to magnetic-field distortions relative to the simple dipole model used in the calculations). It will be noted, however, that the calculated scintillation index in Figure 7 is lower than the observed one by an essentially constant factor throughout the range of latitudes shown. This is suggestive of an

error in relating one or both of the empirical scintillation indices used by Preddey and by Aarons and his coworkers to the scintillation index calculated from the theory of Briggs and Parkin (1963).

Thus, while some progress has been made in recent years in relating scintillation indices used by various workers, it is suggested that more remains to be done. For further discussion of this point, see Section III-D.

Turning to auroral-zone scintillation observations, Figure 8 shows the diurnal variation of observed and calculated scintillation index for the Alaska radio-star data of Little, Reid, Stiltner, and Merritt (1962), and of Fremouw (1966). The fits are considered quite good, although the calculations produced a slightly stronger diurnal variation near solar minimum (sunspot number = 15) than was observed by Fremouw. For the solar-maximum (sunspot number = 200) data of Little et al. the calculated values of scintillation index are heavily dependent on the fourth term of the ΔN model.

Results of the only direct test of frequency dependence made in the modeling are presented in Figure 9, comparing calculations against the two-frequency, scintillation-ratio observations of Lansinger and Fremouw (1967). The fit is considered quite good but is a test of frequency dependence only in the auroral zone near solar minimum. The apparent discontinuity near hour angle = 2 occurs near the geomagnetic zenith and results from performing the calculation only at intervals of integral hour angle. (See Figure 2 of Lansinger and Fremouw, 1967.)

Finally, Figure 10 displays a comparison of scintillation values observed by the Joint Satellite Studies Group (JSSG, 1968), which were not used in model development, against values predicted for the JSSG observational circumstances by the model. The measured values were obtained from zenith observations of the 54-MHz beacon aboard Transit 4A

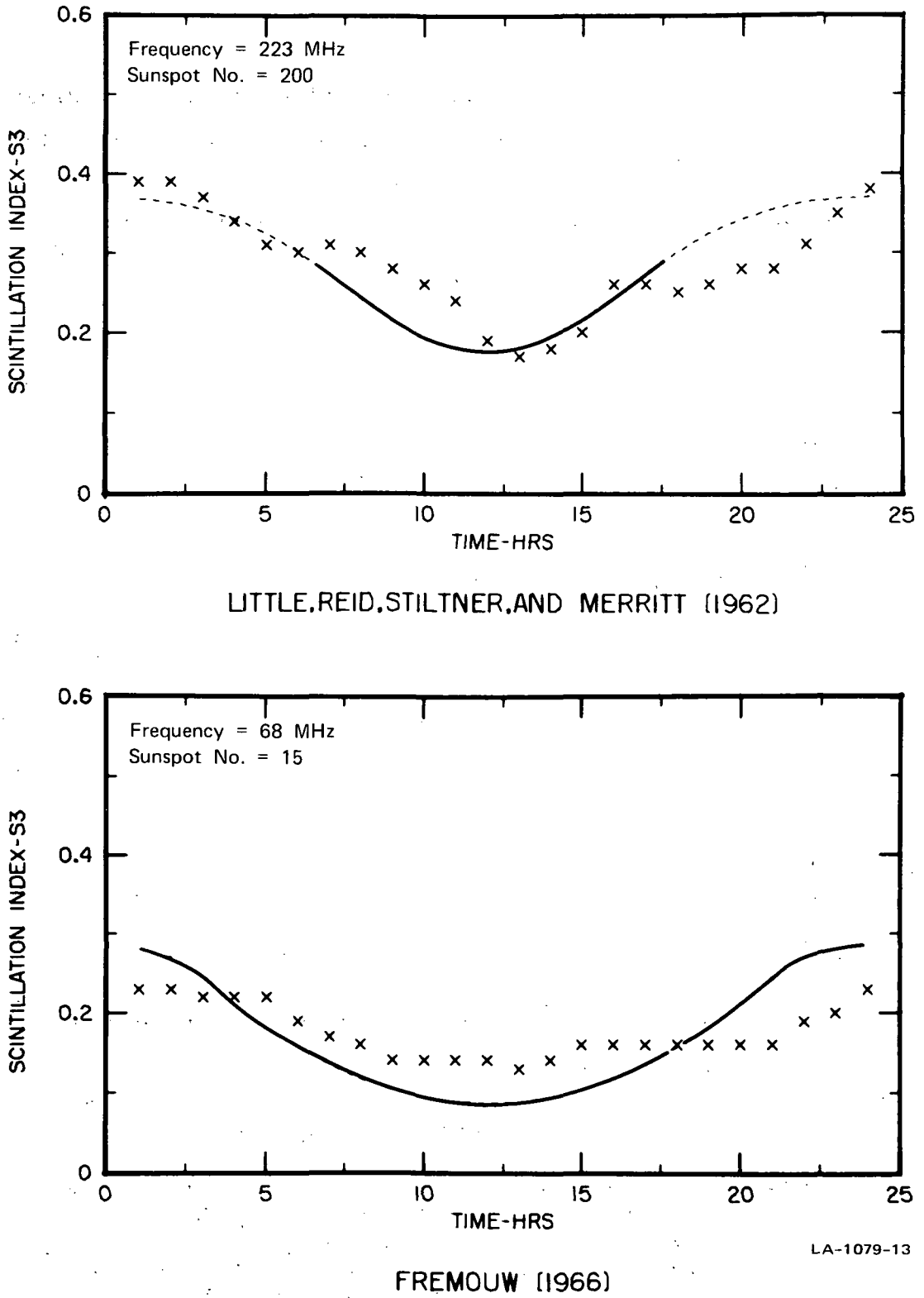

FIGURE 8 COMPARISON OF MODEL CALCULATIONS WITH RADIO-STAR OBSERVATIONS OF THE DIURNAL VARIATION OF SCINTILLATION FROM COLLEGE, ALASKA. Top: a high VHF frequency near solar maximum. Bottom: a low VHF frequency near solar minimum.

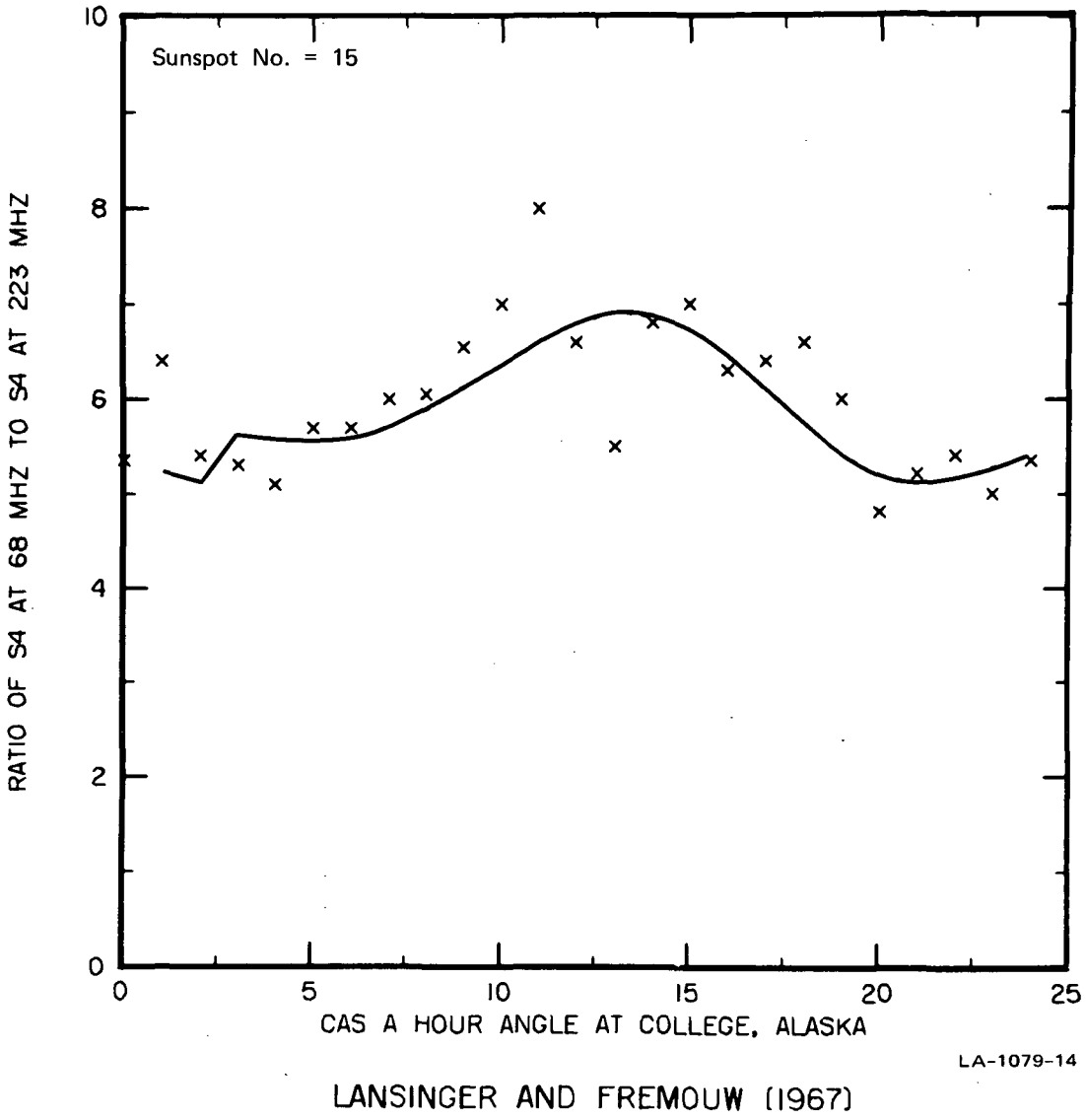

FIGURE 9 COMPARISON OF MODEL CALCULATIONS WITH RADIO-STAR OBSERVATIONS OF THE RATIO OF SCINTILLATION AT TWO FREQUENCIES FROM COLLEGE, ALASKA. The apparent discontinuity in the calculated curve is a magnetic field effect and would be smooth for a denser calculation grid.

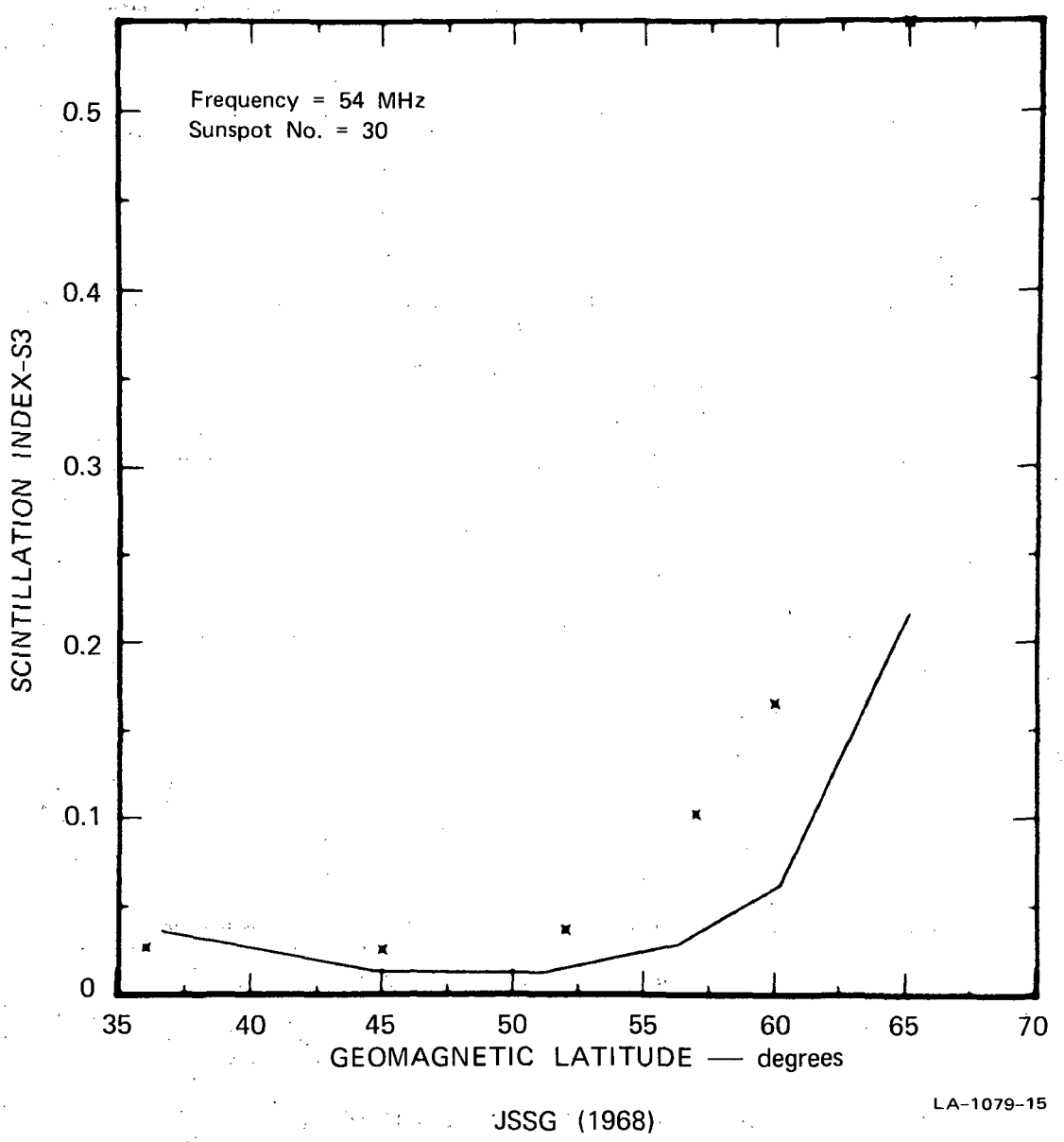

FIGURE 10 COMPARISON OF MODEL CALCULATIONS WITH HIGH-INCLINATION-SATELLITE OBSERVATIONS IN EUROPE

Table 2

QUALITATIVE EVALUATION OF MODEL'S DATA FITS

DEPENDENCE	EQUATORIAL LATITUDES	MIDDLE LATITUDES	BOUNDARY LATITUDES	AURORAL LATITUDES	POLAR LATITUDES
LATITUDE	Untested	Day: Fair Night: Good } (see Fig. 4) Avg: Fair (see Fig. 10)	Low Sunspot Number Day: Fair Night: Good } (see Fig. 4) Avg: Poor (see Fig. 10) Moderate Sunspot Number Avg: Poor (see Fig. 7) High Sunspot Number Day: Poor Night: Fair } (see Fig. 4)	Untested	Untested
TIME	Good (see Fig. 2)	Good (see Fig. 3)	Good (see Fig. 6)	Low Sunspot Number Fair (see Fig. 8) High Sunspot Number Good (see Fig. 8)	Untested
SEASON	Fair (see Fig. 2)	Untested	Untested	Untested	Untested
SUNSPOT NUMBER	Untested	Untested	Untested	Untested	Untested
FREQUENCY	Untested	Untested	Untested	Weak to moderate scintillation Good (see Fig. 9)	Untested
AZIMUTH AND/OR ELEVATION	Untested	Untested	Untested	Untested	Untested

at several European receiving stations, and were presented in Figure 2 of the JSSG (1968) paper. The calculations were performed in a manner similar to that described in Section II-C-2 for the data of Aarons, Mullen, and Basu (1964), except that the satellite was taken to be at the zenith of each observatory, using the station coordinates given in an earlier paper of the Joint Satellite Studies Group (JSSG, 1965).

Figure 10 may be taken as representative of the reliability of results to be obtained by employing the model described at the beginning of this section for predicting average scintillation. An additional indication is given by Figure 4, where the bars on the observed data points represent day-to-day variations from the average values of scintillation index.

By the latter standard, most of the model results appear to be quite meaningful for systems-planning purposes, providing a basis for calculating scintillation index within the range to be encountered in a given situation. Figure 7 shows one of the poorest fits, where the calculated values are consistently lower than the observed values by a factor of about two, which is similar to the discrepancy in Figure 10.* This suggests that calculations based on the model generally should produce somewhat better than order-of-magnitude predictions of average scintillation level. It does not imply uniqueness of the model, however, and geophysical applications should be limited to such uses as experiment planning.

The degree of confidence held for the model under different circumstances of interest is summarized in Table 2 in the form of qualitative evaluations of data fit, where tests have been made. General conclusions and recommendations are offered in Section IV.

---

*It may be of some significance that the observations in both Figures 6 and 10 were given in terms of the AFCRL index (Whitney, Aarons, and Malik, 1969), whereas the model relied rather heavily on observations given in terms of the index used by Preddey (1969).

III STATISTICAL DISTRIBUTION OF SIGNAL AMPLITUDE

In this section theoretical results are presented that will allow prediction of the amplitude probability density for transionospheric VHF-UHF signals. Simple formulas for the probability density parameters are derived that are well suited to system design and evaluation applications. The theory also provides an alternative derivation of the Briggs and Parkin (1963) scintillation index S_4 that provides additional insights into the scattering phenomenon, and a refinement of the Briggs and Parkin formula that can be significant in certain cases to be discussed.

Owing to the complexity of the analysis no rigorous justification of the initial assumption that the constituents of the scattered field satisfy the conditions of the Central Limit Theorem has been attempted. Rather, a qualitative argument and an appeal to the consistency of the results is used. Hopefully the work will stimulate future efforts that will remove this deficiency.

In Sections III-A and B the theoretical basis for the modeling is discussed and the necessary background material is reviewed. The scattering model and the details of the computation are presented in Section III-C. As the details are somewhat lengthy, the main results have been summarized in Section III-D. Hence, for a first or quick reading, Section III-C can be skipped. In Section III-E the theory is applied to observed data.

A. The Theoretical Basis for Amplitude Probability Modeling

At the receiver, the fundamental quantity is the voltage phasor E_R measured at the antenna terminals. Let $X = \mathrm{Re}[E_R]$, and $Y = \mathrm{Im}[E_R]$.

The phasor E_R consists of a non-random or average component $\bar{E}_R$ and a random (noise-like) component E_s. We assume that the random component is a summation of independent constituents of nearly identical probability distribution. (The justification will be deferred until the scattering mechanism is described.)

This assumption allows us to apply the Central Limit Theorem to deduce the asymptotic jointly Gaussian probability density

$$P_{XY}(x,y) = \frac{1}{2\pi\sqrt{\sigma_x^2\sigma_y^2 - C_{xy}^2}} \exp\left\{-\frac{1}{2\left(\sigma_x^2\sigma_y^2 - C_{xy}^2\right)} \times \left[\left(x - \eta_x\right)^2 \sigma_y^2 - 2C_{xy}\left(x - \eta_x\right)\left(y - \eta_y\right) + \left(y - \eta_y\right)^2 \sigma_x^2\right]\right\} \tag{III-1}$$

for X and Y. Here,

$$\eta_x = E[X] \quad , \quad \eta_y = E[Y] \quad , \quad \sigma_x^2 = E[(X - \eta_x)^2] \quad ,$$

$$\sigma_y^2 = E[(Y - \eta_y)^2] \quad ,$$

and

$$C_{xy} = E[(X - \eta_x)(Y - \eta_y)]$$

where $E[\cdot]$ denotes mathematical expectation or average. The consequences of Eq. (III-1) will be discussed. The reader should keep in mind, however, that Eq. (III-1) is a limiting distribution that is approached as the number of constituents becomes arbitrarily large. In practice this means the tails of the density function may not be very accurate.

Ultimately we shall derive an integral expression for the random component of E_R,

$$E_s = E_R - E[E_R] \quad . \tag{III-2}$$

The first quantity we shall compute is the intensity of E_s,

$$\sigma^2 \triangleq E[E_s E_s^*] = \sigma_x^2 + \sigma_y^2 \quad . \tag{III-3}$$

It happens that σ/E_o is identical to $\emptyset_o$ as given by Eq. (II-5)*. Hence, the rms model described in Section II is directly applicable.

In addition, however, we must determine σ_x, σ_y, and σ_{xy}. These parameters are derived from the complex quantity

$$B \triangleq E[E_s E_s] = (\sigma_x^2 - \sigma_y^2) + 2iC_{xy} \quad . \tag{III-4}$$

It follows from Eqs. (III-3) and (III-4) that

$$\sigma_x^2 = \frac{1}{2}\sigma^2(1 + \mathrm{Re}[B]/\sigma^2) \quad , \tag{III-5}$$

$$\sigma_y^2 = \frac{1}{2}\sigma^2(1 - \mathrm{Re}[B]/\sigma^2) \quad , \tag{III-6}$$

and

$$C_{xy} = \frac{1}{2}\sigma^2(\mathrm{Im}[B]/\sigma^2) \quad . \tag{III-7}$$

We shall see later that the quantities in parentheses do not depend on σ^2. They are simply proportionality factors that depend only on the scale-sizes of scattering irregularities and on the propagation geometry. The significance of this will be discussed later. For the present we shall proceed from the fact that Eqs. (III-1), (III-2), (III-5), (III-6), and (III-7) completely specify the first-order statistics of E_R.

The first quantity of interest is the amplitude probability density of E_R. The computation is straightforward in principle. Let $R = |E_R| = \sqrt{x^2 + y^2}$. One can readily show that

*E_o is the magnitude of the field incident upon the scattering region.

$$P_R(r) = \int_0^{2\pi} r\, P_{XY}(r\cos\theta, r\sin\theta)\,d\theta \ . \qquad \text{(III-8)}$$

Moreover, it is possible to obtain a Bessel function series representation for the integral (Beckmann and Spizzichino, 1963). We have found, however, that for computations, numerical integration is the simplest procedure. While this does give the desired result, it is also important to have a qualitative handle on the parameter dependence of $P_R(r)$.

Since σ_x, σ_y, and C_{xy} cannot be varied independently, we proceed in two steps. First we apply a fundamental property of Gaussian variates--namely, that they are derivable from uncorrelated variates, (say, ξ and η), via a unitary transformation (a rotation). Hence,

$$\begin{pmatrix} X \\ Y \end{pmatrix} = \begin{pmatrix} \cos\zeta & -\sin\zeta \\ \sin\zeta & \cos\zeta \end{pmatrix} \begin{pmatrix} \xi \\ \eta \end{pmatrix} \ . \qquad \text{(III-9)}$$

The value of ζ that renders ξ and η uncorrelated (and independent) can be shown to be

$$\zeta = \frac{1}{2} \tan^{-1} \frac{2C_{xy}}{\sigma_x^2 - \sigma_y^2} \ . \qquad \text{(III-10)}$$

Note that 2ζ is the phase angle of B.

Now let $\sigma_1^2 = E[(\xi - \bar{\xi})^2]$, and $\sigma_2^2 = E[(\eta - \bar{\eta})^2]$ where the overbar denotes average, and $E[(\xi - \bar{\xi})(\eta - \bar{\eta})] = 0$. The quantities σ_1^2 and σ_2^2 are readily derived from the relations $\sigma^2 = \sigma_1^2 + \sigma_2^2$ and $|B| = \sigma_1^2 - \sigma_2^2$. Both follow from Eq. (III-9). The fundamental quantities are σ_1, σ_2, and ζ. Once they are computed we can draw the phasor diagram shown in Figure 11. The ellipse is a contour of equal probability for the tip of E_R. The ξ axis is always aligned along the semi-major axis--i.e., $\sigma_1 \geq \sigma_2$.

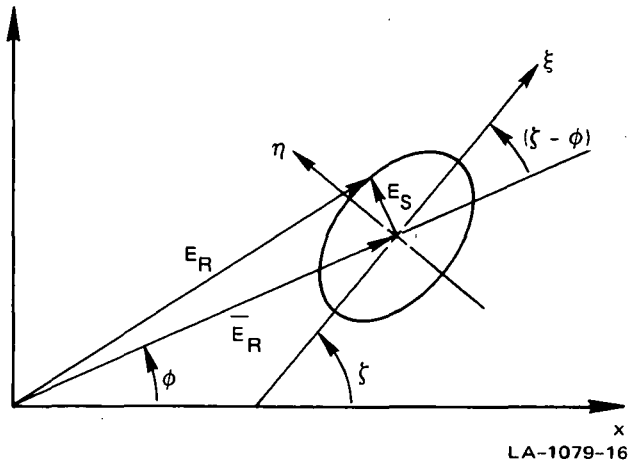

FIGURE 11 EQUIPROBABILITY ELLIPSE FOR E_S

From Figure 11 we can readily deduce that the maximum spread of $|E_R|$ occurs when the ξ-axis is along $\overline{E_R}$, and conversely. Moreover, if $\sigma_1 \approx \sigma_2$, the orientation of the ellipse has little effect on $P_R(r)$. When $\sigma_1 = \sigma_2$ and $C_{xy} = 0$, the density is Rician. The above remark suggests that the Rician distribution is a good approximation as long as $\sigma_1 \approx \sigma_2$. This has some bearing on the validity of an approximating distribution that will be discussed.

We shall first consider the scintillation index S_4, which is a measure of the spread of $|E_R|$. It follows that its dependence on σ_x, σ_y, and C_{xy} (or σ_1, σ_2, and ζ) will quantify the arguments just presented.

B. The Scintillation Index S_4

The scintillation index S_4 is the normalized second moment of intensity (or power). Hence the definition

$$S_4^2 = \frac{E\left[\left(|E_R|^2 - E\left[|E_R|^2\right]\right)^2\right]}{E\left[|E_R|^2\right]^2} \qquad \text{(III-11)}$$

It is convenient to normalize E_R itself so that $E[|E_R|^2] = \sigma^2 + \eta_x^2 + \eta_y^2 = 1$. Then, with $X = \tilde{X} + \eta_x$ and $Y = \tilde{Y} + \eta_y$,

$$S_4^2 = E\left[\tilde{X}^4\right]E\left[\tilde{Y}^4\right] + 2E\left[\tilde{X}^2\tilde{Y}^2\right] - \sigma^4 + 4\left(\sigma_x^2\eta_x^2 + \sigma_y^2\eta_y^2\right) + 8C_{xy}\eta_x\eta_y \quad . \qquad \text{(III-12)}$$

For Gaussian variates, $E[\tilde{X}^4] = 3\sigma_x^2$, $E[\tilde{Y}^4] = 3\sigma_y^2$, and $E[\tilde{X}^2\tilde{Y}^2] = \sigma_x^2\sigma_y^2 + 2C_{xy}^2$. Substituting these results into Eq. (III-12) and performing some algebraic manipulations, we obtain the result

$$S_4^2 = 2\sigma^2\left(1 - \sigma^2\right) + 2\left(\sigma_x^2 - \sigma_y^2\right)\left(\eta_x^2 - \eta_y^2\right) + 8C_{xy}\eta_x\eta_y + \sigma^4 + |B|^2$$

$$= 2\sigma^2\left(1 - \sigma^2\right)\left[1 + \frac{|B|}{\sigma^2}\cos 2\left(\zeta - \phi\right)\right] + \sigma^4\left(1 + |B|^2/\sigma^4\right) \qquad \text{(III-13)}$$

where $\phi = \tan^{-1}\eta_y/\eta_x$ is the phase angle of $\overline{E_R}$.

The first term in Eq. (III-13) arises from the interaction of E_s with $\overline{E_R}$, and it dominates when σ^2 is small ($\sigma^2 \ll 1$). Then

$$S_4^2 \cong 2\sigma^2\left(1 + \frac{|B|}{\sigma^2}\cos 2(\zeta - \phi)\right) \quad . \qquad \text{(III-14)}$$

We can see immediately that Eq. (III-14) is maximized when $\zeta - \phi$ is 0, in agreement with our heuristic argument. The second term in Eq. (III-13) dominates when σ^2 is large. Indeed, if $\sigma^2 = 1$, only the second term contributes to S_4. It is maximized if $\sigma_1^2 = \sigma_2^2 = 0$, and minimized when $\sigma_1^2 = \sigma_2^2 = \sigma^2$, which is what we should expect from the discussion in Section III-A.

Now let us assume that sufficient data are available that an estimate of S_4^2 and its standard deviation can be made. Rewriting Eq. (III-13) to separate the purely deterministic factors, we have

$$S_4^2 = 2\sigma^2\left(1 - \sigma^2\right)g_1 + \sigma^4 g_2$$

$$= 2\sigma^2 g_1 + \sigma^4\left(g_2 - 2g_1\right) , \qquad \text{(III-15a)}$$

where

$$g_1 = \left(1 + \frac{|B|}{\sigma^2}\cos 2\,(\zeta - \phi)\right) \qquad \text{(III-15b)}$$

and

$$g_2 = \left(1 + \frac{|B|}{\sigma^4}\right) \quad . \qquad \text{(III-15c)}$$

The estimate of S_4^2 can be used to estimate σ^2 by solving the quadratic equation in σ^2, Eq. (III-15a). This is related to the approach taken in the rms modeling; however, as we shall show, the quadratic term $\sigma^4(g_2 - 2g_1)$ is not present in the Briggs and Parkin formula. Since the model predicts only an average value for σ^2, it is important to determine its standard deviation as well. The importance for modeling the statistical distribution of amplitude is that the uncertainty in the value of σ^2 determined from the measurement of S_4^2 changes the probability distribution that the system designer must consider.

To state this formally, the theory gives $P_R(r|\sigma^2;\, u_1, u_2)$ that is, the probability density as a function of the given parameters u_1 and u_2, and of σ^2, which must be estimated. The estimate of σ^2 is a random variable with a probability density $P_{\sigma^2}(\sigma^2)$. The system designer must consider the total probability

$$P_R\left(r|u_1, u_2\right) = \int P_R\left(r|\sigma^2; u_1, u_2\right) P_{\sigma^2}\left(\sigma^2\right) d\sigma^2 \quad , \qquad \text{(III-16)}$$

which is always somewhat broader than $P_R(r|\sigma^2;\, u_1, u_2)$, thus automatically accounting for the uncertainty in σ^2. The cummulative distribution $F_R(r) = \int_o^r P_R(r')dr'$ follows immediately.

In the next section we complete the development with the computation of σ^2 and B. As the details are somewhat lengthy, the results are summarized in Section III-D. The assumptions are the same as Briggs and Parkin's, and they are discussed in Section II-A. The approximations used to evaluate the integrals are all valid for F-region scattering.

C. The Computation of σ^2 and B

Uscinski (1967) computed σ^2 and B for a normally incident plane wave within a weakly scattering medium. Following his approach we use the formulas derived by Budden (1965a), which are based on the Booker-Gordon scattering theory. The assumptions and their applicability are discussed in Section II-A. The coordinate system is shown in Figure 12.

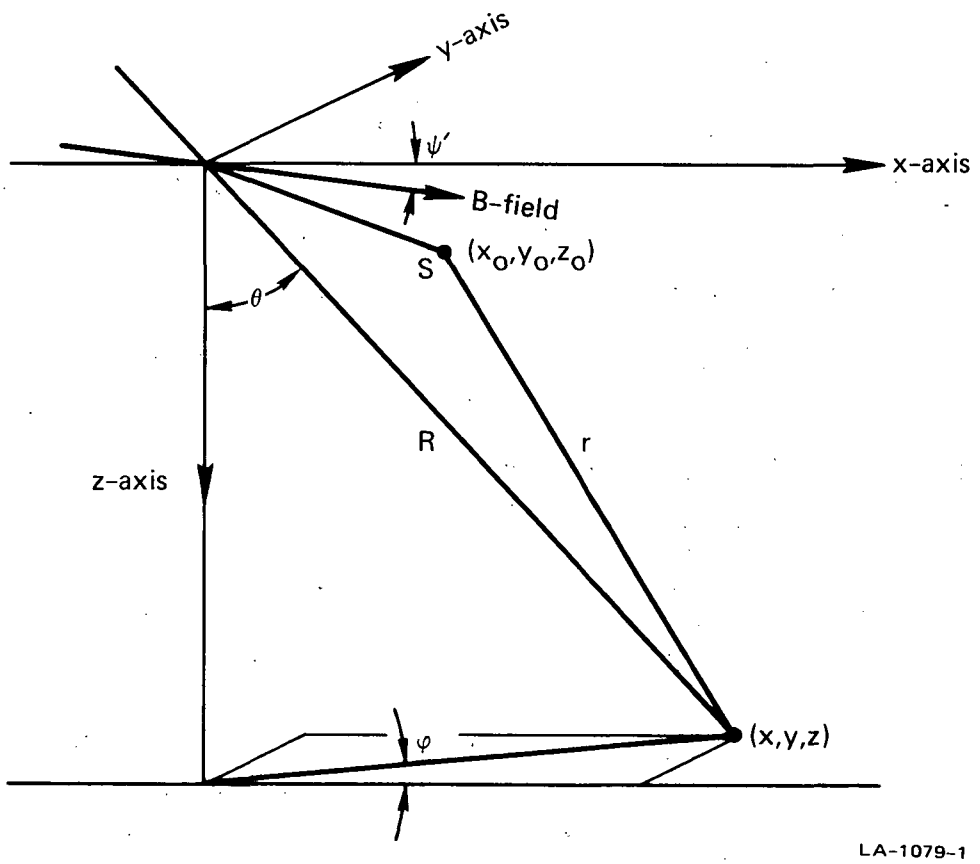

FIGURE 12 SCATTERING GEOMETRY

R is the distance from the center of the scattering region to the receiver. The incident field is $\mathrm{Re}\{E_i \exp(2\pi i f t)\}$, where

$$E_i = E_o \exp\{- ik(z \cos\theta + x \sin\theta \cos\varphi + y \sin\theta \sin\varphi)\} , \tag{III-17}$$

and $k = 2\pi/\lambda$, where λ is the transmitter wavelength.

Consider a small scattering volume centered at S. Assuming weak single scatter as the dominant mechanism, and large irregularities, the contribution to the scattered field at (x,y,z) is

$$dE_s = \frac{k^2 n_1(x_o, y_o, z_o)}{2\pi r} E_{is} \exp\{- ikr\}\, dV \tag{III-18}$$

where n_1 is the deviation of the local index of refraction from its mean value.

Since the frequencies of interest are well above the electron plasma frequency, $n_1 \cong - r_e(\lambda^2/2\pi)N_e$, where r_e is the classical electron radius (2.82×10^{-15} m) and N_e is the local electron-density deviation from its mean value. The scattered field at (x,y,z) is obtained by integrating Eq. (III-18) over the scattering volume. To obtain a mathematically tractable expression, however, certain approximations must be made.

Now,

$$r^2 = (z - z_o)^2 + (x - x_o)^2 + (y - y_o)^2 . \tag{III-19}$$

Let

$$X_o = x_o - z_o \tan\theta \cos\varphi \tag{III-20a}$$

$$Y_o = y_o - z_o \tan\theta \sin\varphi \tag{III-20b}$$

Then

$$r = \left(z - z_o\right) \sec\theta \left[1 - \frac{2\left(z - z_o\right)\tan\theta\left(X_o \cos\varphi + Y_o \sin\varphi\right) + X_o^2 + Y_o^2}{\left(z - z_o\right)^2 \sec^2\theta}\right]^{1/2}$$

$$\cong z \sec\theta - \left(z_o \cos\theta + x_o \sin\theta \cos\varphi + y_o \sin\theta \sin\varphi\right) + H \quad , \tag{III-21a}$$

where

$$H = \frac{X_o + Y_o - \sin^2\theta\left(X_o \cos\varphi + Y_o \sin\varphi\right)^2}{2\left(z - z_o\right)\sec\theta} \quad . \tag{III-21b}$$

In deriving Eq. (III-21a) we retained only quadratic terms in $X_o/(z - z_o)$ and $Y_o/(z - z_o)$. This is valid only if z is much larger than any of the variables x_o, y_o, or z_o. Using Eq. (III-21a) in (III-18) with r in the denominator approximated by $R = z \sec\theta$, we obtain the integral expression for E_s:

$$E_s = E_o r_e \frac{\exp(-ikR)}{R} \int(3) \int N_e\left(x_o, y_o, z_o\right) \exp(-ikH) dV \tag{III-22}$$

We now assume that N_e is a zero-mean random process. Then E_s itself is a zero-mean random process. The integral is well defined if σ^2 is finite. Before computing σ^2, however, we must assign an autocorrelation function to N_e. Following Budden (1965a) we assume that $N_e(x_o, y_o, z_o) = \mu(z_o) N_e'(x_o, y_o, z_o)$, where $\mu(z_o)$ is a deterministic profile function and N_e' is a homogeneous random process to which we assign the autocorrelation function*

$$R_{N_e} = \overline{N_e^2} \exp\left\{-\left[\frac{\Delta x^2}{a^2 \xi_o^2}\left(\cos^2\psi' + a^2 \sin^2\psi'\right) + 2\frac{\Delta x \Delta z}{a^2 \xi_o^2}\left(1 - a^2\right)\cos\psi' \sin\psi'\right.\right.$$

$$\left.\left. + \frac{\Delta z^2}{a^2 \xi_o^2}\left(a^2 \cos^2\psi' + \sin^2\psi'\right)\right]\right\} \exp\left(-\frac{\Delta y^2}{\xi_o^2}\right) \quad . \tag{III-23}$$

*Since we shall not encounter the quantity N_e in subsequent equations, we drop the prime from N_e' at this point.

The quantities ξ_o and a are respectively the transverse scale-size and axial ratio defined in Section II-A.

It is appropriate at this point to discuss the application of the Central Limit Theorem. If N_e is a Gaussian process and the integral in Eq. (III-22) is decomposed into subintegrals that just subtend the size of an average irregularity, the contributions to E_s from each subintegral will be nearly independent and identically distributed. It is certainly of little practical consequence, but to apply the Central Limit Theorem the constituents must be strictly independent. Hence, our results rest on the qualitative but reasonable assessment that the effect is negligible.

To compute B and σ^2, the integrals

$$I_{1,2} = \int (6) \int \mu(z_o)\mu(z_o')\rho_{XZ}(\Delta x,\Delta z)\ \rho_Y(\Delta y)\ \exp\left\{ - ik(H \pm H') \right\} dV dV' \qquad \text{(III-24)}$$

must be evaluated. The subscripts 1 and 2 refer respectively to the upper and lower signs in the exponential, and $\rho_{XZ}(\Delta x, \Delta z)$ and $\rho_Y(\Delta y)$ are simply the Δx-dependent, Δz-dependent, and Δy-dependent factors of $R_{N_e}/\overline{N_e^2}$. From Eqs. (III-3), (III-4), and (III-24) it follows that

$$\sigma^2 = \frac{E_o^2 r_e^2 \overline{N_e^2}}{R^2}\ I_1 \qquad \text{(III-25)}$$

and

$$B = \frac{E_o^2 r_e^2 \overline{N_e^2}}{R^2}\ \exp\left\{ - 2ikR \right\} I_2 \ . \qquad \text{(III-26)}$$

To proceed we must define $\mu(z_o)$. The computations are simplified if we let $\mu(z_o) = \exp\left\{ - z_o^2/L^2 \right\}$. With this definition of $\mu(z_o)$, all the terms in Eq. (III-24) are exponentials with finite quadratic terms in x_o, x_o', y_o, y_o', and z_o, z_o'. The integrals can be evaluated by repeated application of Budden's formula (II) (1965b). As this would require a prohibitive amount of algebra, it is expedient to make some simplifications

before starting. We can write H as

$$H = \left(X_o^2 H_{x^2} + 2 X_o Y_o H_{xy} + Y_o^2 H_{y^2} \right) \qquad \text{(III-27a)}$$

where

$$H_{x^2} = \frac{1 - \sec^2\theta \cos^2\varphi}{2z \sec\theta} \qquad \text{(III-27b)}$$

$$H_{y^2} = \frac{1 - \sec^2\theta \cos^2\varphi}{2z \sec\theta} \qquad \text{(III-27c)}$$

and

$$H_{xy} = - \frac{\sin^2\theta \sin\varphi \cos\varphi}{2z \sec\theta} \qquad \text{(III-27d)}$$

If the coordinate system is rotated so that z-axis is along the propagation direction, and the x-z plane is coincident with the plane defined by the propagation and magnetic field vectors, several simplifications can be realized. (The new coordinate system is identical to that used by Briggs and Parkin, 1963.)

In the new coordinate system, $H_{xy} = 0, H_{x^2} = H_{y^2} = 1/2z$, and, from Eqs. (III-20a) and (III-20b), $X_o = x_o$ and $Y_o = y_o$. The terms in $\rho_Y(\Delta y)$ are unchanged, and

$$\rho_{XY}(\Delta x, \Delta z) = \exp\left\{ - \frac{1}{(a\xi_o)^2} \left[\Delta x^2 B(\psi) + 2\Delta x \Delta y\, C(\psi) + \Delta z^2 B'(\psi) \right] \right\} \qquad \text{(III-28a)}$$

where

$$B(\psi) = (\sin^2\psi + a^2 \cos^2\psi) \quad , \qquad \text{(III-28b)}$$

$$C(\psi) = \sin\psi \cos\psi (1 - a^2) \quad , \qquad \text{(III-28c)}$$

and

$$B' = (a^2 \sin^2\psi + \cos^2\psi) \quad . \qquad \text{(III-28d)}$$

where $\psi = 90^o + \psi' + \theta$ is the angle between the propagation direction and the magnetic field as defined in Section II-A.

Finally, $z_o = \alpha \bar{x}_o + \gamma \bar{y}_o + \cos\theta \bar{z}_o$, where the rotated coordinates are denoted by the overbar and α and γ are geometrical factors. We note that there is only a very small contribution to Eq. (III-24) for

$|z_o - z_o'| \gg a\xi_o$. Hence we can set $\mu(z_o)$ and $\mu(z_o') \cong \mu^2[1/2(z_o + z_o')]$ with only a small error if $L \gg a\xi_o$--that is, if the ionosphere contains many irregularities. Also, the $\alpha\,\bar{x}_o$ and $\gamma\,\bar{y}_o$ terms will contribute to the corresponding terms from ρ_{XY} and ρ_Y reduced by the factor 1/L. Hence, to the same order of approximation they can be ignored. Then

$$\mu(z_o)\,\mu(z_o') \cong \exp\left\{-\frac{\left(\bar{z}_o + \bar{z}_o'\right)^2}{2(\sec\theta\, L)^2}\right\} \qquad \text{(III-29)}$$

With the rotated coordinates and with $\mu(z_o)\,\mu(z_o')$ replaced by Eq. (III-29), the evaluation of Eq. (III-24) is fairly straightforward. The integrations over $\bar{x}_o$, $\bar{x}_o'$, and $\bar{y}_o$, $\bar{y}_o'$ give

$$I_{1,2}\left(\bar{z}_o, \bar{z}_o'\right) = \left(\pi^2/R_1R_2\right)\mu\left(z_o\right)\,\mu\left(z_o'\right)\exp\left\{\Omega\right\} \qquad \text{(III-30a)}$$

where

$$\left\{\Omega\right\} = \left\{-\left[B'(\psi)/(a\xi_o)^2 + \epsilon i\pi^2\lambda^2\, C(\psi)/z^2(a\xi_o)^4\, R_2^2\right]\left(\bar{z}_o - \bar{z}_o'\right)\right\} \qquad \text{(III-30b)}$$

$$R_1^2 = \pm\,(\pi/\lambda z)^2\left[1 \pm \epsilon i\,\lambda z/\pi\xi_o^2\right] \qquad \text{(III-30c)}$$

and

$$R_2^2 = \pm\,(\pi/\lambda z)^2\left[1 \pm \epsilon i\,\lambda z B(\psi)/\pi(a\xi_o)^2\right] \qquad \text{(III-30d)}$$

The factor ϵ is zero for I_1 (upper sign) and 2 for I_2 (lower sign). The remaining integration over $\bar{z}_o$ and $\bar{z}_o'$ gives the final result

$$I_{1,2} = \pi^3/R_1R_2R_3 \qquad \text{(III-31a)}$$

where

$$R_3^2 = \frac{1}{(L\sec\theta)^2}\left[B'(\psi)/(a\xi_o)^2 - \epsilon i C(\psi)\pi/\lambda z(a\xi_o)^4\, R_2^2\right] \qquad \text{(III-31b)}$$

Substituting the appropriate quantities from Eqs. (III-30) and (III-31) into Eqs. (III-25) and (III-26) we obtain, after some algebraic manipulations, our final results:

$$\sigma^2 = E_o^2 r_e^2 \overline{N_e^2} \pi \lambda^2 L \sec i \; a\xi_o/\beta \quad , \tag{III-32}$$

$$B = -\sigma^2 \left(\cos u_1 \cos u_2\right)^{1/2} \exp\left\{ i \frac{1}{2} \left(u_1 + u_2\right)\right\} \tag{III-33}$$

where

$$\tan u_1 = 2\lambda z/\pi\xi_o^2 \quad , \tag{III-34}$$

$$\tan u_2 = 2\lambda z/\pi(\beta\, \xi_o)^2 \quad , \tag{III-35}$$

and

$$\beta = \left(a^2 \sin^2 \psi + \cos^2 \psi\right)^{1/2} \quad . \tag{III-36}$$

The quantities u_1, u_2, and β appeared previously in Section II-A and, in the rotated coordinate system, $\theta \equiv i$. From Eqs. (III-4), (III-10), and (III-33) it follows that $\zeta = \frac{1}{4}(u_1 + u_2)$. To justify the approximations in Eq. (III-21) we note that the contributions to the $\bar{x}_o$, $\bar{x}_o'$ and $\bar{y}_o$, $\bar{y}_o'$ integrals are small for $|\bar{x}_o - \bar{x}_o'|$, $|\bar{y}_o - \bar{y}_o'| \gg a\,\xi_o$. Similarly, the contribution to the $\bar{z}_o$, $\bar{z}_o'$ integral is small for $|\bar{z}_o - \bar{z}_o'| \gg L$. Hence, so long as $z \gg L \gg a\,\xi_o$, the approximations are valid.

In deriving Eq. (III-33) from Eq. (III-26) we have ignored the exp (- 2i kR) term. Since $\phi = kR$ is the phase of the undeviated component of E_R, this is equivalent to referencing the phase to the undeviated component. Since this is what a phase-locked receiver measures, Eq. (III-32) is the quantity of interest to the communications engineer. Hence we shall hereafter set $\phi = 0$. This implies that $\eta_x = \bar{E}_R$ and $\eta_y = 0$.

D. Summary and Discussion of Amplitude-Probability-Density Theory

From the fundamental assumption of Gaussian first-order statistics for the signal at the receiver we have derived formulas for the amplitude probability density, Eq. (III-8), and the scintillation index S_4^2, Eq. (III-15). To evaluate these formulas we must know σ_x^2, σ_y^2, and C_{xy}. They are derived from $\sigma^2 = E[E_s E_s^*]$ and the complex quantity $B = E[E_s E_s]$. In Section III-C we used Budden's (1965a) formula for E_s to calculate these quantities.

To summarize those results,

$$\sigma^2 = E_o^2 \sqrt{\pi}\, r_e^2 (\Delta N)^2 (\Delta h \sec i) \lambda^2 a \xi_o / \beta \quad , \tag{III-37}$$

and

$$B = -\sigma^2 (\cos u_1 \cos u_2)^{1/2} \exp\left\{ i \frac{1}{2} (u_1 + u_2) \right\} \tag{III-38}$$

To obtain Eq. (III-37) we have equated Δh and $\sqrt{\pi}\, L$ in (III-32). The remaining quantities are defined in Section III-A. Substituting from Eq. (III-38) into Eqs. (III-5), (III-6), and (III-7) we obtain

$$\sigma_x^2 = \frac{1}{2} \sigma^2 \left[1 - (\cos u_1 \cos u_2)^{1/2} \cos 2\delta \right] , \tag{III-39}$$

$$\sigma_y^2 = \frac{1}{2} \sigma^2 \left[1 + (\cos u_1 \cos u_2)^{1/2} \cos 2\delta \right] , \tag{III-40}$$

and

$$C_{xy} = \frac{1}{2} \sigma^2 (\cos u_1 \cos u_2)^{1/2} \sin 2\delta \quad , \tag{III-41}$$

where $\delta = \frac{1}{4} (u_1 + u_2) = \zeta - \pi/2$ is the inclination angle of the equiprobability ellipse to the semi-minor axis. The angle is measured to the semi-minor axis rather than the semi-major axis as in Figure 11 because of the negative sign in Eq. (III-38). Finally, recall that $\sigma^2 = \sigma_1^2 + \sigma_2^2$ and that $|B| = \sigma^2 (\cos u_1 \cos u_2) = \sigma_1^2 - \sigma_2^2$.

To compute the scintillation index we substitute $|B|$ into Eqs. (III-15b) and (III-15c). The result is

$$S_4^2 = 2\sigma^2 g_1 - \sigma^4 (g_2 - 2g_1) \quad , \tag{III-42}$$

where

$$g_1 = 1 - (\cos u_1 \cos u_2)^{1/2} \cos \frac{1}{2}(u_1 + u_2) \tag{III-43}$$

and

$$g_2 = 1 + \cos u_1 \cos u_2 \tag{III-44}$$

We set $\phi = 0$ as discussed in Section III-C.

If we retain only the first-order term in σ^2, Eq. (III-42) is identical to the Briggs and Parkin formula (II-1). The weak-single-scatter assumption breaks down if σ^2 becomes too large. It can, however, be large enough that the second-order term in σ^2 cannot be ignored. One difference in behavior of S_4^2 from that predicted by Briggs and Parkin can be seen in Figure 13 where the wavelength dependence is plotted for a large $(\Delta N)^2(\Delta h)$ product. The departure is significant. Moreover, at the long-wavelength end, S_4 departs somewhat from a quadratic dependence on λ.

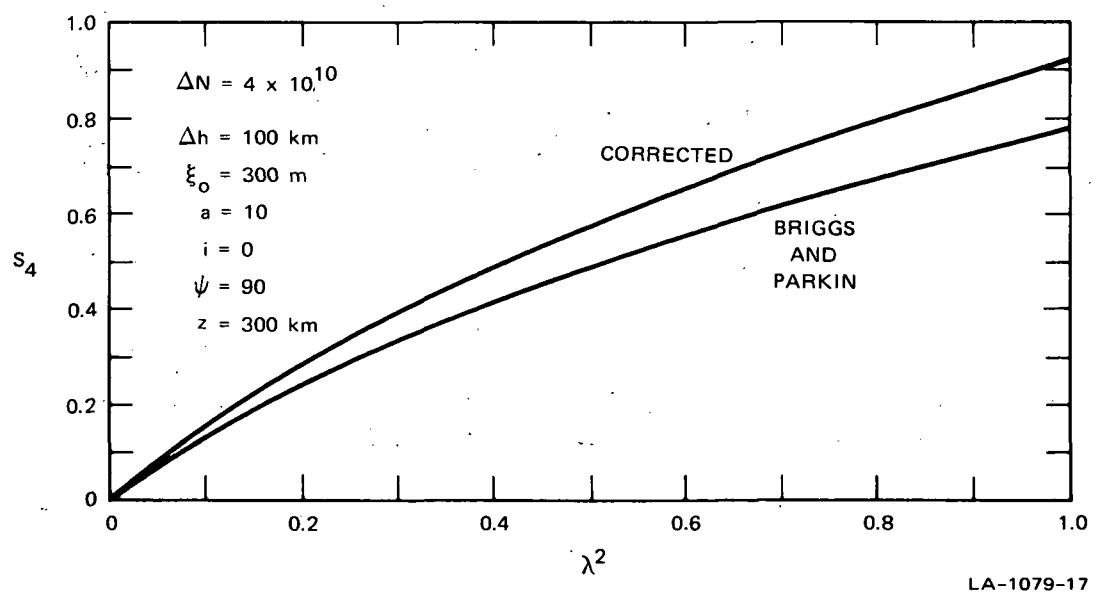

FIGURE 13 WAVELENGTH DEPENDENCE OF S_4 FOR LARGE $(\Delta N)^2(\Delta h)$ PRODUCT

To interpret these results we divide the $0 \leq u_2 \leq u_1 \leq \pi/2$ region into three zones. The near zone is arbitrarily taken to be the region where $|B|/\sigma^2 \geq 0.8$. Similarly we take the far zone to be the region where $|B|/\sigma^2 \leq 0.2$. The intermediate ($0.8 < |B| < 0.2$) region we have named the transition zone (see Figure 14). In the near zone the scattered power is in approximate phase quadrature with the undeviated component, and the scintillation index is generally small, in agreement with Briggs and Parkin's characterization of the near zone. In the far zone the scattered power is almost equally divided between its in-phase and phase-quadrature components.

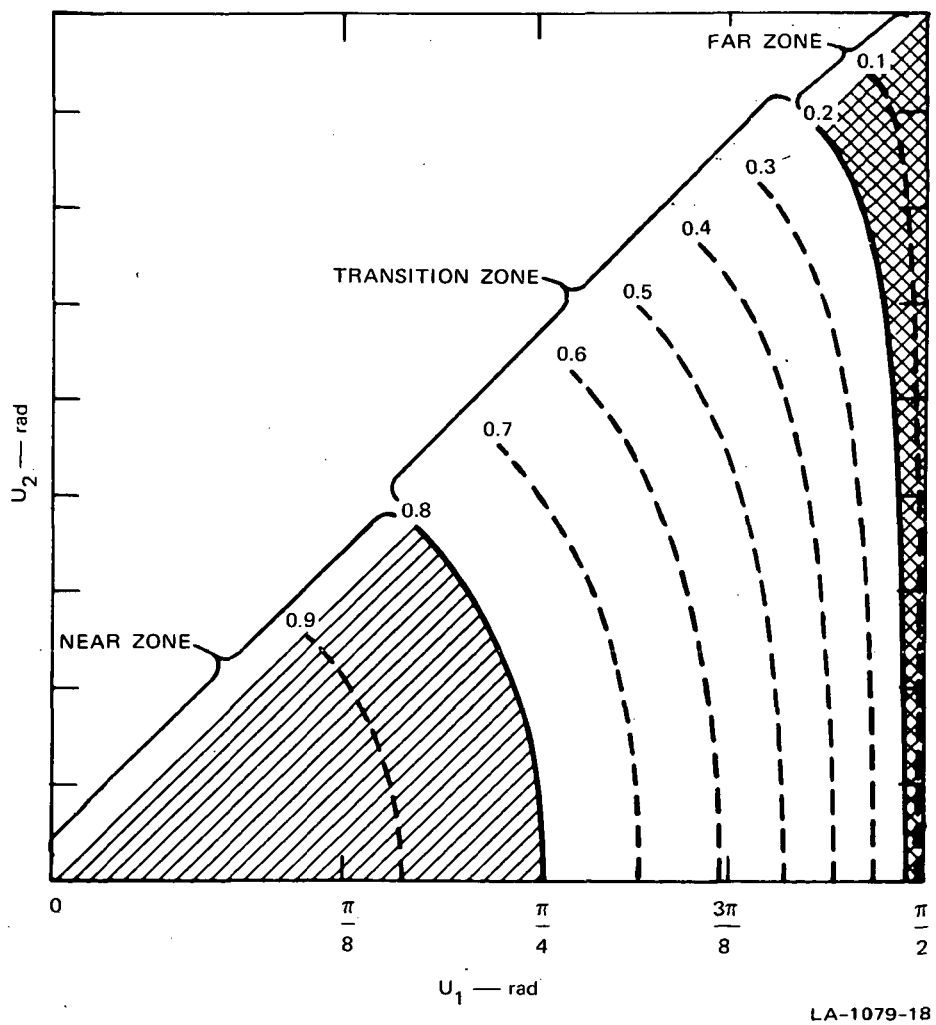

FIGURE 14 CONTOURS OF CONSTANT $|B|/\sigma^2$

If we were to move radially (i.e., along z) from the near to far zones, we would observe a monotonic increase of σ_y^2 to $\sigma^2/2$. We would also observe an initial increase of C_{xy} from zero to a maximum, and then a decrease to zero. This behavior is summarized in Table 3. We note that for typical F-region parameters we are in the transition zone and generally closer to the near zone than to the far zone at VHF and UHF frequencies.

Table 3

BEHAVIOR OF PROBABILITY-DENSITY PARAMETERS

Parameter	Near Zone	Transition Zone	Far Zone
σ_x^2	~ 0	Intermediate, increasing	$\sim \sigma^2/2$
σ_y^2	$\sim \sigma^2$	Intermediate, decreasing	$\sim \sigma^2/2$
C_{xy}	~ 0	Maximum	~ 0
S_4^2	$\sim 2\sigma^4$	Intermediate, increasing for small σ^2, decreasing for large σ	$\sim 2\sigma^2 - \sigma^4$

The consequences of this for applications are important. First, for large $|B|/\sigma^2$, $\sigma_1 \gg \sigma_2$. Hence the equiprobability ellipse is highly elongated, and the amplitude probability density is sensitive to its orientation. This means that the Rice, or even the Nakagami distribution (see Appendix C) suggested by Bischoff and Chytil (1969), will be a poor approximation to the true density. Secondly, changes in the scintillation index are due to parameter changes in the probability density. Hence, the conversion factors used in relating the various scintillation measures

are not constant. We have not analyzed the degree of this variation; however, we believe it is most important for strong scintillation. Both of these points will be demonstrated in the next section.

One point remains to be discussed. We must estimate the undeviated component η_x. The procedure we have adopted is the following: We assume that the receiver uses a well calibrated square-law detector. For a period of time when the output is approximately stationary we assume ergodicity and approximate the first and second moments of power by the time averages $\langle P \rangle$ and $\langle P^2 \rangle$. We can then estimate S_4^2 as

$$\hat{S}_4^2 = \frac{\langle P^2 \rangle - \langle P \rangle^2}{\langle P \rangle^2} \qquad \text{(III-45)}$$

Our working parameters are $\hat{S}_4^2$ and $\langle P \rangle$.

Applying Eq. (III-42) with a presumably known scale size and axial ratio, we can estimate σ^2 as

$$\hat{\sigma}^2 = \frac{-g_1 \pm \sqrt{g_1^2 - \left(g_2 - 2g_1\right) \hat{S}_4^2}}{g_2 - 2g_1} \langle P \rangle \qquad \text{(III-46)}$$

We choose the sign so that $0 < \hat{\sigma}^2 < 1$. We can then estimate η_x as

$$\hat{\eta}_x = \sqrt{\langle P \rangle (1 - \hat{\sigma}^2)} \qquad \text{(III-47)}$$

Finally, we use σ^2 in Eqs. (III-39), (III-40), and (III-41) to compute σ_x, σ_y, and C_{xy}. With $\eta_y = 0$ and η_x determined by Eq. (III-47), we can compute the amplitude probability density. An example of this procedure is given in the next subsection.

E. Application of Probability-Distribution Theory to ATS-3 Satellite Data

To test the theory we have applied the technique described in Section III-D to data from the ATS-3 synchronous satellite provided by NASA. The receiving station was located at Lima, Peru. Two channels of data were received, both at 136.4 MHz. The antennas were separated approximately 1200 feet along an east-west baseline. The data were recorded on December 17, 1969 from 0400 to 0440 GMT. The scintillation was described as average.

Histograms were made on one-minute segments of the data with a sampling interval of 5 ms. Hence, each histogram contains 12,000 samples. The interval used in making the histograms was 10^{-13} milliwatts. The scintillation index S_4 and average power were estimated on 25 consecutive segments. The average of the 25 values was 0.475 for Channel 1 and 0.487 for Channel 2. The standard deviation for both channels was less than 0.01.

Having determined scintillation index S_4 and the average power, we applied the technique described at the end of Section III-D to determine first σ^2, and then σ_x^2, σ_y^2, C_{xy} and η_x. Two different scale-sizes were used: ξ_o = 300 meters, which is in the rms electron density fluctuation model, and, for comparison, ξ_o = 1 km. The results are summarized in Table 4.

Channel 1 and Channel 2 should differ only in average power. As the differences in the estimated values of S_4 are on the order of the standard deviation of the estimate, we have a good check on the consistency of our estimates. Now, with ξ_o = 1 km, $|B|/\sigma^2$ = 0.926, and we are in the near-zone. Note that σ^2 is 0.31, so that the quadratic terms in Eq. (III-46) cannot be neglected. Indeed, if we estimate σ^2 as $S_4^2/2g_1$--i.e., neglecting the quadratic terms in σ^2--the result is greater than unity.

Table 4

COMPUTED PARAMETERS FOR ATS-3 DATA

Parameters	Channel 1	Channel 2	Channel 1	Channel 2	Comments
	ξ_o = 300 m		ξ_o = 1 km		
S_4	0.475	0.487	-	-	From Data
$\langle P \rangle$	1.747×10^{-12} milli-watts	2.307×10^{-12} milli-watts	-	-	From Data
$\sigma^2/\langle P \rangle$	0.162	0.171	0.310	0.320	Eq.(III-46)
$\sigma_x^2/\langle P \rangle$	0.0583	0.0614	0.0168	0.0173	Eq.(III-39)
$\sigma_y^2/\langle P \rangle$	0.104	0.110	0.2936	0.302	Eq.(III-40)
$\lvert B \rvert/\sigma^2$	0.385	-	0.926	-	Eq.(III-38)
δ	21.40^o	-	7.80	-	$\frac{1}{4}(u_1 + u_2)$

With the 300-meter transverse scale-size, which is closer to the observed values for the equatorial region, $|B|/\sigma^2$ is 0.385. This is in the transition zone, but there is still nearly twice as much power in phase quadrature as there is in phase with the undeviated component. Hence, neither the Rice nor the Nakagami distributions are applicable. To underscore this point, note that S_4 is a constant independent of the scale size we use, yet we observe a large difference in the parameters that enter into the computation of $P_R(r)$.

In Figure 15 we have plotted the computed probability densities using the parameters in Table 4 and η_x computed from Eq. (III-47) together with the average of the 25 measured histograms. The cumulative distributions are plotted in Figure 16. While we have not computed a measure of confidence for the theoretical curves, it is clear that the fit for ξ_o = 300 meters is very good. Moreover, the computed densities are very sensitive to the particular values of the parameters that are used.

We conclude that the theory is adequate to describe the probability distribution for average equatorial scintillation. Moreover, since only 16 percent of the total power is scattered in this case we expect the theory to be applicable for moderate to strong scintillation as well. In addition, the technique can be used to discriminate among possible combinations of values for ξ_o, a, and z.

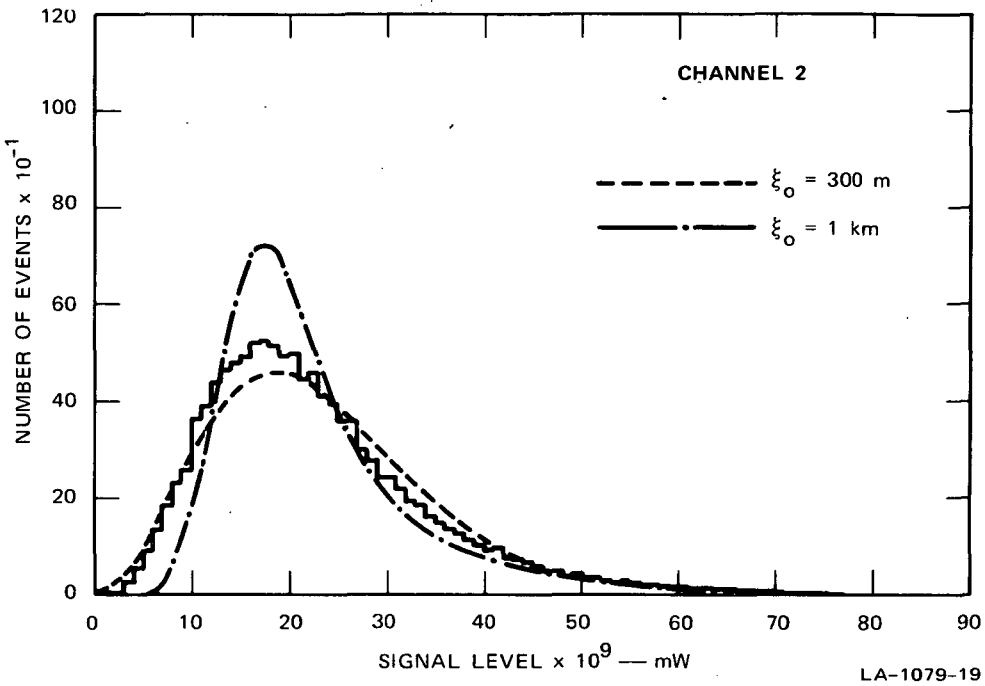

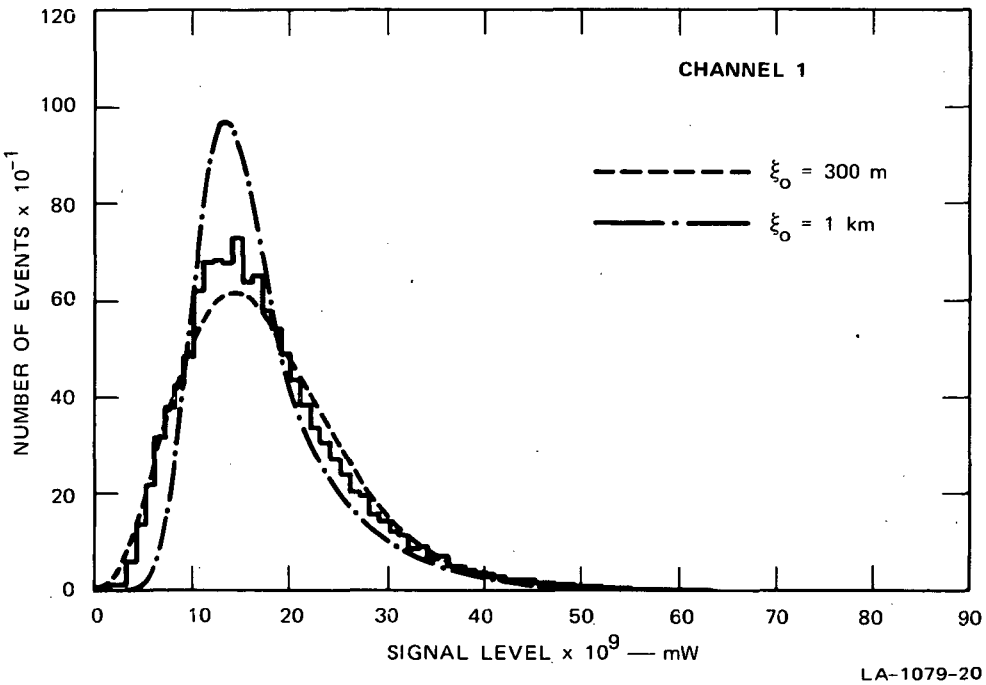

FIGURE 15 OBSERVED AND COMPUTED PROBABILITY DENSITY

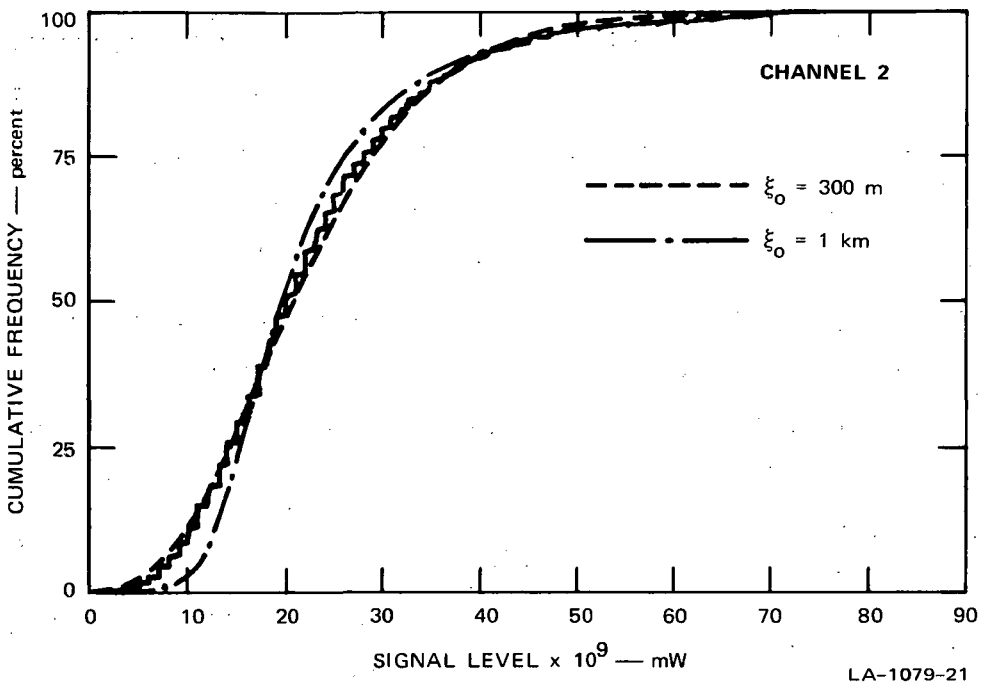

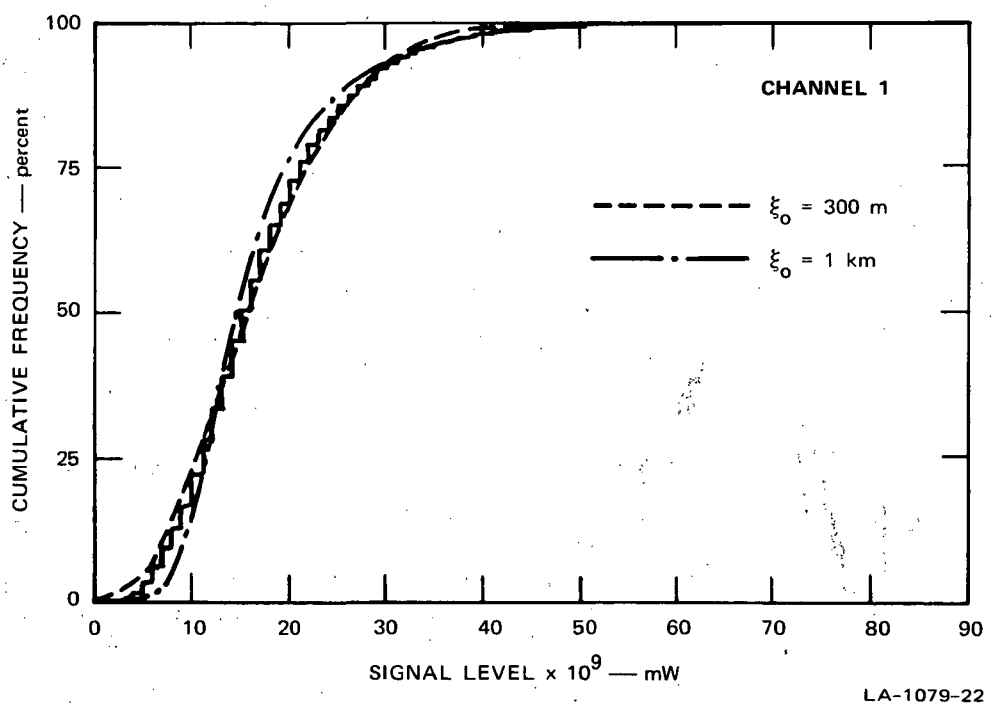

FIGURE 16 OBSERVED AND COMPUTED CUMULATIVE DISTRIBUTIONS

IV CONCLUSION AND RECOMMENDATIONS

The first major objective of this work was to develop an empirical model of F-layer irregularities that could be used to estimate the rms fluctuation of signal strength to be expected, due to scintillation, on an arbitrary satellite-to-earth communication path. Such a model has been presented at the beginning of Section II-D of this report and has been coded in a computer program being released simultaneously to NASA. The model and the program are offered as probably the best synoptic tools currently available for systems planning; for geophysical purposes, they should be used only for experiment design or as guides to intuition and/or more refined modeling.

The model has been tested against a sufficient number of published scintillation observations that it is thought to describe most major trends in scintillation activity, at least relatively. In most instances, the model is expected to produce better than order-of-magnitude estimates of the strength of scintillation to be expected under average ionospheric conditions. It is believed that the calculated value will usually fall within the range of day-to-day variation to be experienced in a given circumstance (i.e., for a given time of day, season, geometry, etc.).

There are, however, a number of significant limitations to the model. Table 2, on page 53, lists six scintillation dependences in five regimes of geomagnetic latitude that appear pertinent to scintillation evaluation. Among these 30 categories, it has been possible within the scope of this work to completely test the model quantitatively in only eight.

However, among the remaining categories partial tests were conducted in three, qualitative review of the scintillation literature revealed no significant trend in four others, four more were essentially redundant

with other categories, and there was sound basis for estimating behavior in an additional five. The remaining categories are the six scintillation dependences at polar latitudes (above 70 degrees geomagnetic latitude).

The (geomagnetic) polar region is probably of little importance for most currently envisioned engineering applications (even for airliners at very high latitudes utilizing geostationary-satellite communications, assuming F-layer irregularities*). This may not be true, however, for all users (e.g., the military), and the region is of decided geophysical interest. Furthermore, it is not difficult to imagine future increased NASA interest in a purely applied sense (viz., a series of polar-orbiting communication and/or navigation satellites to augment geostationary coverage).

There appears to be little hope of performing truly quantitative scintillation modeling at polar latitudes by means of data currently available in the published literature. This situation may be mitigated soon by means of data from Thule, Greenland (Aarons, private communication). Additional observations are needed, however, expecially above 136 MHz.

At latitudes of more immediate interest for NASA applications--equatorial, boundary, and auroral--the most generally absent type of data for complete quantitative modeling are those extending over sufficiently long periods to test sunspot dependence and over wide frequency ranges. It was possible to perform quantitative tests at decidedly different solar-cycle epochs even though continuous testing was not performed; testing of frequency dependence, however, was quite limited.

The most acute need is for long-term data from near the geomagnetic equator. It is suggested that useful data may exist at the University of Ghana (awaiting quantitative calibration) and possibly in NASA's own archives. In addition to long-term observations, data are needed for detailed evaluation of the latitudinal dependence of scintillation near the geomagnetic equator.

---

*Scintillations produced in the disturbed polar E layer might be of concern.

The above equatorial data could be combined with some published data from boundary and auroral latitudes that could not be in included in the scope of the present work, to fill in several of the gaps in complete quantitative testing of the existing model. However, filling of two other, more pressing needs would make a greater contribution to refining our ability to accurately predict average scintillation on a worldwide basis.

The two most pressing needs are for higher quality--not greater quantity--in scintillation data, and for complimentary measurements of the scale-size of scintillation-producing irregularities. For purposes of modeling, continued collection of qualitative and semi-quantitative scintillation indices will be of little value. In spite of progress in recent years in relating various indices, the conversions used probably are not reliable in all instances (see discussions of this point in Sections II-D and III-D).

What is needed are digitally recorded data from which various moments of the amplitude distribution could be calculated. Except at middle latitudes, these data should be collected near or above about 100 MHz in order to avoid the serious complication of strong or multiple scatter. NASA's widely used frequencies near 136 MHz are very useful for the purpose, whereas 40 and 54 MHz, which have been widely used for scintillation observations, often are too low.

In addition to measurements of scintillation, per se, accompanying measurements of irregularity scale-size are necessary for evaluation of scintillation frequency dependence; the most direct means is by dual- or multiple-frequency observations. In practice, it is not necessary to measure irregularity scale-size as an independent parameter (although this will suffice if the height is known or can be reasonably assumed). Rather, it is the Fresnel-zone parameter, u_1 (and, usually less importantly, u_2) defined in Eqs. (II-2) and (III-34) that is needed.

We turn now to the second major objective of this work: assessing the feasibility of modeling the first-order statistical distribution of amplitude under scintillation conditions. It is not recommended that such modeling be undertaken now on a worldwide basis, primarily due to the lack of appropriate data cited above. The theoretical basis for such modeling has been laid in the present work, however, and a suggested approach has been demonstrated quantitatively in Section III-E.

Appropriate data for limited distribution modeling in the geomagnetic equatorial region (Golden, private communication), in the auroral region (Lansinger, private communication), and possibly in the scintillation-boundary region (Aarons, private communication) do exist. Hence, a limited model could be developed.

We have shown that the suggested approach is quite good for average scintillation and probably applicable for moderate to strong scintillation. Hence we recommend that additional data be analyzed to determine empirically the limitations of the approach. Also, the result is very sensitive to changes in irregularity scale-size and height, and, to a lesser extent, to changes in axial ratio. If two of these quantities are known or were measured independently, the theory could be applied to determine the third parameter. The improved parameter estimates could then be used to refine the rms electron-density fluctuation model and/or a full-distribution model.

Finally, it is recommended that the next step in scintillation modeling be an intensive effort toward modeling amplitude distribution as regards a limited number of dependences (e.g., diurnal and seasonal behavior) near the geomagnetic equator. A secondary effort toward similar modeling in the auroral region could also be undertaken. In either case, data would have to be carefully edited to ensure validity of the weak-single-scatter assumption. Simultaneously, an effort should be initiated to extend the theory into the regime of stronger scatter, either in closed form or by means of numerical integrations.

Appendix A

A BRIEF CATALOGUE OF SCINTILLATION CALCULATIONS

Appendix A

A BRIEF CATALOGUE OF SCINTILLATION CALCULATIONS

This appendix contains graphs of scintillation index, calculated from the model described in Section II-D of the main text, for some cases of potential NASA interest. The ordinate values are of fractional rms fluctuation in received power, which is identical to the scintillation index S_4, defined in Eq. (II-8) of the main text. The values calculated are those expected for average ionospheric conditions at the times and places specified. They are subject to the limitations of the model and the assumptions underlying the calculations, which are described in Sections II-D and II-A of the main text, respectively. Missing values indicate either breakdown of the weak-single-scatter condition--with the corresponding expectation of severe scintillation--or that the transmitter is below the receiver's local horizontal.

The cases calculated are of two types: first, a polar orbiting satellite at 1000 km altitude, passing from north to south directly over a ground-based receiving station; second, an aircraft at 10.6 km (35,000 ft) altitude located at various points on a specified great-circle path, receiving from a geostationary satellite located at 75°W longitude. There are six cases of each type, as specified below. For all 12 cases, two values of sunspot number have been assumed: 30, which is applicable to the year 1972, and 100, which is applicable to solar maximum. Curves are presented for three frequencies--as indicated on the graphs--for each case and for each value of sunspot number.

In the order of their appearance, the 1000-km polar-orbiting satellite cases are as follows:

- Case 1 Receiver at Lima, Peru; pass time is local midnight at solstice.
- Case 2 Same as Case 1, except pass is at equinox.
- Case 3 Receiver is at Washington, D.C.; pass time is local noon (any season).
- Case 4 Same as Case 3, except pass time is local midnight.
- Case 5 Receiver is at Fiarbanks, Alaska; pass time is local noon.
- Case 6 Same as Case 5, except pass time is local midnight.

In the order of their appearance on the following pages, the cases for an aircraft observing a 75°W geostationary satellite are as follows:

- Case 7 Aircraft en route from London to New York; time at the ionospheric penetration point of the radio line of sight (for any aircraft location) is noon.
- Case 8 Same as Case 7, except time is midnight.
- Case 9 Aircraft en route from London to Seattle; time is noon.
- Case 10 Same as Case 9, except time is midnight.
- Case 11 Aircraft en route from London to Anchorage; time is noon.
- Case 12 Same as Case 11, except time is midnight.

Again, for all of the above, solar conditions appropriate to 1972 (near solar minimum) and to solar maximum have been assumed, and curves are presented for three frequencies in each case (Figures A-1 through A-6).

Of the above 12 cases, the least confidence in the calculations is held for Cases 1 and 2 (especially for sunspot number = 30), because of lack of data for testing the model near the geomagnetic equator at more than one epoch of the solar cycle. In general, the results are expected to be within the range of day-to-day variation of scintillation index, but individual observations may yield either higher or lower values.

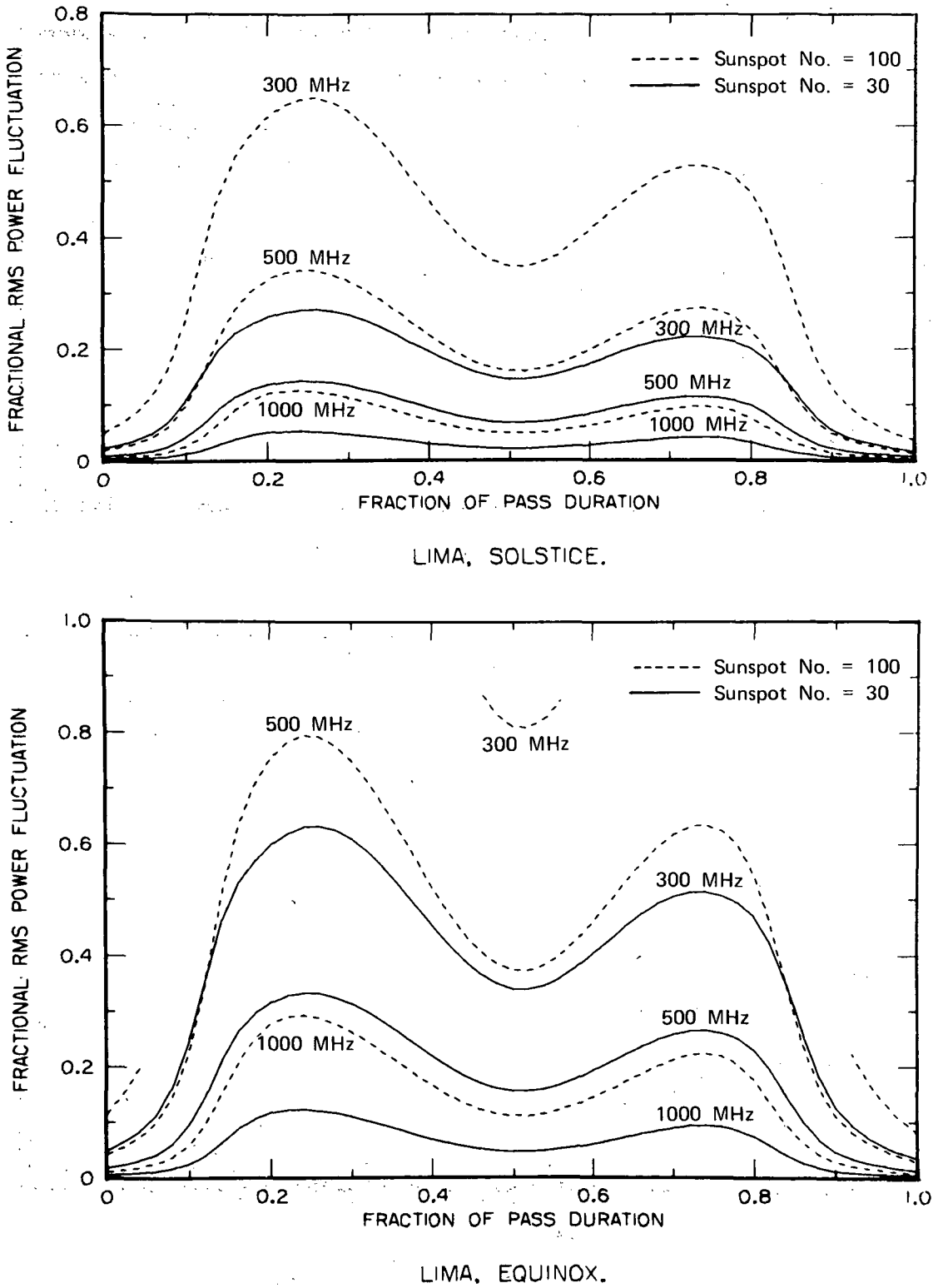

FIGURE A-1 CALCULATED SCINTILLATION INDEX FOR MIDNIGHT PASSES OF A 1000-km, POLAR-ORBITING SATELLITE OVER AN EQUATORIAL STATION

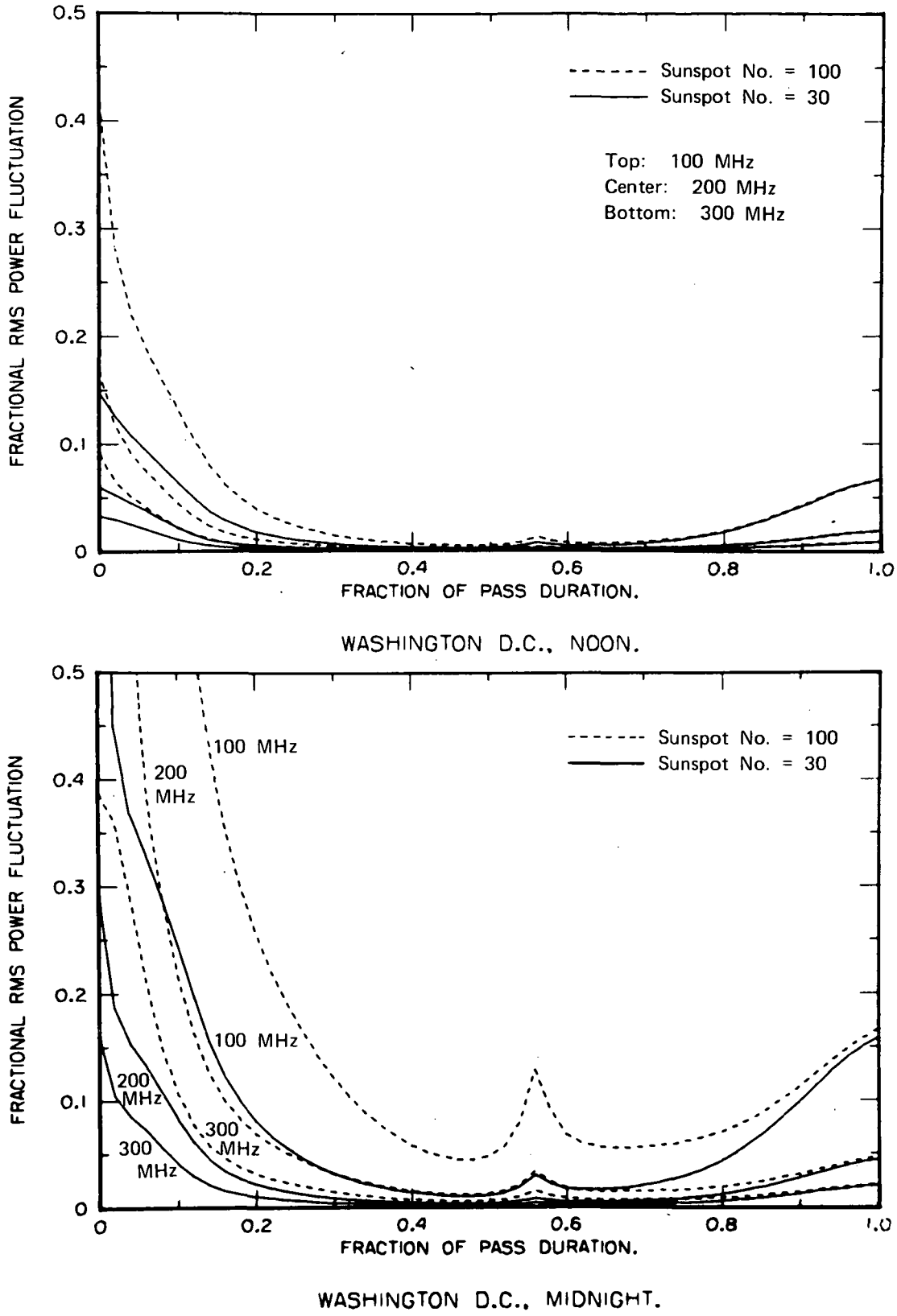

FIGURE A-2 CALCULATED SCINTILLATION INDEX FOR EQUATORWARD PASSES OF A 1000-km, POLAR-ORBITING SATELLITE OVER A MID-LATITUDE STATION

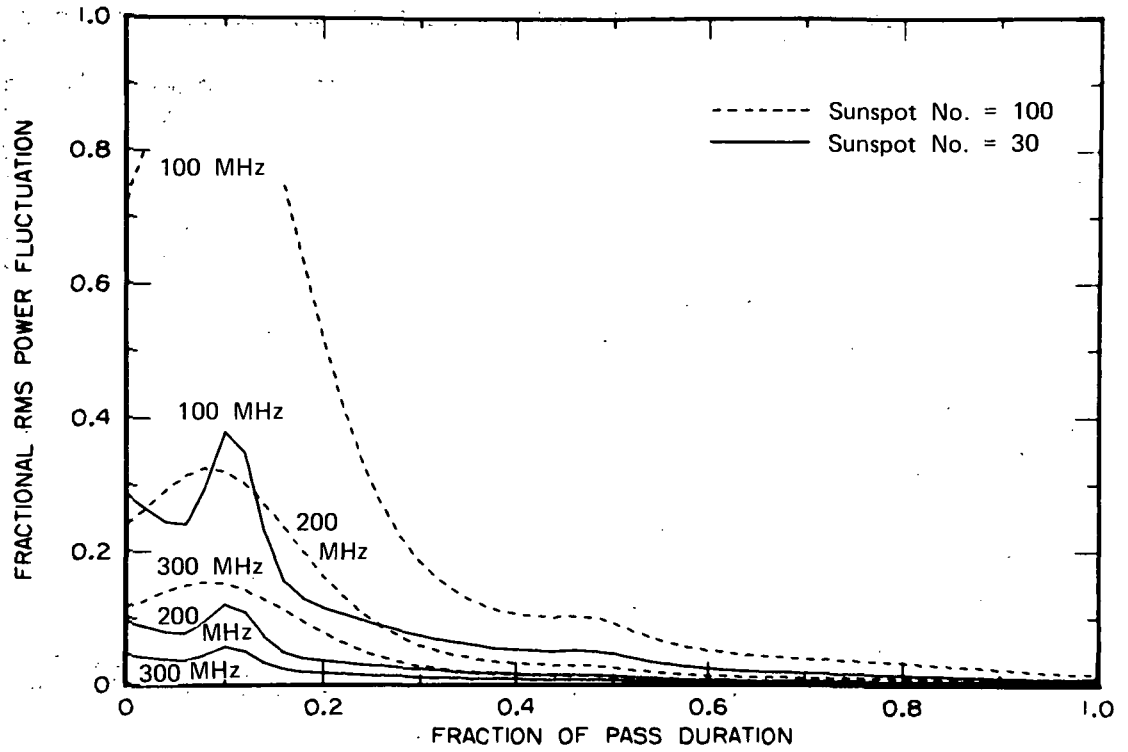

FAIRBANKS, NOON.

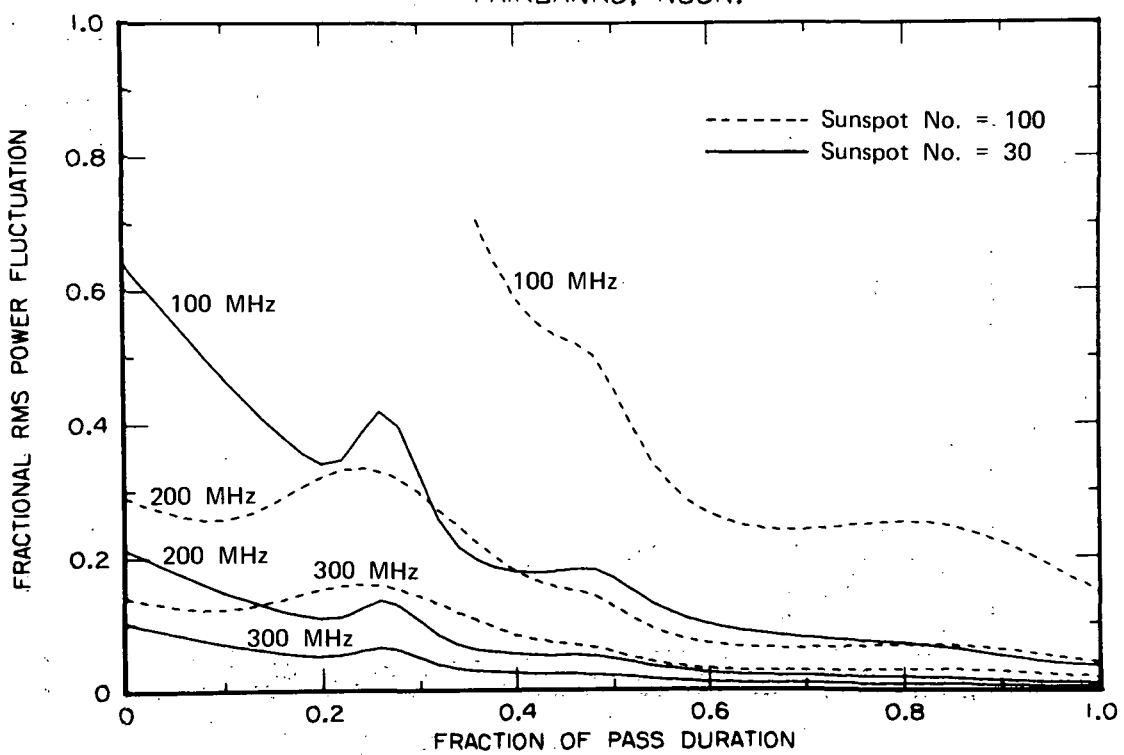

FAIRBANKS, MIDNIGHT.

FIGURE A-3. CALCULATED SCINTILLATION INDEX FOR EQUATORWARD PASSES OF A 1000-km, POLAR-ORBITING SATELLITE OVER AN AURORAL-ZONE STATION

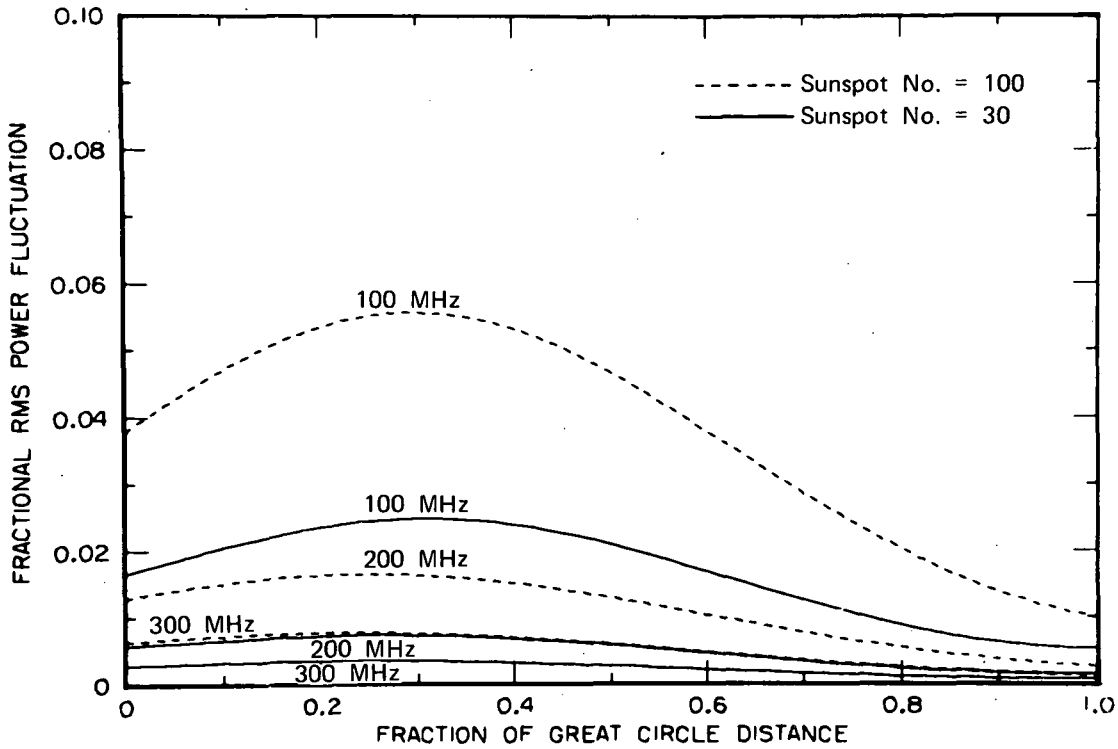

LONDON - NEW YORK, NOON MERIDIAN

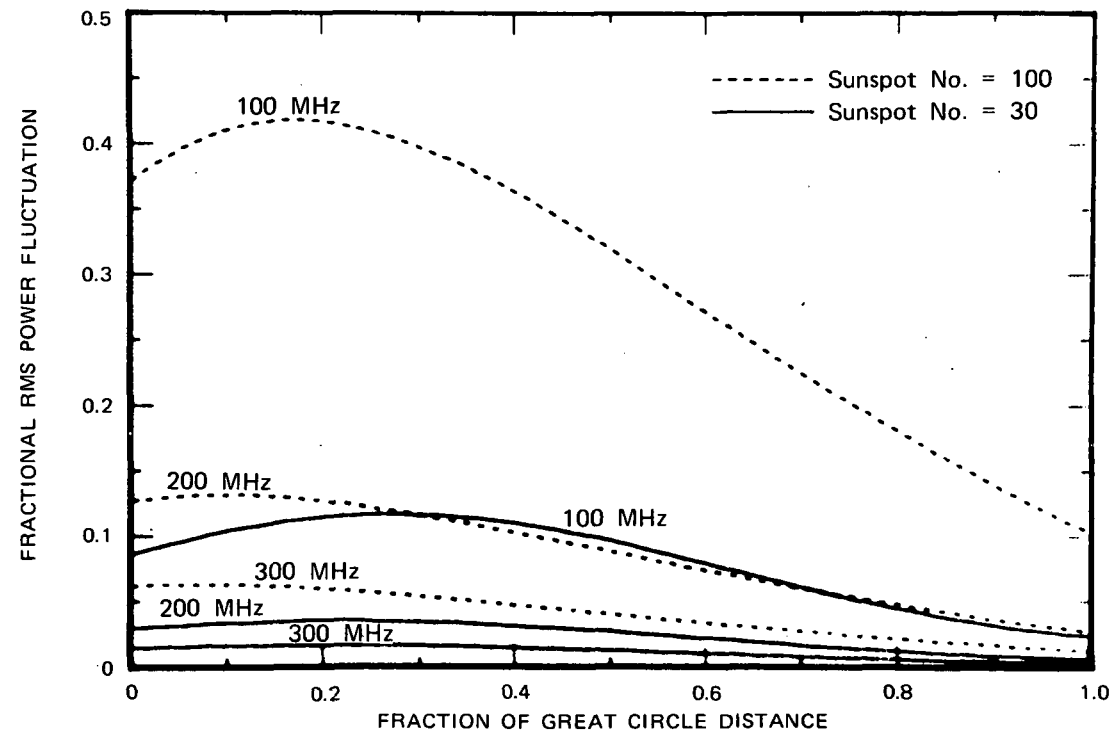

LONDON — NEW YORK, MIDNIGHT MERIDIAN

FIGURE A-4 CALCULATED SCINTILLATION INDEX ALONG A NORTH-ATLANTIC AIRLANE, FOR OBSERVATION OF A GEOSTATIONARY SATELLITE AT 75° W LONGITUDE

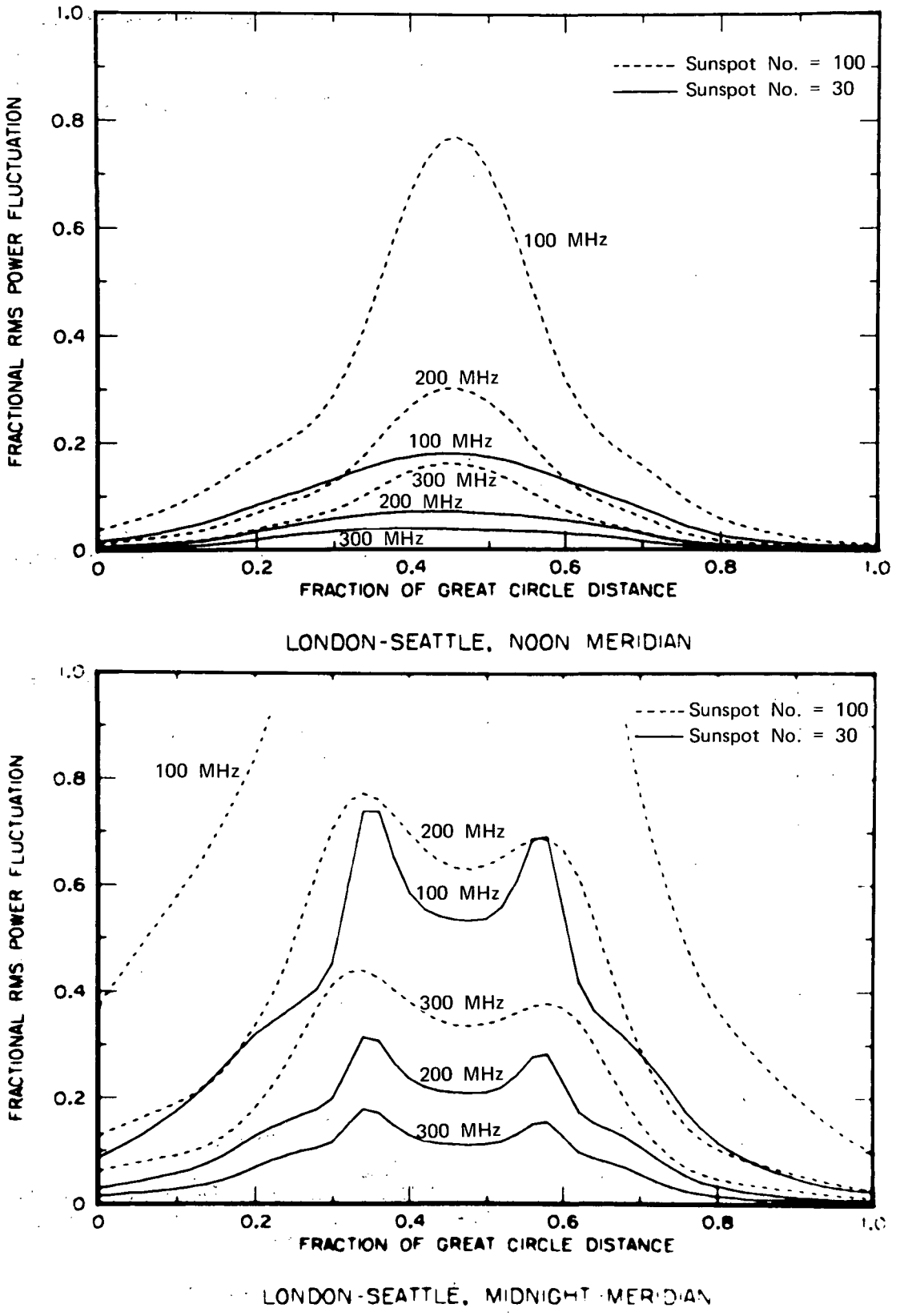

FIGURE A-5 CALCULATED SCINTILLATION INDEX ALONG A HIGH-LATITUDE AIRLANE, FOR OBSERVATION OF A GEOSTATIONARY SATELLITE AT 75° W LONGITUDE

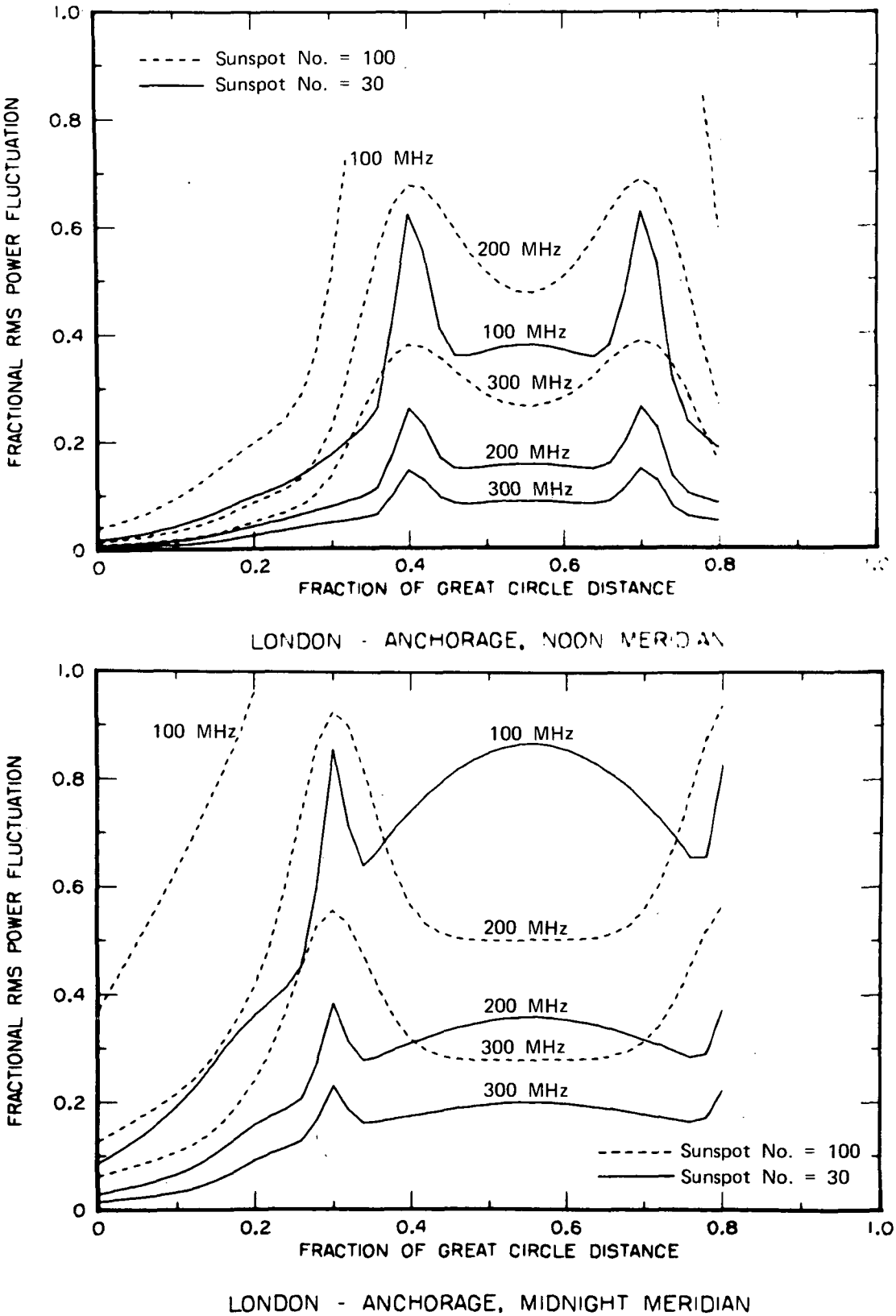

FIGURE A-6 CALCULATED SCINTILLATION INDEX ALONG A NEARLY POLAR AIRLANE, FOR OBSERVATION OF A GEOSTATIONARY SATELLITE AT 75° W LONGITUDE

Appendix B

A PARTIAL GUIDE TO THE SCINTILLATION LITERATURE

Appendix B

A PARTIAL GUIDE TO THE SCINTILLATION LITERATURE

This appendix lists approximately 75 contributions to the scintillation literature, grouped in the following five categories:

- Category I Theory (very abbreviated list)
- Category II Scintillation Index Definitions and Conversions
- Category III Scintillation Index Measurements
- Category IV Measurements of Ionospheric-Irregularity Parameters
- Category V Special Topics.

The contributions are identified fully in the List of References at the end of this report.

Category I

1. Hewish (1952)
2. Briggs and Parkin (1963)
3. Budden (1965a)
4. Budden (1965b)
5. Chytil (1970)
6. Pomalaza, Woodman, Tisnado, Sandoval, and Guillen (1970)
7. Singleton (1970a)

Category II

1. Little, Reid, Stiltner, and Merritt (1962)
2. Chytil (1967)
3. Bischoff and Chytil (1969)
4. Whitney, Aarons, and Malik (1969)
5. Whitney (1969)

Category III

1. Koster (1958)
2. Jones (1960)
3. Forsyth and Paulson (1961)
4. Lawrence, Jespersen, and Lamb (1961)
5. Little, Reid, Stiltner, and Merritt (1962)
6. Aarons, Mullen, and Basu (1963)
7. Koster (1963)
8. Koster and Wright (1963)
9. Liszka (1963)
10. Aarons, Mullen, and Basu (1964)
11. Basu, Allen, and Aarons (1964)
12. Briggs (1964)
13. Jespersen and Kamas (1964)
14. Lawrence and Martin (1964)

15. Liszka (1964a)
16. Yeh and Swenson (1964)
17. Millman and Moceyunas (1965)
18. Frihagen and Liszka (1965)
19. Aarons and Giudice (1966)
20. Aarons, Silverman, and Ramsey (1966)
21. Fremouw (1966)
22. Kent and Koster (1966)
23. Aarons, Allen, and Elkins (1967)
24. Whitney, Allen, and Aarons (1967)
25. Coates and Golden (1968)
26. Frihagen (1968)
27. JSSG (1968)
28. Kaiser and Preddy (1968)
29. Titheridge and Stuart (1968)
30. Aarons, Mullen, and Whitney (1969)
31. Allen (1969)
32. Frihagen (1969)
33. Preddy (1969)
34. Preddy, Mawdsley, and Ireland (1969)
35. Singleton (1969)
36. Stuart and Titheridge (1969)
37. Allen (1970)
38. Allen and Aarons (1970)
39. Bandyopadhyay and Aarons (1970)
40. Huang (1970)
41. Singleton (1970b)
42. Walker and Chan (1970)
43. Aarons and Allen (1971)
44. Aarons, Whitney, and Allen (1971)

Category IV		Parameter Measured
1.	Basler and DeWitt (1962)	Height
2.	Hook and Owren (1962)	Height
3.	Lawrence and Martin (1964)	Height
4.	Liszka (1964b)	Height
5.	Yeh and Swenson (1964)	Height
6.	Aarons and Guidice (1966)	Scale-size
7.	Kent and Koster (1966)	Scale-size and axial ratio
8.	Lansinger and Fremouw (1967)	Scale-size
9.	Allen (1969)	Height and scale-size
10.	Titheridge (1969)	Axial ratio
11.	Clark, Mawdsley, and Ireland (1970)	Height
12.	Dixon and Forsyth (1970)	Scale-size and axial ratio
13.	Golden (1970)	Scale-size
14.	Kidd (1970)	Height
15.	Paul, Yeh, and Flaherty (1970)	Height
16.	Pomalaza, Woodman, Tisnado, Sandoval, and Guillén (1970)	Scale-size

Category V		Topic Considered
1.	Little and Maxwell (1952)	Aurorae and magnetic storms
2.	Nakagami (1960)	Distribution*
3.	Little, Reid, Stiltner, and Merritt (1962)	Distribution
4.	Fremouw (1966)	Distribution
5.	Aarons, Allen, and Elkins (1967)	Distribution
6.	Whitney, Allen, and Aarons (1967)	Distribution

*"Distribution" refers to the statistical distribution of scintillation index or of instantaneous amplitude.

7.	Jones (1968)	Sporadic E
8.	JSSG (1968)	Distribution
9.	Aarons (1969)	Tropospheric scintillations, polar-cap scintillations, magnetic storm
10.	Allen (1969)	Distribution, K index
11.	Elkins (1969)	Ionospheric physics, observational summary
12.	Anastassiadis, Matsoukas, and Moraitis (1970)	Sporadic E
13.	Houminer (1970)	Distribution
14.	Huang (1970)	Spread F
15.	Singleton (1970a)	Focusing and saturation
16.	Aarons and Allen (1971)	K index, distribution
17.	Aarons, Whitney, and Allen (1971)	Distribution
18.	Craft (1971)	4-6 GHz
19.	Paulson and Tyner (1971)	Distribution

Appendix C

THE NAKAGAMI DISTRIBUTION

Appendix C

THE NAKAGAMI DISTRIBUTION

Nakagami (1960) has derived the probability density function

$$P(r) = \frac{2m^m r^{2m-1}}{\Omega^{2m-1}\Gamma(m)} \exp\left\{- mr^2/\Omega \right\} \qquad \text{(C-1)}$$

where $\Omega = E[r^2]$, and $m = \Omega^2/\left(E[r^4] - \Omega^2\right)$. Hence, m is the inverse of S_4^2, and Eq. (C-1) is an attractive candidate for the amplitude probability density. Nakagami pursued this possibility both experimentally and theoretically.

He found that Eq. (C-1) fitted the distribution of amplitude fades observed on long-range HF (9.67 to 20.02 MHz) communications channels fairly well. He also showed (Nakagami, Wada, and Fujimura, 1953) that Eq. (C-1) can be derived as an approximation to Eq. (III-8). Unfortunately Nakagami gives no criterion by which to determine the parameter range over which the approximation is accurate.

Consider first the case of very strong scintillation, where $\sigma^2 = 1$. From Eq. (III-15) we have $S_4^2 = 1/m = 1 + |B|^2$. Hence, $\sigma_1^2 - \sigma_2^2 = \sqrt{1/m - 1}$, and using the fact that $\sigma_1^2 + \sigma_2^2 = 1$, we deduce that $\sigma_1^2 = \frac{1}{2} - \frac{1}{2}\sqrt{1/m - 1}$. Now neither the amplitude probability density nor the scintillation index S_4^2 depend on ζ. Hence we can let $\sigma_y^2 = \sigma_1^2$ and $\sigma_x^2 = \sigma_2^2$. Nakagami showed that Eq.(C-1) is a good approximation to the true (Hoyt) density in this case.

For trans-ionospheric VHF-UHF signals, $\sigma^2 = 1$ is not typical. Indeed, our own analysis is only valid for $\sigma^2 \ll 1$. In that case we deduce formally that

$$\sigma^2 = - \frac{g_1 \pm \sqrt{g_1^2 - \left(g_2 - 2g_1 \right) \frac{1}{m}}}{g_2 - 2g_1} \qquad \text{(C-2)}$$

where

$$g_1 = 1 + |B|/\sigma^2 \cos 2\zeta \qquad \text{(C-3)}$$

and

$$g_2 = 1 + |B|^2/\sigma^4 \quad . \qquad \text{(C-4)}$$

Once this is done we can compute σ_x^2 and σ_y^2 as a function of m.

Nakagami has shown that Eq. (C-1) approximates a Rice distribution with $\sigma_x^2 = \sigma_y^2 = \frac{1}{2}\left(1 - \sqrt{1 - 1/m}\right)$. From Eqs. (C-2), (C-3), and (C-4), we see that this is the case only when $|B| = 0$, so that $g_1 = g_2 = 1$. From our own analysis (Sections III-C and D) we have seen that this is strictly true only in the limit as we move infinitely far from the scattering region. It is approximately true in the far zone as we defined it in Section III-E.

We conclude that Nakagami's distribution is a better approximation to the true density in the far zone than is Rice's. However, as we have shown, far-zone scintillation is not typical for the accepted values of the transverse scale-size and axial ratio at VHF and UHF frequencies. Hence one must exercise some caution in approximating the amplitude probability distribution.

REFERENCES

Aarons, J., "Special Problems - Equatorial Scintillations - Polar Cap Scintillations - Lower Atmosphere Scintillations," in "A Survey of Scintillation Data and Its Relationship to Satellite Communications," J. Aarons, Ed., Agardograph Interim Report, Air Force Cambridge Research Laboratories, Bedford, Mass., pp. 90-144 (1969).

Aarons, J., and R. S. Allen, "Scintillation Boundary during Quiet and Disturbed Magnetic Conditions," J. Geophys. Res., Vol. 76, No. 1, pp. 170-177 (January 1, 1971).

Aarons, J., R. S. Allen, and T. J. Elkins, "Frequency Dependence of Radio Star Scintillations," J. Geophys. Res., Vol. 72, No. 11, pp. 2891-2902 (June 1, 1967).

Aarons, J., and D. A. Guidice, "The Size of Low-Latitude Ionospheric Irregularities Determined from Observations of Discrete Sources of Different Angular Diameter," J. Geophys. Res., Vol. 71, pp. 3277-3280 (1966).

Aarons, J., J. P. Mullen, and S. Basu, "Geomagnetic Control of Satellite Scintillations," J. Geophys. Res., Vol. 68, No. 10, pp. 3159-3168 (1963).

Aarons, J., J. P. Mullen, and S. Basu, "The Statistics of Satellite Scintillations at a Subauroral Latitude," J. Geophys. Res., Vol. 69, No. 9 (May 1, 1964).

Aarons, J., J. P. Mullen, and H. E. Whitney, "The Scintillation Boundary," J. Geophys. Res., Vol. 74, No. 3, pp. 884-889 (1969).

Aarons, J., H. M. Silverman, and B. A. Ramsey, "Latitudinal Effects on Satellite Scintillations," Ann. Geophys., Vol. 22, pp. 349-355 (1966).

Aarons, J., H. E. Whitney, and R. S. Allen, "Global Morphology of Ionospheric Scintillations," Proc. IEEE, Vol. 59, pp. 159-172 (1971).

Allen, R. S., "Comparison of Scintillation Depths of Radio Star and Satellite Scintillations," J. Atmos. Terr. Phys., Vol. 31, pp. 289-297 (1969).

Allen, R. S., "Application of the Statistics of Ionospheric Scintillation to VHF and UHF Systems," in "A Survey of Scintillation Data and Its Relationship to Satellite Communications," J. Aarons, Ed., Agardograph Interim Report, Air Force Cambridge Research Laboratories, Bedford, Mass., pp. 64-89 (August 1970).

Anastassiadis, M., D. Matsoukas, and G. Moraitis, "40-MHz Ionospheric Scintillation and the Sporadic-E Layer," Radio Sci., Vol. 5, No. 6, pp. 953-957 (1970).

Bandyopadhyay, P., and J. Aarons, "The Equatorial F-Layer Irregularity Extent as Observed from Huancayo, Peru," Radio Sci., Vol. 5, pp. 931-938 (1970).

Basler, R. P., and R. N. DeWitt, "The Height of Ionospheric Irregularities in the Auroral Zone," J. Geophys. Res., Vol. 67, No. 2 (February 1962).

Basu, S., R. S. Allen, and J. Aarons, "A Detailed Study of a Brief Period of Radio Star and Satellite Scintillations," J. Atmos. Terr. Phys., Vol. 26, pp. 811-823 (1964).

Beckmann, P., and A. Spizzichino, "The Scattering of Electromagnetic Waves from Rough Surfaces" (Pergamon Press, Oxford, 1963).

Bischoff, K., and B. Chytil, "A Note on Scintillation Indices," Planet. Space Sci., Vol. 17, No. 5, pp. 1059-1066 (1969).

Briggs, B. H., "Observations of Radio Star Scintillations and Spread-F Echoes over a Solar Cycle," J. Atmos. Terr. Phys., Vol. 26, pp. 1-23 (1964).

Briggs, B. H., and I. A. Parkin, "On the Variation of Radio Star and Satellite Scintillations with Zenith Angle," J. Atmos. Terr. Phys., Vol. 25, No. 6, pp. 339-366 (1963).

Budden, K. G., "The Amplitude Fluctuations of a Radio Wave Scattered from a Thick Ionospheric Layer with Weak Irregularities," J. Atmos. Terr. Phys., Vol. 27, No. 2, p. 155 (1965a).

Budden, K. G., "The Theory of the Correlation of Amplitude Fluctuations of Radio Signals at Two Frequencies Simultaneously Scattered by the Ionosphere," J. Atmos. Terr. Phys., Vol. 27, pp. 883-897 (1965b).

Cain, J. C., and S. J. Cain, "Derivation of the International Reference Field [IGRF (10/68)]--A Report to IAGA Commission II Working Group 4," X-612-68-501, Goddard Space Flight Center, Greenbelt, Maryland (1968).

Christiansen, R. M., "Preliminary Report of S-Band Propagation Disturbance During Alsep Mission Support (November 19, 1969 - June 30, 1970)," X-861-71-239, Goddard Space Flight Center, Greenbelt, Maryland (1971).

Chytil, B., "The Distribution of Amplitude Scintillation and the Conversion of Scintillation Indices," J. Atmos. Terr. Phys., Vol. 29, No. 9, pp. 1175-1177 (1967).

Chytil, B., "Amplitude and Phase Scintillations of Spherical Waves," J. Atmos. Terr. Phys., Vol. 32, pp. 961-966 (1970).

Clark, D. H., J. Mawdsley, and W. Ireland, "Mid-Latitude Radio-Satellite Scintillation: The Height of the Irregularities," Planet. Space Sci., Vol. 18, pp. 1785-1791 (1970).

Coates, R. J., and T. S. Golden, "Ionospheric Effects on Telemetry and Tracking Signals from Orbiting Spacecraft," X-520-68-78, Goddard Space Flight Center, Greenbelt, Maryland (1968).

Craft, H. D., Jr., "Some Measurements of Ionospheric Scintillation at 4 GHz and 6 GHz," paper presented at the spring meeting of URSI, Washington, D.C., April 1971.

Davis, T. N., "An Investigation of the Morphology of the Auroral Displays of 1957-58," Scientific Report 1, NSF Grant No. G14782, Report UAG-R117, Geophysical Institute of the University of Alaska, College, Alaska (1961).

Dixon, A. F., and P. A. Forsyth, "Measurements of the Shape of Ionospheric Irregularities Using Satellite Transmission," Can. J. Phys., Vol. 48, pp. 2097-2100 (1970).

Dyson, P. L., "Direct Measurement of the Size and Amplitude of Irregularities in the Topside Ionosphere," J. Geophys. Res., Vol. 74, pp. 6291-6303 (1969).

Dyson, P. L., "On the Significance of Electrostatic Probe Observations of Electron Density Irregularities," J. Geophys. Res., Vol. 76, pp. 4689-4690 (1971).

Elkins, T. J., "Summary of Properties of F-Region Irregularities," in "A Survey of Scintillation Data and Its Relationship to Satellite Communications," J. Aarons, Ed., Agardograph Interim Report, Air Force Cambridge Research Laboratories, Bedford, Mass., pp. 22-63 (August 1969).

Feldstein, Y. I., and G. V. Starkov, "Dynamics of Auroral Belt and Polar Geomagnetic Disturbances," Planet. Space Sci., Vol. 15, pp. 209-229 (1967).

Forsyth, P. A., and K. V. Paulson, "Radio-Star Scintillations and the Auroral Zone," Can. J. Phys., Vol. 39, pp. 502-509 (1961).

Fremouw, E. J., "Aberrations of VHF-UHF Signals Traversing the Auroral Ionosphere," Final Report, Contract NAS5-3904, Report UAG R-181, Geophysical Institute of the University of Alaska, College, Alaska (1966).

Fremouw, E. J., and H. F. Bates, "Worldwide Behavior of Average VHF-UHF Scintillation," Radio Sci., Vol. 6, No. 10 (1971).

Frihagen, J., "Spaced Receiver Measurements of the Height of Ionospheric Irregularities over Europe," J. Atmos. Terr. Phys., Vol. 30, pp. 1913-1918 (1968).

Frihagen, J., "Satellite Scintillation at High Latitudes and its Possible Relation to Precipitation of Soft Particles," J. Atmos. Terr. Phys., Vol. 31, pp. 81-92 (1969).

Frihagen, J., and L. Liszka, "A Study of Auroral Zone Ionospheric Irregularities Made Simultaneously at Tromso, Norway, and Kiruna, Sweden," J. Atmos. Terr. Phys., Vol. 27, pp. 513-523 (1965).

Golden, T. S., "A Note on Correlation Distance of VHF Fading from Irregularities in the Equatorial Ionosphere," Radio Sci., Vol. 5, No. 6, pp. 943-947 (1970).

Hewish, A., "The Diffraction of Galactic Radio Waves as a Method of Investigating the Irregular Structure of the Ionosphere," Proc. Roy. Soc. London, A, Vol. 214, pp. 494-514 (1952).

Hook, J. L., and L. Owren, "The Vertical Distribution of E-Region Irregularities Deduced from Scintillations of Satellite Radio Signals," J. Geophys. Res., Vol. 67, No. 13, pp. 5353-5356 (December 1962).

Houminer, Z., "Scintillation Studies of a Synchronous Satellite's Radio Signals at a Low-Latitude Station," Radio Sci., Vol. 5, No. 6, pp. 949-951 (1970).

Huang, Chun-ming, "F-Region Irregularities which Cause Scintillation and Spread-F Echoes at Low Latitude," J. Geophys. Res., Vol. 75, No. 25, pp. 4833-4841 (September 1, 1970).

Jespersen, J. L., and G. Kamas, "Satellite Scintillation Observations at Boulder, Colorado," J. Atmos. Terr. Phys., Vol. 26, No. 4, pp. 457-473 (1964).

Jones, I. L., "Further Observations of Radio Stellar Scintillation," J. Atmos. Terr. Phys., Vol. 19, No. 1, pp. 26-36 (September 1960).

Jones, K. L., "Radio Scintillations Produced by Irregularities at Sporadic-E Level," Planet. Space Sci., Vol. 16, pp. 1475-1482 (1968).

JSSG (Joint Satellite Studies Group), "A Synoptic Study of Scintillations of Ionospheric Origin in Satellite Signals," Planet. Space Sci., Vol. 13, pp. 55-62 (1965).

JSSG (Joint Satellite Studies Group), "On the Latitude Variation of Scintillations of Ionosphere Origin in Satellite Signals," Planet. Space Sci., Vol. 16, No. 6, pp. 775-781 (1968).

Kaiser, A. B., and G. F. Preddey, "Observations of Transitions in Satellite Scintillation," J. Atmos. Terr. Phys., Vol. 30, pp. 285-291 (1968).

Kent, G. S., "High Frequency Fading Observed on the 40 Mc/s Wave Radiated from Artificial Satellite 1957 α," J. Atmos. Terr. Phys., Vol. 16, pp. 10-20 (1959).

Kent, G. S., and J. R. Koster, "Some Studies of Nighttime F-Layer Irregularities at the Equator Using Very High Frequency Signals Radiated from Earth Satellites," in "Spread-F and its Effects Upon Radiowave Propagation and Communications," P. Newman, Ed., Technivision, Maidenhead, England, pp. 333-356 (1966).

Kidd, W. C., "Heights of Ionospheric Irregularities at a Sub-Auroral Latitude," Radio Sci., Vol. 5, No. 6, pp. 975-978 (1970).

Koster, J. R., "Radio Star Scintillations at an Equatorial Station," J. Atmos. Terr. Phys., Vol. 12, pp. 100-109 (1958).

Koster, J. R., "Some Measurements of the Irregularities Giving Rise to Radio-Star Scintillations at the Equator," J. Geophys. Res., Vol. 68, No. 9, pp. 2579-2590 (May 1, 1963).

Koster, J. R., "Equatorial Studies of the VHF Signal Radiated by Intelsat II, F-3, 1. Ionospheric Scintillation," Progress Report No. 3, Contract No. F61052-67-C-0027, University of Ghana-Legon, Accra, Ghana (September 1968).

Koster, J. R., I. Katsriku, and M. Tete, "Studies of the Equatorial Ionosphere Using Transmissions from Active Satellites," Annual Summary Report No. 1, Contract AF61(052)-800, University of Ghana-Legon, Accra, Ghana (1966).

Koster, J. R., and R. W. Wright, "Radio Star Scintillations and Associated Effects in Equatorial Regions," in Radio Astronomical and Satellite Studies of the Atmosphere, J. Aarons, Ed., pp. 114-134 (Interscience Publishers, New York, N. Y., 1963).

Kuegler, G. K., "Equatorial Scintillations Experienced during Apollo 11 Support July 12 to July 24," X-460-69-534, Goddard Space Flight Center, Greenbelt, Maryland (1969).

Lansinger, J. M., and E. J. Fremouw, "The Scale Size of Scintillation-Producing Irregularities in the Auroral Ionosphere," J. Atmos. Terr. Phys., Vol. 29, pp. 1229-1242 (1967).

Lawrence, R. A., J. L. Jespersen, and R. C. Lamb, "Amplitude and Angular Scintillations of the Radio Source Cygnus-A Observed at Boulder, Colorado," J. Res. NBS, 65D, pp. 333-350 (1961).

Lawrence, J. D., Jr., and J. D. Martin, "Diurnal, Seasonal, Latitudinal, and Height Variations of Satellite Scintillation," J. Geophys. Res., Vol. 69, No. 7, pp. 1293-1300 (April 1, 1964).

Liszka, L., "A Study of Ionospheric Irregularities Using Transmissions at 54 Mc/s," Ark. Geofys., Vol. 4, pp. 227-246 (1963).

Liszka, L., "The Geographical Distribution of Satellite Activity above Northern Scandinavia," Ark. Geofys., Vol. 4, pp. 453-463 (1964a).

Liszka, L., "An Investigation of the Height of Scintillation-Producing Irregularities," Ark. Geofys., Vol. 4, pp. 523-528 (1964b).

Little, C. G., and A. Maxwell, "Scintillation of Radio Stars during Aurorae and Magnetic Storms," J. Atmos. Terr. Phys., Vol. 2, No. 6, pp. 356-360 (1952).

Little, C. G., G. C. Reid, E. Stiltner, and R. P. Merritt, "An Experimental Investigation of Radio Stars Observed at Frequencies of 223 and 456 Megacycles per Second from a Location Close to the Auroral Zone," J. Geophys. Res., Vol. 67, No. 5, pp. 1763-1784 (1962).

McIlwain, C. E., "Coordinates for Mapping the Distribution of Magnetically Trapped Particles," J. Geophys. Res., Vol. 66, pp. 3681-3691 (1961).

Millman, G. H., and A. J. Moceyunas, "Observations of Ionospheric Scintillations by Ultra High Frequency Radar Reflection from Earth's Satellites," J. Geophys. Res., Vol. 70, No. 1, p. 81 (January 1, 1965).

Muldrew, D. B., "F-Layer Ionization Troughs Deduced from Alouette Data," J. Geophys. Res., Vol. 70, pp. 2635-2650 (1965).

Nakagami, M., "The m-Distribution--A General Formula of Intensity Distribution of Rapid Fading," in "Stat. Methods in Radio Wave Prop.," W. C. Hoffman, Ed., pp. 3-36 (Pergamon Press, Oxford, 1960).

Nakagami, M., S. Wada, and S. Fujimura (in Japanese), J. Inst. Elec. Commun. Engrs.--Japan, Vol. 36, pp. 595-602 (1953).

Paul, L. M., K. C. Yeh, and B. J. Flaherty, "Measurements of Irregularity Heights by the Spaced Receiver Technique," Radio Sci., Vol. 5, No. 6, pp. 967-973 (1970).

Paulson, M. R., and J. C. Tyner, "An Investigation of Equatorial Fading of TACSAT I UHF Signals," TN 1837, Naval Electronic Laboratory Center, San Diego, California (1971).

Pomalaza, J., R. F. Woodman, G. Tisnado, J. Sandoval, and A. Guillén, "A Progress Report on Scintillation Observations at Ancon and Jicamarca Observatories," Report No. X-520-70-398, Goddard Space Flight Center, Greenbelt, Maryland (October 1970).

Preddey, G. F., "Midlatitude Radio-Satellite Scintillation: The Variation with Latitude," Planet. Space Sci., Vol. 17, No. 8, pp. 1557-1561 (1969).

Preddey, G. F., J. Mawdsley, and W. Ireland, "Mid-Latitude Radio-Satellite Scintillation--The Morphology near Sunspot Minimum," Planet. Space Sci., Vol. 17, pp. 1161-1171 (1969).

Singleton, D. G., "The Occurrence of Scintillation-Producing Irregularities over Australasia," J. Geophys. Res., Space Physics, Vol. 74, No. 7, pp. 1772-1785 (April 1, 1969).

Singleton, D. G., "Saturation and Focusing Effects in Radio-Star and Satellite Scintillations," J. Atmos. Terr. Phys., Vol. 32, pp. 187-208 (1970a).

Singleton, D. G., "Dependence of Satellite Scintillations on Zenith Angle and Azimuth," J. Atmos. Terr. Phys., Vol. 32, pp. 789-803 (1970b).

Skinner, N. J., R. F. Kelleher, J. B. Hacking, and C. W. Benson, "Scintillation Fading of Signals in the SHF Band," Nature Physical Science, Vol. 232, pp. 19-21 (1971).

Stringer, W. J., and A. E. Belon, "The Morphology of the IQSY Auroral Oval, 1. Interpretation of Isauroral Diagrams," J. Geophys. Res., Vol. 72, p. 4415 (September 1, 1967).

Stuart, G. F., and J. E. Titheridge, "The Distribution of Irregularities in the Antarctic Ionosphere--II, Diurnal, Magnetic and Solar Cycle Effects," J. Atmos. Terr. Phys., Vol. 31, pp. 905-924 (1969).

Titheridge, J. E., "A Regular Disturbance in the Topside Ionsophere," J. Geophys. Res., Space Physics, Vol. 74, No. 5, p. 1195 (March 1, 1969).

Titheridge, J. E., and G. F. Stuart, "The Distribution of Irregularities in the Antarctic Ionosphere--II, Mean Seasonal Maps at Sunspot Minimum," J. Atmos. Terr. Phys., Vol. 30, pp. 85-98 (1968).

Uscinski, B. J., "The Multiple Scattering of Waves in Irregular Media," Phil. Trans. Roy. Soc. London, A, Vol. 262(1133), pp. 609-643 (1967).

Walker, G. O., and T. Chan, "A Study of Scintillations at Low Latitudes during a Period from Sunspot Minimum to Sunspot Maximum," J. Geophys. Res., Space Physics, Vol. 75, No. 13, pp. 2517-2528 (May 1, 1970).

Whitney, H. E., "The Definition of Scintillation Index and its Use for Characterizing Ionospheric Effects," in "A Survey of Scintillation Data and its Relationship to Satellite Communications," J. Aarons, Ed., Agardograph Interim Report, Air Force Cambridge Research Laboratories, Bedford, Mass., pp. 4-20 (1969).

Whitney, H. E., J. Aarons, and C. Malik, "A Proposed Index for Measuring Ionospheric Scintillations," Planet. Space Sci., Vol. 17, pp. 1069-1073 (1969).

Whitney, H. E., R. S. Allen, and J. Aarons, "Studies of the Latitudinal Variations of Irregularities by Means of Synchronous and 1000 km Satellites," Space Res., VII, pp. 1358-1369 (1967).

Yeh, K. C., and G. W. Swenson, Jr., "F-Region Irregularities Studied by Scintillation of Signals from Satellites," J. Res. Nat. Bur. Stand., Vol. 68D, No. 8, pp. 881-894 (August 1964).

1. Report No.	2. Government Accession No.	3. Recipient's Catalog No.
Final Report		

4. Title and Subtitle	5. Report Date
DEVELOPMENT OF A WORLDWIDE MODEL FOR F-LAYER-PRODUCED SCINTILLATION	November 1971
	6. Performing Organization Code
7. Author(s)	8. Performing Organization Report No.
E. J. Fremouw and C. L. Rino	Project 1079
9. Performing Organization Name and Address	10. Work Unit No.
Stanford Research Institute Menlo Park, California 94025	11. Contract or Grant No. NAS5-21551
12. Sponsoring Agency Name and Address	13. Type of Report and Period Covered
Mr. Thomas S. Golden Goddard Space Flight Center Greenbelt, Maryland 20071	Final Report 3 Feb. 1971 to 3 Dec. 1971
	14. Sponsoring Agency Code

15. Supplementary Notes

16. Abstract (Condensed)

An empirical approach to modeling the electron-density irregularities in the F layer of the earth's ionosphere that are primarily responsible for scintillation of transatmospheric VHF-UHF signals has been devised and tested. The work consisted of two major tasks: first, development of a worldwide model for describing the rms fluctuation in signal strength to be expected on an arbitrary satellite-to-earth communication link under average ionospheric conditions; and, second, investigation of the feasibility of similar modeling for description of the complete first-order distribution of signal strength. In the work on rms fluctuation, a model for scintillation-producing irregularities was postulated as a function of geomagnetic latitude, local time of day, season, and sunspot number. The model was tested against scintillation observations reported in the literature and improved by iteration. The feasibility investigation into modeling amplitude distribution involved a theoretical development of scattering in the complex domain, based solely on requirements of the Central Limit Theorem. From the theoretical results, a technique for evaluating the expected amplitude distribution in a given observational circumstance was devised and successfully tested. As a result, it is concluded that distribution modeling is feasible for conditions of moderate scintillation. The rms model developed is offered as a tool for systems planning on a worldwide basis, except poleward from about 70 degrees geomagnetic latitude, where testing was not possible. It is expected to yield better than order-of-magnitude estimates in most circumstances.

17. Key Words	18. Distribution Statement
Ionospheric Scintillation Transatmospheric Radio Signals Amplitude Distribution	

19. Security Classif. (of this report)	20. Security Classif. (of this page)	21. No. of Pages	22. Price
Unclassified	Unclassified	128	

Form DOT F 1700.7 (8-69)